University of Windsor
Scholarship at UWindsor

Electronic Theses and Dissertations | Theses, Dissertations, and Major Papers

2002

The second law analysis of a spark ignition engine fueled with compressed natural gas

Shengmei Zhang
University of Windsor

Follow this and additional works at: https://scholar.uwindsor.ca/etd

Recommended Citation

Zhang, Shengmei, "The second law analysis of a spark ignition engine fueled with compressed natural gas" (2002). *Electronic Theses and Dissertations*. 4260.
https://scholar.uwindsor.ca/etd/4260

This online database contains the full-text of PhD dissertations and Masters' theses of University of Windsor students from 1954 forward. These documents are made available for personal study and research purposes only, in accordance with the Canadian Copyright Act and the Creative Commons license—CC BY-NC-ND (Attribution, Non-Commercial, No Derivative Works). Under this license, works must always be attributed to the copyright holder (original author), cannot be used for any commercial purposes, and may not be altered. Any other use would require the permission of the copyright holder. Students may inquire about withdrawing their dissertation and/or thesis from this database. For additional inquiries, please contact the repository administrator via email (scholarship@uwindsor.ca) or by telephone at 519-253-3000ext. 3208.

INFORMATION TO USERS

This manuscript has been reproduced from the microfilm master. UMI films the text directly from the original or copy submitted. Thus, some thesis and dissertation copies are in typewriter face, while others may be from any type of computer printer.

The quality of this reproduction is dependent upon the quality of the copy submitted. Broken or indistinct print, colored or poor quality illustrations and photographs, print bleedthrough, substandard margins, and improper alignment can adversely affect reproduction.

In the unlikely event that the author did not send UMI a complete manuscript and there are missing pages, these will be noted. Also, if unauthorized copyright material had to be removed, a note will indicate the deletion.

Oversize materials (e.g., maps, drawings, charts) are reproduced by sectioning the original, beginning at the upper left-hand corner and continuing from left to right in equal sections with small overlaps.

ProQuest Information and Learning
300 North Zeeb Road, Ann Arbor, MI 48106-1346 USA
800-521-0600

UMI®

Reproduced with permission of the copyright owner. Further reproduction prohibited without permission.

Reproduced with permission of the copyright owner. Further reproduction prohibited without permission.

The Second Law Analysis of a Spark Ignition Engine Fueled with Compressed Natural Gas

By

Shengmei Zhang

A Thesis
Submitted to the Faculty of Graduate Studies and Research
through Mechanical, Automotive and Materials Engineering Department
in Partial Fulfillment of the Requirements for
the Degree of Master of Applied Science at the
University of Windsor

Windsor, Ontario, Canada

2002

© 2002 Shengmei Zhang

Reproduced with permission of the copyright owner. Further reproduction prohibited without permission.

National Library of Canada
Acquisitions and Bibliographic Services
395 Wellington Street
Ottawa ON K1A 0N4
Canada

Bibliothèque nationale du Canada
Acquisitions et services bibliographiques
395, rue Wellington
Ottawa ON K1A 0N4
Canada

Your file Votre référence

Our file Notre référence

The author has granted a non-exclusive licence allowing the National Library of Canada to reproduce, loan, distribute or sell copies of this thesis in microform, paper or electronic formats.

The author retains ownership of the copyright in this thesis. Neither the thesis nor substantial extracts from it may be printed or otherwise reproduced without the author's permission.

L'auteur a accordé une licence non exclusive permettant à la Bibliothèque nationale du Canada de reproduire, prêter, distribuer ou vendre des copies de cette thèse sous la forme de microfiche/film, de reproduction sur papier ou sur format électronique.

L'auteur conserve la propriété du droit d'auteur qui protège cette thèse. Ni la thèse ni des extraits substantiels de celle-ci ne doivent être imprimés ou autrement reproduits sans son autorisation.

0-612-75811-7

Canada

Reproduced with permission of the copyright owner. Further reproduction prohibited without permission.

962009

APPROVED BY:

Dr. Andrzej Sobiesiak, Ph.D., P.Eng., Academic Advisor
NSERC / DaimlerChrysler Canada Industrial Research Chair in Alternate Fuels;
Mechanical, Automotive and Materials Engineering

Dr. Amir Fartaj, Ph.D., Department Reader
Mechanical, Automotive and Materials Engineering

Dr. Paul Henshaw, Ph.D., P.Eng.
Outside Department Reader
Civil and Environmental Engineering

Dr. Gary Rankin, Ph.D., P.Eng., Chair of Defense
Mechanical, Automotive and Meaterials Engineering

Reproduced with permission of the copyright owner. Further reproduction prohibited without permission.

ABSTRACT

This thesis presents a fundamental thermodynamic modeling approach to study internal combustion engines. The computations of the thermodynamic functions, especially availability, have been developed to seek better energy utilization, analyze engine performance and optimize design of spark ignition (SI) engines fueled with compressed natural gas (CNG), by using both the first and the second law analyses.

Compared with the first law, the second law of thermodynamics provides a framework leading to a more thorough understanding of energy conversion processes, illustrates a quantitative measure of capability to produce useful work, and identifies the processes which are destructive to the goals of high performance and high efficiency. When considering the problem of better energy utilization, it is essential to take into account both the quantity and quality (potential to produce useful work) of energy, which are captured by the first and second law respectively. Therefore, energy analysis based on both is required, and one complements the other. Moreover, the examination of the detailed, time-resolved characteristics of a number of thermodynamic properties, such as specific heat ratio, internal energy, entropy, and availability, allows a complete interpretation of the overall engine performance.

A single-zone heat release model with constant thermodynamic properties is built into the air cycle simulation, while a more comprehensive two-zone combustion model with burning rate as a sinusoidal function of crank angle is built into the fuel/air thermodynamic engine cycle simulation. The computations mainly include pressure, unburned and burned zone temperature, indicated work, heat loss, mass blowby, availability destruction due to combustion, fuel chemical availability, availability transfer with heat, availability transfer with work and availability exhaust to the environment. The validation of the simulation results with the experimental data is performed for a DaimlerChrysler 4.7 Liter CNG fueled V8 engine at wide open throttle (WOT), and 4000 rpm.

Reproduced with permission of the copyright owner. Further reproduction prohibited without permission.

The engine parametric studies of sparking timing, combustion duration, equivalence ratio, residual gas fraction and compression ratio, are used for engine performance analysis and optimum design for CNG engine operation.

The comparisons of natural gas and alcohol with conventional gasoline fueled SI engines according to the second law analysis have brought out fairly different perspectives on potential benefits and advantages for alternative fuels operation in SI engines.

The highest second law efficiency is found at the lean engine operation condition, while the peak engine output reflected in the indicated mean effective pressure (IMEP) is at slightly rich mixture condition. Clearly, there has to be a trade off between the second law efficiency and the indicated mean effective pressure. In order to obtain better engine performance, higher power and torque, and better emission control by three-way catalytic converters, a slight rich condition with equivalence ratio of 1.1 is chosen for the optimal design of CNG fuelling.

Reproduced with permission of the copyright owner. Further reproduction prohibited without permission.

ACKNOWLEDGEMENTS

I wish to thank my supervisor Dr. Sobiesiak, for introducing me to this subject and for generously sharing his thoughts about it. During my graduate studies, I have learned a great deal from him. Many thanks to my Mother, Father and Sister for their support and Ethan Barbour for his encouragement and help.

In the preparation of the thesis, several people have made contribution by reviewing, making suggestions, and assisting this work. Thanks are due to the following individuals: Dr. Gary Rankin, Dr. Amir Fartaj, Dr. Paul Henshaw, Dr. Nader Zamani, Mohsen Battoei, Biao Zhou, Rafal Jarnicki, Chunyi Xia, and Kevin Roth.

Many thanks for the resources supplied by the DaimlerChrysler/NSERC Industrial Office at the University of Windsor.

The financial support of the Natural Science and Engineering Research Council, DaimlerChrysler Canada, and the University of Windsor School of Graduate Studies is gratefully acknowledged.

Reproduced with permission of the copyright owner. Further reproduction prohibited without permission.

TABLE OF CONTENTS

ABSTRACT iii

ACKNOWLEDGEMENTS v

TABLE OF CONTENTS vi

LIST OF FIGURES viii

LIST OF TABLES xi

NOMENCLATURE xii

CHAPTER 1 INTRODUCTION OF AVAILABILITY ANALYSIS 1

1.1 Better Energy Utilization and Availability Analysis
1.2 Spark Ignition Engine with Alternative Fuels
1.3 Summary

CHAPTER 2 MOTIVATION AND OBJECTIVE 5

2.1 Natural Gas and Methanol in Canada
2.2 Motivation
2.3 Objective

CHAPTER 3 DEFINITIONS 8

3.1 Equilibrium
3.2 Environment
3.3 Restricted Dead State and Dead State
3.4 Thermomechanical Availability—A^{th}
3.5 Availability Destruction
3.6 Chemical Availability—A^{ch}
3.7 Availability and Exergy

CHAPTER 4 AVAILABILITY 12

4.1 Introduction to Availability
4.2 Thermomechanical and Chemical Availability

CHAPTER 5 LITERATURE REVIEW 16

5.1 Strong and Weak Points from Previous Work
5.2 Summary

Reproduced with permission of the copyright owner. Further reproduction prohibited without permission.

CHAPTER 6 METHODOLOGY AND PROCEDURE **20**

6.1 Compositions and Thermodynamic Properties for In-Cylinder Mixtures
6.1.1 Fuel-Air-Residual Gas (FARG) Simulation
6.1.2 Equilibrium Combustion Products (ECP) Simulation
6.2 Thermodynamic Engine Cycle Simulations
6.2.1 Ferguson Models
6.2.2 Current Models: Air Cycle Availability Simulation
6.2.3 Current Models: Fuel/air Cycle Availability Simulation
6.2.4 Current Models: DaimlerChrysler 4.7 Liter-V8 engine Simulation

CHAPTER 7 RESULTS AND DISCUSSIONS **64**

7.1 Air Cycle Thermomechanical Availability Results
7.2 Discussion of Air Cycle Availability Results
7.3 Fuel/air Cycle Thermomechanical and Fuel Chemical Availability Results
7.4 Discussion of Fuel/air Cycle Availability Results
7.4.1 Indicated Mean Effective Pressure & Second Law Efficiency
7.4.2 Distributions of Fuel Energy and Fuel Availability Analyses
7.5 Parametric Study on DaimlerChrysler V8 Engine Performance
7.5.1 Spark Timing and Combustion Duration
7.5.2 Equivalence Ratio
7.5.3 Residual Gas Fraction
7.5.4 Compression Ratio
7.6 Comparison of Optimized CNG and Gasoline Fueled SI Engine Operations
7.7 Thermodynamic Properties Studies for CNG Engine Simulation
7.8 Comparison of Experimental with Simulated Pressure Data

CHPATER 8 SUMMARY, CONCLUSIONS AND RECOMMENDATIONS **104**

8.1 Summary of the Approach
8.2 Conclusion—Trends in Energy and Availability Changes with Engine Operating Variables
8.3 Recommendations for Future Work

CHAPTER 9 REFERENCES **108**

CHAPTER 10 APPENDIXES **110**

VITA AUCTORIS **138**

Reproduced with permission of the copyright owner. Further reproduction prohibited without permission.

LIST OF FIGURES

Figure 3.1	The combined system (System & Environment).	9
Figure 6.1	The procedure of the current study.	22
Figure 6.2	Schematic diagram of the two-zone model and the combined system for determining availability in fuel/air cycle analysis.	49
Figure 6.3	(a) Experimental pressure-volume diagram at WOT, 4000rpm for V8 engine; (b) Experimental log (p/p_0)-log (V/V_0) plot at WOT, 4000 rpm for V8 engine.	58
Figure 6.4	Predicted and measured mass fraction burned (MFB) versus crank angles at WOT, 4000 rpm for V8 engine.	60
Figure 6.5	Heat transfer coefficient changes with crank angle at WOT, 4000rpm, equivalence ratio (1.1), start of combustion (-30°), combustion duration (70°), and residual gas fraction (0).	63
Figure 7.1	Air cycle thermomechanical availability from Method I for arbitrary heat release (AHR), arbitrary heat release with heat loss(AHR-HL), arbitrary heat release with heat and mass losses (AHR-HML).	64
Figure 7.2	Air cycle thermomechanical availability from Method II for arbitrary heat release (AHR), arbitrary heat release with heat loss(AHR-HL), arbitrary heat release with heat and mass losses (AHR-HML).	64
Figure 7.3	Air cycle arbitrary heat release with heat and mass losses (AHR-HML) from Method I & II.	65
Figure 7.4	Effects of constant and changing specific heat on air cycle thermomechanical availability simulation for arbitrary heat release with heat and mass losses (AHR-HML).	65
Figure 7.5	(a) Pressure and temperature versus crank angle for air cycle arbitrary heat release with heat and mass loss (AHR-HML). (b) Constant and varying specific heats for air cycle arbitrary heat release with heat and mass loss (AHR-HML).	66
Figure 7.6	Fuel/air cycle indicated mean effective pressure (IMEP) for gasoline, CNG and methanol.	67
Figure 7.7	Fuel/air cycle second law efficiency for gasoline, CNG and methanol.	67

Reproduced with permission of the copyright owner. Further reproduction prohibited without permission.

Figure 7.8 The distributions of fuel energy and fuel availability (I) in engine cycle processes for gasoline, CNG and methanol at Φ=0.8. 68

Figure 7.9 The distributions of fuel energy and fuel availability (II) in engine cycle processes for gasoline, CNG and methanol at Φ=0.8. 69

Figure 7.10 Effects of sparking timing on unburned and burned mixtures temperature, for V8 engine at equivalence ratio (1.1), residual gas fraction (0.0), combustion duration (70°), WOT, and 4000 rpm. 73

Figure 7.11 (a) V8 engine simulated cylinder pressure versus crank angle for overadvanced spark timing (40°), MBT timing (30°), and retarded timing (20°). (b) Effects of spark advance on indicated torque and the second law efficiency for V8 engine at combustion duration (70°), equivalence ratio (1.1), residual gas fraction (0.0), WOT and 4000rpm. 74

Figure 7.12 (a) Effects of spark timing on availability transfer with work for V8 engine at combustion duration (70°), equivalence ratio (1.1), residual gas fraction (0.0), WOT and 4000rpm. (b) Effects of combustion duration on availability transfer with work for V8 engine at spark timing (-30° before TDC), equivalence ratio (1.1), residual gas fraction (0.0), WOT and 4000 rpm. 75

Figure 7.13 Effects of spark timing on availability destruction due to combustion for V8 engine at combustion duration (70°), equivalence ratio (1.1), residual gas fraction (0.0), WOT and 4000rpm. 76

Figure 7.14 Effects of spark timing on availability with heat transfer for V8 engine at combustion duration (70°), equivalence ratio (1.1), residual gas fraction (0.0), WOT and 4000rpm. 77

Figure 7.15 Effects of combustion duration on the availability destruction due to combustion for V8 engine at spark timing (-30° before TDC), equivalence ratio (1.1), residual gas fraction (0.0), WOT and 4000 rpm. 77

Figure 7.16 Effects of combustion duration on unburned and burned mixtures temperature for V8 engine at spark timing (-30° before TDC), equivalence ratio (1.1), residual gas fraction (0.0), WOT and 4000 rpm. 78

Figure 7.17 Effects of combustion duration on availability with heat for V8 engine at spark timing (-30° before TDC), equivalence ratio (1.1), residual gas fraction (0.0), WOT and 4000 rpm. 78

Reproduced with permission of the copyright owner. Further reproduction prohibited without permission.

Figure 7.18 Fuel/air cycle simulation results for the second law efficiency as a function of equivalence ratio and compression ratio at spark timing (-30° before TDC), combustion duration (70°), residual gas fraction (0.0), WOT and 4000 rpm. 79

Figure 7.19 Fuel/air cycle simulation results for indicated mean effective pressure as a function of equivalence ratio and compression ratio at spark timing (-30° before TDC), combustion duration (70°), residual gas fraction (0.0), WOT and 4000 rpm. 79

Figure 7.20 Effects of the fuel/air equivalence ratio variations on indicated mean effective pressure, and specific fuel consumption for V8 engine at spark timing (-30° before TDC), combustion duration (70°), residual gas fraction (0.0), WOT and 4000 rpm. 80

Figure 7.21 Effects of equivalence ratio on the total availability for V8 engine at spark timing (-30° before TDC), combustion duration (70°), residual gas fraction (0.0), WOT and 4000 rpm. 81

Figure 7.22 Effects of equivalence ratio on the fuel chemical availability transferred to the environment for V8 engine at spark timing (-30° before TDC), combustion duration (70°), residual gas fraction (0.0), WOT and 4000 rpm. 81

Figure 7.23 Effects of equivalence ratio on the thermomechanical availability for V8 engine at spark timing (-30° before TDC), combustion duration (70°), residual gas fraction (0.0), WOT and 4000 rpm. 82

Figure 7.24 Effects of equivalence ratio on availability transfer with work for V8 engine at spark timing (-30° before TDC), combustion duration (70°), residual gas fraction (0.0), WOT and 4000 rpm. 82

Figure 7.25 Effects of equivalence ratio on availability destruction due to combustion in V8 engine simulation for V8 engine at spark timing (-30° before TDC), combustion duration (70°), residual gas fraction (0.0), WOT and 4000 rpm. 83

Figure 7.26 Effects of residual gas fraction on the total availability for V8 engine at spark timing (-30° before TDC), combustion duration (70°), equivalence ratio (1.1), WOT and 4000 rpm. 84

Reproduced with permission of the copyright owner. Further reproduction prohibited without permission.

Figure 7.27 Effects of residual gas fraction on the availability transfer with work for V8 engine at spark timing (-30° before TDC), combustion duration (70°), equivalence ratio (1.1), WOT and 4000 rpm. 84

Figure 7.28 Effects of residual gas fraction on availability destruction due to combustion for V8 engine at spark timing (-30° before TDC), combustion duration (70°), equivalence ratio (1.1), WOT and 4000 rpm. 85

Figure 7.29 Effects of compression ratio on indicated mean effective pressure and the second law efficiency at spark timing (-30° before TDC), combustion duration (70°), equivalence ratio (1.1), residual gas fraction (0.0), WOT and 4000 rpm. Equivalence ratio and spark timing are set for maximum torque and indicated mean effective pressure. 86

Figure 7.30 Effects of compression ratio on the availability destruction due to combustion at spark timing (-30° before TDC), combustion duration (70°), equivalence ratio (1.1), residual gas fraction (0.0), WOT and 4000 rpm. 87

Figure 7.31 Availability simulation versus crank angles in the predicted optimum engine operation conditions: equivalence ratio (1.1), spark timing (-30°), combustion duration (70°), residual gas fraction (0.0) at WOT and 4000 rpm for DaimlerChrysler V8 engine fueled with CNG. 89

Figure 7.32 CNG and gasoline operations at the predicted optimal engine conditions for best indicated mean effective pressure (IMEP). 90

Figure 7.33 CNG and gasoline operations at the same equivalence ratio, $\Phi = 1.1$. 91

Figure 7.34 The distributions of fuel energy and fuel availability of CNG and gasoline fueled SI engines at the same equivalence ratio, $\Phi = 1.1$. 92-93

Figure 7.35 Entropy-temperature diagram at the predicted optimal conditions for CNG fueled V8 engine. 94

Figure 7.36 Specific availability and internal energy vs. temperature at the predicted optimal conditions for CNG fueled V8 engine. 95

Figure 7.37 Major species and cylinder mixtures temperature as a function of crank angles for CNG optimal operating conditions. 96

Reproduced with permission of the copyright owner. Further reproduction prohibited without permission.

Figure 7.38 (a) The mole fractions of minor species (CO, H_2, OH) and the cylinder mixtures temperature as a function of crank angles for CNG optimal operating conditions. (b) Minor species (OH, NO, O,H) and the cylinder mixture temperature as a function of crank angles for CNG optimal operating conditions. 97

Figure 7.39 Wet exhaust gas compositions as a function of fuel/air equivalence ratio for CNG fueled SI engine operations (at the end of the expansion stroke). 99

Figure 7.40 NO emission and minor species (OH,H,O) as a function of fuel/air equivalence ration for CNG fueled SI engine (30° after TDC). 99

Figure 7.41 Pressure-Volume diagram for simulated (fuel/air cycle and air cycle) results and experimental data at WOT, 4000rpm. 100

Figure 7.42 Log (p/p_0)-log (V/V_0) plot for simulated and experimental pressure data for V8 engine at WOT, 4000rpm, with the current MFB model. 101

Figure 7.43 Log (p/p_0)-log (V/V_0) plot for simulated and experimental pressure data for V8 engine at WOT, 4000rpm, with the Wiebe function. 101

Figure 7.44 The distributions of fuel energy and fuel availability of CNG and gasoline fueled SI engines with the Wiebe function and the current MFB model. 103

Reproduced with permission of the copyright owner. Further reproduction prohibited without permission.

LIST OF TABLES

Table 1-1	Alternative fuels of interest and their properties	3
Table 5-1	Summary of previous work (Part 1)	16
Table 5-1	Summary of previous work (Part 2)	18
Table 5-1	Summary of previous work (Part 3)	19
Table 6-1	In-cylinder mixture constituents	23
Table 6-2	Combustion products	27
Table 6-3	SI engine parameters for simulation	54
Table 6-4	Calorific value, fuel chemical availability, air/fuel ratio for three different fuels	55
Table 6-5	Baseline case for 4.7 Liter V8 SI engine model	56
Table 7-1	Total in-cylinder mass, calorific value, and total specific availability per unit of the in-cylinder mixture for three different fuels	70
Table B-1	Curve Fit Coefficients for Thermodynamic Properties (300<T<1000 K)	135
Table B-2	Curve Fit Coefficients for Thermodynamic Properties (1000<T<4000 K)	136
Table B-3	Curve Fit Coefficients for Thermodynamic Properties of Selected Fuels (300<T<100K)	137

Reproduced with permission of the copyright owner. Further reproduction prohibited without permission.

NOMENCLATURE

A	Total availability (J)
A^{th}	Thermomechanical availability (J)
A^{ch}	Chemical availability (J)
A_W	Availability associated with work (J)
A_Q	Availability associated with heat transfer (J)
a_f^{ch}	Specific fuel chemical availability (J/g)
b	Engine bore (m)
c_v	Specific heat at the constant volume (J/g · K)
c_p	Specific heat at the constant pressure (J/g · K)
ΔE_c	Energy change of the combined system (J)
F	Gravimetric fuel air ratio at actual condition
F_s	Gravimetric fuel air ratio at stoichiometric condition
h	Specific enthalpy (J/g)
h	Heat transfer coefficient of in-cylinder mixtures ($W/m^2 \cdot K$)
I_c'	Rate of availability destruction due to combustion (J/crank angle)
$I_{heat\ transfer}'$	Rate of availability destruction due to heat transfer (J/crank angle)
k	Thermal conductivity of in-cylinder mixtures (W/m·K)
K_p	Equilibrium constant
L	Characteristic length for Reynolds number (m)
m	Total mass in the cylinder (g)
m_f	Mass of fuel in the cylinder (g)
$\dot{m}_l$	Instantaneous leakage or blowby rate (g/s)
Nu	Nusselt number
N_k	Number of moles of substance k
N_k^0	Number of moles of substance k in the environment (mol)
p	Pressure (Pa)
p_m	Motered cylinder pressure (Pa)
p_0	Pressure of the environment (Pa)
Q	Heat transfer (J)
Q_{in}	Heat addition due to the combustion (J)
Q_l	Heat losses by the gases in the cylinder due to convection (J)
r	Compression ratio
R	Universal gas constant (= 8.314 J/mol · K)
Re	Reynolds number
S	Entropy (J/K)
s	Specific entropy (J/g · K)
s^0	Specific entropy at the atmospheric pressure (J/g · K)

Reproduced with permission of the copyright owner. Further reproduction prohibited without permission.

S^0	Entropy of the environment (J/K)
S_0	Entropy at the restricted dead state (J/K)
T	Temperature (K)
T_w	Cylinder wall temperature (K)
T_0	Temperature of the environment (K)
u	Specific internal energy (J/g)
U	Internal energy (J)
U^0	Internal energy of the environment (J)
U_0	Internal energy at the restricted dead state (J)
v	Specific volume (m^3/g)
V	Volume (m^3)
V^0	Volume of the environment (m^3)
V_0	Volume at the restricted dead state (m^3)
w	Average in-cylinder gas velocity (m/s)
W	Work done by the control mass or control volume (J)
$(W_C)_{max}$	Maximum potential of work from the combined system (J)
W_C	Work produced from the combined system (J)
$W_{environment}$	Work produced by the environment (J)
x	Heat release rate or Mass burn rate

Greek symbols

Φ	Fuel/air equivalence ratio
γ	Specific heat ratio
μ	Dynamic viscosity of the fluid (N·s)
μ_k^0	Chemical potential of the substance k present in the environment (J/mol)
μ_{k0}	Chemical potential of substance k at the restricted dead state (J/mol)
θ	Instantaneous crank angle (˚CA)
θ_s	Crank angle of start of the combustion (˚CA)
θ_b	Crank angle of combustion duration (˚CA)
ρ	Density of in-cylinder mixtures (g/m^3)
σ	Entropy production of the combined system (J/K)
σ_c	Entropy production due to combustion (J/K)
σ'	Entropy production rate (J/K/ crank angle)
ω	Engine speed (rev/s)

Reproduced with permission of the copyright owner. Further reproduction prohibited without permission.

Abbreviations

LCV	Low Calorific Value
RON	Research Octane Number
AHR	Arbitrary Heat Release
AHR-HL	Arbitrary Heat Release with Heat loss
AHR-HML	Arbitrary Heat Release with Heat and Mass losses
CV	Calorific Value
$(AFR)_{stoich}$	Gravimetric Air-Fuel Ratio at the stoichiometric condition
TDC	Top Dead Center
ECP	Equilibrium Combustion Products
FARG	Fuel-Air-Residual Gas
rpm	Revolutions per minute
WOT	Wide Open Throttle
$^{\circ}CA$	Degree crank angle
MFB	Mass fraction Burned
IMEP	Indicated Mean Effective Pressure

Reproduced with permission of the copyright owner. Further reproduction prohibited without permission.

CHAPTER 1 INTRODUCTION OF AVAILABILITY ANALYSIS

1.1 Better Energy Utilization and Availability Analysis

For the past half century, global energy growth has marched in lockstep with economic growth. Energy use has increased 400 percent to accommodate a doubling of world population and a quadrupling of Gross World Product. A tremendous amount of energy resources have been used for comfort, transportation, and industrial production. For example, the world now consumes the equivalent of 175 million barrels of oil each day [1]. Until recently, most energy analysts expect growth in the future to reflect the past. It means they anticipate another 400 percent growth in energy over the next 50 years to accommodate another doubling of world population and a quadrupling of Gross World Product.

As we know, a certain amount of energy is wasted due to a variety of inefficiencies and poor practices. Improving energy efficiency of buildings, appliances, office equipment, factories, and vehicles is of major concern. Better energy utilization is a worthy goal for our society, economy, and environment as well.

When considering better energy utilization, it is essential to take into account both the quantity and quality (potential to produce a useful work) of energy, which are reflected in the first and second law of thermodynamics respectively. Therefore, processes analyses based on both are required.

This thesis presents an effective methodology, rooted in the concept of availability as a thermodynamic state function, to evaluate the distribution of the initial total availability, identify and qualify the processes causing state degradation in SI engines. Employing both the first and second law, the methodology is named as availability analysis. The fuel and air mixture is well mixed at the beginning of simulation, and the compression, combustion and expansion processes in SI engines can be viewed as a control mass

Reproduced with permission of the copyright owner. Further reproduction prohibited without permission.

application. Another term for such type of analysis, frequently used outside the U.S., is exergy analysis.

1.2 Spark Ignition Engines and Alternative Fuels

Future SI engines will require engine technology which could utilize a wide range of alternative fuels. Important alternative fuels for vehicles include natural gas, liquid petroleum gas (LPG), alcohols, and hydrogen. As of the year 2000, the most commonly used alternative fuels for vehicles are LPG, followed by natural gas, and methanol [2]. This thesis focuses on the studies of compressed natural gas[1] (CNG) and methanol.

It is well known that alternative fuels are of interest since they can be used as replacements if there are availability problems with crude oil. Most alternative fuels can be refined from renewable feed stocks, and their emission levels can be much lower than those of gasoline fueled conventional engines. Table 1.1 lists the alternative fuels of interest and their properties. When comparing the mass of CO_2 to the mass of fuel in the last column of Table 1.1, alcohol fuels seem to have an advantage. Methanol produces only 1.375 g of CO_2 (per gram of fuel), and ethanol produces 1.913 g of CO_2 (per gram of fuel). However, this changes when comparison on energy base is done as in the second last column. Now the best fuel is CNG followed by LPG and methanol. Conventionally, gasoline fueled SI engines are the worst case for greenhouse gas carbon dioxide with a value of 69.2 g/ MJ, while CNG operation is the best with a value of 55.0 g/MJ at the stoichiometric condition. CNG has the highest research octane number (RON) of 120, while gasoline has the lowest RON of 95. However, one of the major challenges for CNG operation is its storage problem to obtain a comparable mileage with gasoline. CNG is in the gaseous phase requiring a pressure of 245 bar with ambient temperature. Such high pressure causes potential dangers and inconvenience for drivers. Whereas, LPG only requires a pressure of 10 bar with ambient temperature for storage, and can be maintained in the liquid phase with a high in-cylinder charge density. Ethanol is also a popular

[1] Because of the gaseous nature of natural gas, it must be stored onboard a vehicle in either a compressed gaseous state (CNG) or in a liquefied state (LNG).

Reproduced with permission of the copyright owner. Further reproduction prohibited without permission.

alcohol fuel with high energy density for SI engine operation. For example, E85 is a blend of 85% ethanol and 15% of gasoline. In Brazil, about half of the vehicles use an ethanol-based fuel, produced from sugar cane.

Table 1-1 Alternative fuels of interest and their properties

Fuel	Model	LCV (MJ/kg)	(AFR)stoich	RON	Storage Capacity	CO_2 (g/MJ) $\Phi=1$	$\frac{CO_2\ (g)}{Fuel\ (g)}$
Gasoline	C_8H_{18}	44.651	14.7	95	Liquid at ambient T & p	69.2	3.088
CNG	CH_4	50.031	17.2	120	Gas at ambient T, p= 245 bar	55.0	2.750
LPG	C_3H_8	46.334	15.6	112	Liquid at ambient T, p= 10 bar	64.7	3.000
Methanol	CH_3OH	21.104	6.4	107	Liquid at ambient T & p	65.2	1.375
Ethanol	C_2H_5OH	27.731	9.0	108	Liquid at ambient T & p	69.0	1.913

The interest for CNG and methanol mainly stems from their clean burning qualities, the domestic resource base, and their environmental, economic and commercial benefits. Natural gas is a natural-occurring fossil fuel. It is primarily composed of 90-95% methane, with small amount of additional compounds such as 0-4% nitrogen, 4% ethane, and 1-2% propane. Natural gas has an octane number (RON) of 120, and it can operate at a compression ratio of 11-13, higher than that for gasoline fueled engines. Methanol is an alcohol fuel formed from natural gas, coal, or renewable sources such as biomass feed stocks. Pure methanol is labeled M100, and a mix of 85% methanol and 15% gasoline is labeled M85. M85 has an octane number rating of 107. Adding gasoline to methanol provides more volatile components that can vaporize easily at low temperatures. Such substantial evaporative cooling effect leads to an improvement in the volumetric efficiency, and thus the power output. The lower combustion temperature associated with

Reproduced with permission of the copyright owner. Further reproduction prohibited without permission.

methanol will reduce the heat transfer from the combustion chamber, which means the arbitrary overall efficiency of methanol fueled engines should be higher. Methanol has been adopted as a racing fuel, for both performance and safety reasons.

Existing gasoline or diesel fueled engines can be retrofitted easily to operate with alternative fuels. The DaimlerChrysler 4.7 Liter-V8 engine is a good example of converting from gasoline to CNG operation. However, different combustion characteristics of alternative fuel operations require changes in the ignition timing. The parametric studies of alternative fuels in this thesis have demonstrated such requirement and shed a new light on engine operation. The development and optimization efforts on CNG fueled SI engines are directed toward meeting higher engine torque, and maintaining relatively higher second law efficiency, since there is a trade-off between the indicated mean effective pressure and the second law efficiency when choosing the optimal equivalence ratio.

1.3 Summary

In view of energy deficiencies of many processes in SI engines, it is feasible to improve the energy utilization and optimize the engine operating conditions by using the availability analysis method. Improved utilization could come with the reduction of availability destruction or with the decrease of availability transfer losses. This knowledge should be useful in directing the attention of engineers and researchers to the aspects of engine process design, and offers the greatest opportunities for improving energy utilization.

Research and comparison of SI engine operations fueled with conventional gasoline fuel, compressed natural gas and methanol should broaden the present understanding of SI engine technologies and engine performance.

Reproduced with permission of the copyright owner. Further reproduction prohibited without permission.

CHAPTER 2 MOTIVATION AND OBJECTIVE

2.1 Natural Gas and Methanol in Canada

Fossil fuels, including coal, oil products and natural gas, will remain in use in Canada well into the next century. Especially, demands for natural gas continue to grow, and reserves are plentiful. 31% of Canada's primary energy is provided by natural gas. Forecasts to 2010 indicate that the growth in volume of natural gas consumed in Canada is expected to continue at about 2% per year [3]. The Western Canada Sedimentary Basin is currently the largest reservoir in North America for natural gas. Natural gas fueled vehicles (NGV) have been in use since the 1950s, and conversion kits are available for both spark and compression ignition engines. The natural gas industry in Canada, being new in comparison of some other countries, has taken advantage of the latest low emission technology and techniques. Natural gas is the cleanest burning alternative fuel. Exhaust emissions from NGVs are much lower than those from gasoline-powered vehicles. For instance, carbon monoxide are approximately 70% lower, non-methane organic gas emissions are 89% lower, and oxides of nitrogen emission are 87% lower. In addition to these reductions in pollutants, NGVs also emit significantly lower amounts of greenhouse gases and toxins than do gasoline vehicles, which is shown in Table 1.1 and discussed in Chapter 1. Dedicated NGVs produce little or no evaporative emissions during fueling and use.

Methanol is predominantly produced by steam reforming of natural gas to create a synthesis gas, which is then fed into a reactor vessel in the presence of a catalyst to produce methanol and water vapor. While a variety of feedstocks other than natural gas can be used, today's economics favor natural gas. Although there is an "energy cost" associated with the production of methanol from natural gas, it results in a fuel which can much more readily stored in a vehicle compared with CNG, as shown in Table 1.1. The alternative methanol fuel currently being used is M-85. In the future, neat methanol M-100 may also be used. Cars, trucks and buses running millions of miles on methanol have proven its use as a total replacement for gasoline and diesel fuels in conventional engines.

Reproduced with permission of the copyright owner. Further reproduction prohibited without permission.

As a practical alternative, methanol is similar to gasoline, compatible with the existing gasoline infrastructure, and methanol stations cost about the same.

This thesis focuses on the studies of CNG and methanol fueled SI engines. Due to their clean burning characteristics, their domestic resource base, their environmental, economic and commercial benefits, natural gas and methanol are viable alternative fuels to be used as substitutes in vehicles, in order to mitigate the dependence on conventional gasoline and diesel fuels. In addition, high engine performance and engine output can be achieved by raising the compression ratio in engine operations, due to their high octane number rating.

2.2 Motivation

The fundamental thermodynamic research of alternative fuels in SI engine operations based on the second law analysis has not been extensively developed, although thermodynamic engine cycle simulations have been used for over 40 years. Only one-third of the existing second-law based engine analysis literature refers to SI engines, and about two-thirds is for Compressed Ignition (CI) engines [4]. SI engines fueled with CNG have been analyzed in this thesis by applying the principles of the second law analysis, so as to gain a better understanding of energy utilization in SI engine operation.

2.3 Objective

Better energy utilization can be achieved by identifying and correcting processes which waste and destroy the thermodynamic state function, availability. This is accomplished by using the second law in conjunction with the first law analysis. The objectives of the current studies are as follows:

- To identify, qualify, and catalog the processes causing thermodynamic state degradation in SI engines

Reproduced with permission of the copyright owner. Further reproduction prohibited without permission.

- To quantify the effects of main operating variables on engine optimum performance
- To gain an insight of the effects of thermodynamic properties on engine performance

SI engine operation could be optimized in order to reach better engine performance, while maintaining higher second law efficiency, by adjusting the following engine operation variables:

- Alternative fuels, such as CNG and methanol
- Compression ratio
- Equivalence ratio
- Start of combustion
- Combustion duration
- Residual gas fraction

Finally, thermodynamic properties which are considered here are fuel/air mixture compositions, specific internal energy, specific entropy and specific availability. The purpose of studying both air cycle with constant properties and fuel/air cycle with variable properties is to illustrate the detailed characteristics of these properties and the implications for engine performance.

Reproduced with permission of the copyright owner. Further reproduction prohibited without permission.

CHAPTER 3 DEFINITIONS

The basic thermodynamic definitions and principles, which are required to gain an understanding of the availability concept, are given as follows. The classical thermodynamics, which concerns the macroscopic characteristics of large aggregations of molecules, is used in this study.

3.1 Equilibrium

Equilibrium means a condition of balance. Thermal equilibrium refers to an equality of temperature, mechanical equilibrium to an equality of pressure, and chemical equilibrium to an equality of chemical potentials.

3.2 Environment

When the thermomechanical availability is the objective, the composition of the environment is of no interest. The state of the environment is adequately defined by its temperature and pressure.

Otherwise, when the system is brought into thermal, mechanical, and chemical equilibrium with the environment, it is necessary to consider the compositions of both the system and the environment.

The state of the environment is described by both the extensive properties such as the internal energy, volume and entropy, and the intensive properties, like temperature, pressure and chemical potentials, related by Eq.(3.1).

$$U^0 = T_0 S^0 - p_0 V^0 + \sum_{k=1}^{n} N_k^0 \mu_k^0 \qquad (3.1)$$

Reproduced with permission of the copyright owner. Further reproduction prohibited without permission.

The relationships among the system, environment, combined system, and surroundings are shown in Figure 3.1. The environment is viewed as part of the surroundings. The system and the environment form the combined system. The combined system is used for availability analysis in the current study. The system is viewed as a control mass, because only the compression, combustion and expansion processes are studied in the current engine cycle simulation. The control mass interacts with the environment until both the control mass and the environment come to equilibrium. The work derived from the combined system W_C is defined as availability.

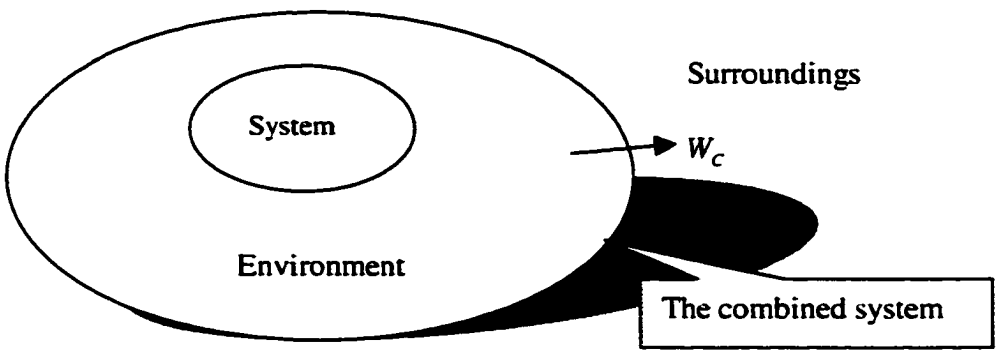

Figure 3.1 The combined system (System & Environment).

3.3 Restricted Dead State and Dead State

At the restricted dead state, the system is in the thermal and mechanical equilibrium with the environment. But it does not reach the chemical equilibrium with the environment, because the contents of the system are not permitted to mix with the environment or enter into chemical reaction with environmental components.

At the dead state, the system is in thermal, mechanical, and chemical equilibrium with the environment.

Reproduced with permission of the copyright owner. Further reproduction prohibited without permission.

3.4 Thermomechanical availability—A^{th}

Thermomechanical availability refers to the maximum work extractable from a combined system, as the system comes into thermal and mechanical equilibrium with the environment. It is represented in Eq.(3.2).

$$A^{th} = (U - U_0) + p_0(V - V_0) - T_0(S - S_0) - T_0\sigma \tag{3.2}$$

Its magnitude cannot be negative. It always has a positive value when the temperature of the system is different from the temperature of the environment. Similarly, it is positive when the pressure of the system is different from that of the environment.

3.5 Availability Destruction

Unlike energy, availability is not conserved. It can be destroyed by irreversibilities, which is expressed in Eq. (3.3). The effect of irreversibilities is to keep the work done by the combined system below a maximum, which is represented in Eq.(3.4).

$$I = T_0\sigma \tag{3.3}$$

$$W_c = (W_c)_{\max} - T_0\sigma \tag{3.4}$$

3.6 Chemical Availability—A^{ch}

In principle, the difference between the composition of the system at the restricted dead state and that of the environment can be exploited to obtain additional work, in order to reach chemical equilibrium. The maximum work obtained in this way is the chemical availability, expressed in Eq. (3.5). It can be obtained in two ways.

$$A^{ch} = \sum_{k=1}^{n} N_k(\mu_{k0} - \mu_k^0) \tag{3.5}$$

Reproduced with permission of the copyright owner. Further reproduction prohibited without permission.

First, the chemical availability can be calculated from the chemical potential differences associated with the same environmental species present in the system at the restricted dead state and those in the reference environment.

Second, species such as a fuel not present in the reference environment could be allowed to enter into chemical reactions with species from the reference environment to produce environmental species. More specifically, take a unit mass of hydrocarbon fuel for example. C_aH_b is at the restricted dead state, and the environment consists of N_2, O_2, CO_2, H_2O . The fuel is at the ambient temperature and pressure. No thermomechanical availability is associated with it. However, its fuel chemical availability can be utilized by reacting with air drawn from the environment.

3.7 Availability and Exergy

Availability is the maximum work obtained from a combined system of the control mass and the environment, as the control mass comes into thermal, mechanical, and chemical equilibrium with the environment. The maximum is obtained only when the process of the combined system is internally reversible. Generally, the availability destruction is to keep the work done by the combined system below a maximum.

The availability can be viewed as the sum of the thermomechanical availability and the chemical availability, represented in Eq.(3.6).

$$A = A^{th} + A^{ch} = [(U - U_0) + p_0(V - V_0) - T_0(S - S_0) - T_0\sigma] + \sum_{k=1}^{n} N_k(\mu_{k0} - \mu_k^0) \quad (3.6)$$

In the literature, exergy is often referred to as the flow availability, which is maximum work obtained from a combined system of the control volume (with mass flowing through the control surface) and the environment in a reversible process.

Reproduced with permission of the copyright owner. Further reproduction prohibited without permission.

CHAPTER 4 AVAILABILITY

4.1 Introduction to Availability

The concept of availability has been introduced in chapter 3. The purpose of this chapter is to present a more comprehensive understanding of availability. As we known, energy is conserved and cannot be destroyed. This principle is expressed by the first law of thermodynamics. However, the second law of thermodynamics limitations, imposed on thermodynamic function called availability, not only identify energy quality but also lead to availability destruction and deterioration of energy quality.

We can see manifestations of the second law of thermodynamics every day, as it describes the direction and consequences of processes to take over things left to themselves. The second law is a rich and powerful statement of related physical observations with respect to engineering design and operation of thermal systems. It can be used to determine the direction of processes, to establish the conditions of equilibrium, to specify the maximum possible performance of thermal systems, and to identify those aspects of processes which are deteriorative to overall performance.

The method of availability analysis is particularly suited for furthering the goal of efficient energy resource use, because it enables one to determine the locations, types, and magnitudes of the waste and destruction of energy. This information can be used to design thermal systems such as internal combustion engines and to guide efforts to reduce sources of inefficiency in existing systems.

The availability concept distinguishes the energy quality or potential from its quantity. For instance, it is easy to accept that energy potential existing in the mixture of combustion products is not the same as that in the initial fuel/air mixture in an isolated system. While the energy quantity is constant as the engine cycle progresses, energy potential (quality) decreases. It is obvious that the initial fuel/air mixture would be intrinsically more useful than the final warm mixture. A precise formulation of these

Reproduced with permission of the copyright owner. Further reproduction prohibited without permission.

ideas is achieved through the property availability which takes into account both the quantity and potential of energy.

Availability can not only be destroyed by irreversibilities, but also transferred to and from a system, such as availability transfer with heat, availability transfer with exhaust, and availability transfer with work. Improved energy resource utilization can be realized by reducing availability destruction and transfer losses.

4.2 Thermomechanical and Chemical Availability

Availability can be considered as the sum of two contributions, thermomechanical and chemical availability. Availability is a measure of the potential for extracting work from the combined system at any other state than the dead state.

Thermomechanical availability is the maximum work that can be extracted from a combined system as the system passes from a given state to the restricted dead state, and comes into thermal and mechanical equilibrium with the environment in a reversible process. An example of the thermal aspect of availability is a case where the system temperature is above the environmental temperature. By utilizing an ideal heat engine, such as a Carnot engine, the availability from the system could be converted to work until the system temperature equaled the environmental temperature. An example of the mechanical aspect of availability is a system which is at a pressure above the environmental pressure. By utilizing an ideal expansion device, the energy of the system could be converted to work until the system pressure equaled the environmental pressure.

At the restricted dead state the system is in thermal and mechanical equilibrium with the environment, but not necessarily in chemical equilibrium [5]. The concentration differences between the composition of the system at the restricted dead state and that of the environment can be exploited to obtain additional work to achieve chemical equilibrium. The maximum work obtainable in this way is the chemical availability.

Reproduced with permission of the copyright owner. Further reproduction prohibited without permission.

Chemical availability, in principle, can be obtained by two means. First, environmental species, present in the system at the restricted dead state, could diffuse into the environment to produce the chemical availability. The composition of the system is assumed to be frozen, existing at certain temperature and pressure, and the system is brought to a non-equilibrium restricted dead state. Hence, further potential exists to develop work from the combined system by allowing the system to proceed to reach its composition equilibrium without exchanging mass with the environment [6]. Second, species, present in the system but not in the environment, could be allowed to enter into chemical reactions with species from the environment to produce environmental species. For example, fuel can react with air to produce environmental species. After these processes occur, the chemical potential of each specie in the system would equal its respective chemical potential in the environment, and no further interactions would be possible.

The following paragraphs summarize some important points related to the availability concept.

- Availability is a state function and an extensive thermodynamic property. The numerical value of availability depends explicitly on the choices for the ambient temperature and pressure.

- Availability is a measure of the departure of the state of control mass from that of the environment. The greater the difference between temperature and pressure at a given state and those of the environment, the greater the value for thermomechanical availability. Similarly, the greater the difference between chemical potential at a given state and that of the environment, the greater the chemical availability.

- Availability is the maximum work that can be extracted from the combined system of control mass and environment, as the control mass passes from a given state to the dead state and comes into thermal, mechanical and chemical equilibrium with the environment in a reversible process.

Reproduced with permission of the copyright owner. Further reproduction prohibited without permission.

- Unlike energy, availability is not a conservative property. When availability destruction occurs, the potential of the system to do useful work is permanently diminished. Availability destruction keeps availability below a maximum.

- For all states, availability is no less than zero.

- At the dead state, both control mass and environment possess energy, but the availability is zero.

If the system is in any state other than the dead state, it is able to change its condition spontaneously toward the dead state. This tendency ceases when the dead state is reached. No work needs to be done on the combined system for such spontaneous change.

Reproduced with permission of the copyright owner. Further reproduction prohibited without permission.

CHAPTER 5 LITERATURE REVIEW

5.1 Strong and Weak Points from Previous Work

Over two-dozen previous investigations employing the second law of thermodynamics or availability analysis with respect to internal combustion engines have been identified [7]. These previous investigations have used thermodynamic cycle simulations, experimental data, or a combination of simulations and experiments. The majority of them were completed for CI engines. Only 9 related to SI engines, such as van Gerpen and Shapiro [8] who extended their earlier work to include SI engines cycle simulation in 1989, and Caton [9] who examined the effects of operating characteristics on SI engines using the second law analysis in 2000. However, still fewer are for alternative fuel research in SI engines.

These previous work is summarized in a chronological order in Table 5-1. Comments on their unique points and limitation of their research are also presented.

Table 5-1 Summary of previous work (Part 1)

Date	Researchers	Engine	Comments
1957	Traupel [4]	CI	Availability calculations were based on measured energy terms. Availability destruction due to combustion process was considered, as well as losses related to cooling, exhaust, mechanical, and aerodynamic processes.
1964	Patterson and van Wylen [4]	SI	It was a pioneering work of thermodynamic cycle simulation for SI engine. Some of the simplifications included: idealized induction and exhaust processes; compression process was assumed adiabatic.
1976	Clarke [4]	SI/CI	Clarke suggested strategies to achieve minimum destruction of availability.
1984	Edo and Foster [4]	SI & dissociated methanol	A simple Otto cycle with an instantaneous heat release was used in availability analysis. The use of dissociated methanol was motivated by the potential to capture the exhaust energy. No intake or exhaust processes were considered.
1984	Flynn et al. [15]	CI	Thermodynamic cycle simulation was used to obtain the availability balance, including fuel availability, irreversibility, availability associated

Reproduced with permission of the copyright owner. Further reproduction prohibited without permission.

			with heat and work, for a given engine cycle.
1984	Primus [4]	CI	This was a companion study to Flynn's work. It focused on exhaust system optimization.
1984	Primus [4]	CI	This was another continuation of earlier Flynn's work. They used the second law to assess the benefits of turbocharging, insulating techniques, and etc.
1985	Primus and Flynn [4]	CI	It was the other continuation of their earlier work. They examined the effects of engine parameters, such as engine speed, load, compression ratio, intake air temperature, injection timing and heat release rate, on thermodynamic processes of the engine operation.
1986	Primus and Flynn [12]	CI	As a further study, they focused on itemizing the various loss mechanisms associated with a CI engine.
1987 & 1990	Van Gerpen and Shapiro [6]	CI	The second law with a thermodynamic cycle simulation was used. Simplifications included: only compression and expansion strokes were considered; the initial conditions were assumed to be ambient conditions. In contrast to previous investigations, availability of "chemical component[2]" was included.
1988 & 1989	Alkidas [16,17]	CI	This work was different from others in two major ways. First, Alkidas defined the thermodynamic system as outside the cylinder. Second, he used experimental measurements of energy rejected to the coolant and lubricating oil; of the brake work, and of the air and fuel flow rates. The availability calculations were based on the measured values.
1988	McKinley and Primus [4]	CI	They described an assessment of a number of turbocharging systems from both first law and second law perspective.
1989	Kumar et al. [18]	CI	They used a complete simulation model, but only preliminary results were in their report.
1989	Lipkea and DeJoode [19]	CI	Both experimental and simulation results were used to assess the CI engine. They completed availability analysis for various engine components, such as turbocharger, intercooler, manifolds, and cylinder.
1989	Shapiro and van Gerpen [8]	SI & CI	They extended their earlier work to include a two-zone combustion model in both CI and SI engines. No intake and exhaust processes were considered. They presented that time-resolved availability values, varying with engine parameters.

[2] The "chemical component" refers to the potential to do work due to the species concentrations relative to the concentrations in the surroundings. It is different from fuel chemical availability, because fuel does not originally exist in the environment.

Reproduced with permission of the copyright owner. Further reproduction prohibited without permission.

Table 5-1 Summary of previous work (Part 2)

Date	Researchers	Engine	Comments
1991	Bozza et al. [4]	CI	They used experimental measurements to for heat release and flow expression simulation.
1992	Gallo and Milanez [20]	SI (ethanol & gasoline)	Cycle simulation was used to determine the instantaneous irreversibilities. They found that ethanol provided more effective use of fuel energy than gasoline.
1992	Al-Najem and Diab [4]	CI	They presented brief results about availability destruction, combustion, exhaust to ambient, relative to the fuel availability.
1993	Rakopoulos [21]	SI	Engine cycle simulation and experiment were used for SI engine. No intake and exhaust strokes were considered. They discussed possible ways for improving engine cycle performance.
1993	Rakopoulos and Andritsakis [22]	CI	They used experimental information to determine the fuel burn rate, and then calculated availability and the irreversibilities rate.
1993	Rakopoulos et al. [4]	CI	They completed their earlier experiments, and then computed the related second law quantities including irreversibility. Only compression and expansion strokes were studied. They completed this work for a range of speeds and loads.
1997	Rakopoulos and Giakoumis [23]	CI	They used cycle simulation to assess the engine performance over a range of engine speeds, loads, and compression ratios. A number of engine sub-assemblies, such as compressor, turbine, inlet and exhaust system, were also studied.
1997	Rakopoulos and Giakoumis [4]	CI	They used engine cycle simulation to study energy and exergy performance of a CI engine under stead-state and transient conditions.
1997	Alssfour [4]	SI (gasoline & 30% butanol-gasoline blend)	The availability analysis was completed for a single cylinder SI engine. The majority of this work was an experimental study of the energy terms. Then Alssfour used these results to determine the related second law quantities.
1997	Rakopoulos and Giakoumis [4]	CI	They described the engine cycle simulation, including both closed valve and open valve portions, to assess the availability balance for a CI engine.
1998	Anderson et al. [24]	SI	They studied a naturally aspirated Miller cycle SI engine using late intake valve closure. Using a quasi-dimensional engine cycle simulation, they compared the Miller cycle with a conventional SI engine.

Reproduced with permission of the copyright owner. Further reproduction prohibited without permission.

Table 5-1 Summary of previous work (Part 3)

Date	Researchers	Engine	Comments
1999, 2000	Caton [7,9,25,26,27]	SI	The work was based on the complete thermodynamic cycle simulation. He examined the effects of engine load and speed on the engine performance, energy and availability terms.
2001	Rakopoulos and Kyritsis [28]	CI	They studied the effects of engine parameters, such as engine speed, injection timing, and fuel composition, on CI engine operation. Experimental data were used to determine the fuel reaction rate. A method of analytic calculation of various terms in availability balance was presented. They examined the use of alternative fuel for increased second law efficiency.

5.2 Summary

The earlier availability analysis work was mainly based on the measured energy terms. Pioneering thermodynamic engine cycle simulations was limited by using simple assumptions and approximations such as using Otto cycle with instantaneous heat release models for SI engine simulations. Since the mid-1980s, the complete availability balance with comprehensive cycle simulation has been reported for CI engines. While most of the previous work has related to conventional engine research, fewer studies have included non-conventional characteristics. These non-conventional characteristics included the use of alternative fuels, such as butanol, ethanol and methanol, and a Miller cycle engine. Recently, engine researchers have been more and more concerned with the effects of various engine parameters and alternative fuels on the availability analysis.

Reproduced with permission of the copyright owner. Further reproduction prohibited without permission.

CHAPTER 6 METHODOLOGY AND PROCEDURE

As far as methodology is concerned, all engine simulations, from the simplest constant-volume and constant-pressure ideal cycle approximations to the most complex fluid-dynamic-based multidimensional simulations, require models for:

- Compositions and thermodynamic properties for in-cylinder mixture
- The individual processes, such as intake, compression, combustion, expansion, and exhaust.

The compositions for the unburned mixture during the compression process do not change significantly, and it is sufficiently accurate to assume its composition is frozen or unchanged. The combustion products or the burned mixture during the combustion process and the expansion process are in thermodynamic equilibrium.

One-dimensional thermodynamic-based models, based on energy conservation and the availability analysis, have been developed without considering the flow modeling or the geometric features of the fluid motion. Through availability analysis, the processes where destruction or losses occur can be identified and ranked in order. This knowledge can be used in the design of internal combustion engines and to guide efforts to reduce sources of inefficiency and find opportunities for improvement in existing systems. The finite heat release model or the mass fraction burned model is used to simulate the combustion process. Only compression, combustion, and expansion processes are simulated in the current study.

Point of departure in this thesis is a series of programs (called the Ferguson models), which simulate engine cycles from the energy balance and the first law point of view. Then, these programs were rewritten and modified to include associated availability calculations.

Reproduced with permission of the copyright owner. Further reproduction prohibited without permission.

The procedure and pathway in this work are presented in Figure 6.1.

- The dashed arrows indicate the simulations that follow the original Ferguson models.
- The solid arrows represent the availability simulations that have been added and applied with various levels of complexity.

Figure 6.1 is followed by detailed descriptions of components used in the current methodology and procedure for SI engine cycle simulations in this thesis.

Reproduced with permission of the copyright owner. Further reproduction prohibited without permission.

Reproduced with permission of the copyright owner. Further reproduction prohibited without permission.

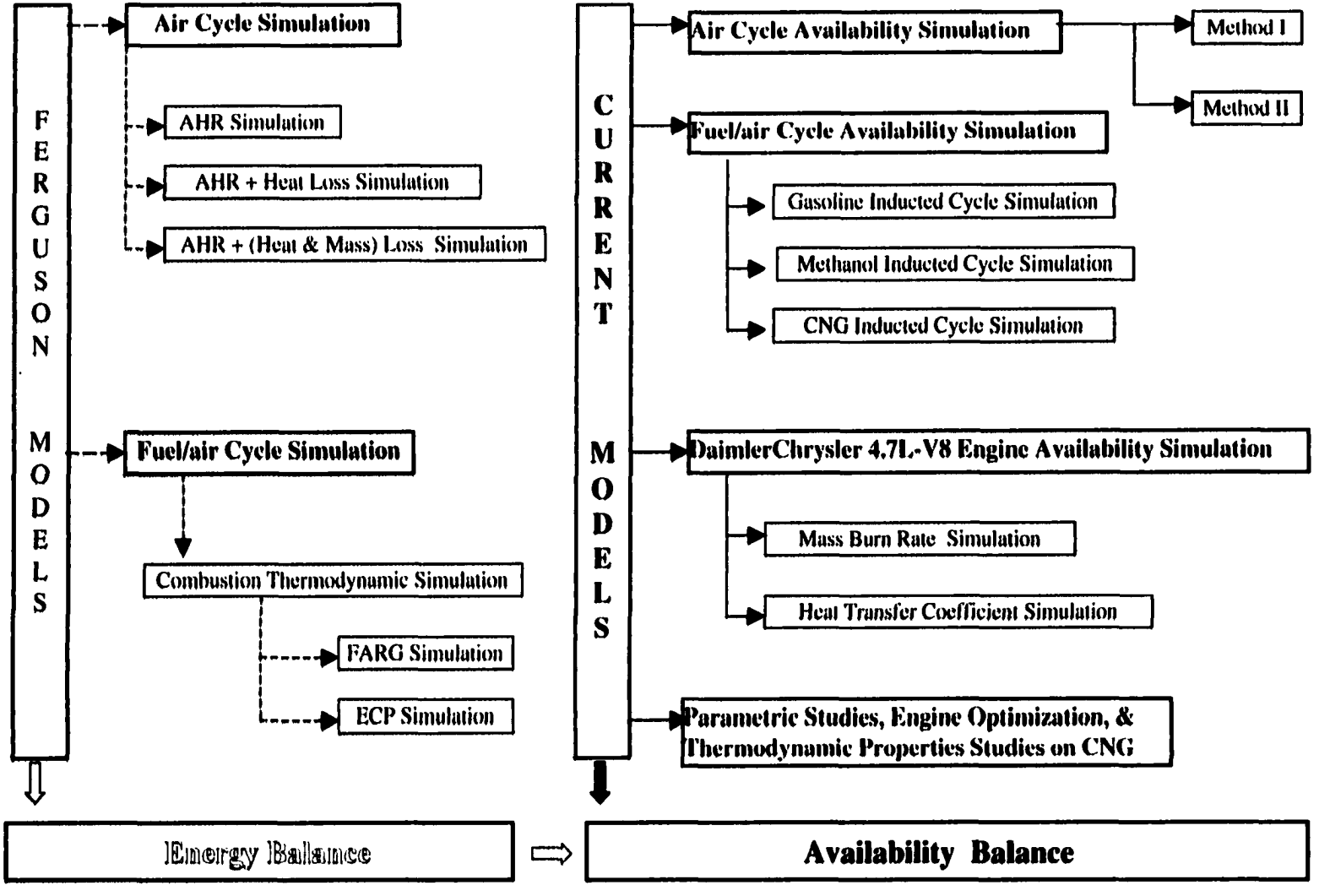

Figure 6.1 The procedure of the current study.

6.1 Compositions and Thermodynamic Properties for In-Cylinder Mixtures

The compositions of the in-cylinder mixtures during the compression, combustion and expansion processes are indicated in Table 6-1.

Table 6-1 In-cylinder mixture constituents

Process	Spark Ignition Engines
Compression	Air (O_2 and N_2) Fuel (gasoline, CNG, and methanol) Residual gas (N_2,CO_2,H_2O,O_2,CO,H_2,NO,OH,O and H)
Combustion and Expansion	Combustion products ($\Phi < 1$) mixture of N_2,H_2O,CO_2,O_2,NO,OH,O,and H ($\Phi > 1$) mixture of N_2,H_2O,CO_2,CO,H_2,NO,OH,O,and H

The computer subroutines, namely as fuel-air-residual gas (FARG) and equilibrium combustion products (ECP), are used for predicting compositions and thermodynamic properties for unburned and burned mixtures.

The computer models are based on curve fits to the thermodynamic properties data for elements, combustion products, and many pollutants in a compilation published by the National Bureau of Standards, called the JANAF tables (1971). For the engine cycle simulation of each species in the mixture, assumptions are made as (1) the unburned mixture is frozen in composition and (2) the burned mixture is in equilibrium. The thermodynamic quantities of the specific heat, enthalpy, and entropy as functions of temperature are curve fitted to polynomials by minimizing the least-squares error:

$$\frac{c_P}{R} = a_1 + a_2 T + a_3 T^2 + a_4 T^3 + a_5 T^4 \tag{6.1}$$

$$\frac{h}{RT} = a_1 + \frac{a_2}{2} T + \frac{a_3}{3} T^2 + \frac{a_4}{4} T^3 + \frac{a_5}{5} T^4 + \frac{a_6}{T} \tag{6.2}$$

$$\frac{s^0}{R} = a_1 \ln T + a_2 T + \frac{a_3}{2} T^2 + \frac{a_4}{3} T^3 + \frac{a_5}{4} T^4 + a_7 \tag{6.3}$$

Reproduced with permission of the copyright owner. Further reproduction prohibited without permission.

Usually two sets of coefficients are used for two adjacent temperature ranges, which are 300K to 1000K and 1000K to 4000K. The temperature range from 300K to 1000K is appropriate for compositions and properties of the unburned mixture simulations, while the temperature range from 1000K to 4000 K is appropriate for those of the burned mixture property calculations.

For fuels, the thermodynamic quantities of the specific heat, enthalpy, and entropy as functions of temperature are curve fitted in the forms:

$$\frac{c_P}{R} = a_0 + b_0 T + c_0 T^2 \tag{6.4}$$

$$\frac{h}{RT} = a_0 + \frac{b_0}{2} T + \frac{c_0}{3} T^2 + \frac{d_0}{T} \tag{6.5}$$

$$\frac{s^0}{R} = a_0 \ln T + b_0 T + \frac{c_0}{2} T^2 + e_0 \tag{6.6}$$

The tables of coefficients of CO_2, H_2O, CO, H_2, O_2, N_2, OH, NO, O, H in the temperature range from 300K to 4000K and different fuels in the temperature range from 300K to 1000K are given in Appendix B.

The inputs of the FARG and ECP subroutines are temperature, pressure, fuel/air equivalence ratio, and residual gas fraction. The programs calculate the following:

- Thermodynamic properties: h, u, s, v, c_p, $(\partial \ln V / \partial \ln p)_T$, and $(\partial \ln V / \partial \ln T)_p$
- Equilibrium compositions: mole fractions of major species which are fuel, O_2, N_2, CO_2 and H_2O, and minor species which are CO, OH, H_2, NO, H and O.

The detailed descriptions of FARG and ECP subroutines are given in the following sections.

Reproduced with permission of the copyright owner. Further reproduction prohibited without permission.

6.1.1 Fuel-Air-Residual Gas (FARG) Simulation

A chemical formula of a fuel as $C_\alpha H_\beta O_\gamma N_\delta$. Fuel/air equivalence ratio is defined as the actual fuel/air ratio divided by the stoichiometric fuel/air ratio

$$\Phi = F/F_S \tag{6.7}$$

If $\Phi < 1$, it is called a lean mixture. If $\Phi > 1$, it is called a rich mixture. If $\Phi = 1$, the mixture is said to be stoichiometric.

The molar fuel/air ratio is defined as ε. Therefore, the gravimetric fuel/air ratio at stoichiometric condition is

$$F_S = \frac{\varepsilon\,(12.01\alpha + 1.008\beta + 16.00\gamma + 14.01\delta)}{28.85} \tag{6.8}$$

Consider combustion of a fuel $C_\alpha H_\beta O_\gamma N_\delta$ with air. If the products of combustion are limited to CO_2, CO, H_2O, H_2, O_2, and N_2, the generalized combustion equation with air can be written as

$$\varepsilon\Phi C_\alpha H_\beta O_\gamma N_\delta + (0.21O_2 + 0.79N_2) \rightarrow \upsilon_1 CO_2 + \upsilon_2 H_2O + \upsilon_3 N_2 + \upsilon_4 O_2 + \upsilon_5 CO + \upsilon_6 H_2 \tag{6.9}$$

Four atomic balances can be written:

C balance: $\varepsilon\Phi\alpha = \upsilon_1 + \upsilon_5$ (6.10)

H balance: $\varepsilon\Phi\beta = 2\upsilon_2 + 2\upsilon_6$ (6.11)

O balance: $\varepsilon\Phi\gamma + 2(0.21) = 2\upsilon_1 + \upsilon_2 + 2\upsilon_4 + \upsilon_5$ (6.12)

N balance: $\varepsilon\Phi\delta + 2(0.79) = 2\upsilon_3$ (6.13)

Reproduced with permission of the copyright owner. Further reproduction prohibited without permission.

With six unknowns and only four simultaneous equations, two further equations are required. A simplification is to assume no oxygen in the products of rich combustion, and no hydrogen or carbon monoxide in the products of lean combustion.

Rich mixtures ($\Phi > 1$): $\upsilon_5 = 0$ (6.14)

Lean mixtures ($\Phi < 1$): $\upsilon_5 = \upsilon_6 = 0$ (6.15)

Stoichiometric mixtures ($\Phi = 1$): $\upsilon_4 = \upsilon_5 = \upsilon_6 = 0$ (6.16)

For lean or stoichiometric cases, there are four equations for four unknowns, which are $\upsilon_1, \upsilon_2, \upsilon_3, \upsilon_4$. The atomic balance equations are sufficient to determine the product compositions.

For rich mixtures, there are four atomic balance equations for five unknowns, which are $\upsilon_1, \upsilon_2, \upsilon_3, \upsilon_4, \upsilon_6$. A further equation is required. It is provided by the water gas equilibrium:

$$CO_2 + H_2 \Leftrightarrow CO + H_2O \tag{6.17}$$

for which the equilibrium constant is K_P :

$$K_P = \frac{\upsilon_2 \upsilon_5}{\upsilon_1 \upsilon_6} \tag{6.18}$$

Simultaneous solutions of equations from (6.9) to (6.16) and (6.18) yield the results for lean or rich mixtures, which are summarized in Table 6.2.

Reproduced with permission of the copyright owner. Further reproduction prohibited without permission.

Table 6-2 Combustion products

No.	Species	$\Phi \le 1$	$\Phi > 1$
1	CO_2	$\varepsilon\Phi\alpha$	$\varepsilon\Phi\alpha - \upsilon_5$
2	H_2O	$\varepsilon\Phi\beta/2$	$0.42 - \varepsilon\Phi(2\alpha-\gamma) + \upsilon_5$
3	N_2	$0.79 + \varepsilon\Phi\delta/2$	$0.79 + \varepsilon\Phi\delta/2$
4	O_2	$0.21(1-\Phi)$	0
5	CO	0	υ_5
6	H_2	0	$0.42(\Phi-1) - \upsilon_5$

With compositions known, the simulations of thermodynamic properties, such as enthalpy, entropy, specific volume, specific heats and internal energy, can consequently be computed by FARG subroutine.

6.1.2 Equilibrium Combustion Products (ECP) Simulation

In general, the chemical reaction equation for equilibrium combustion products is

$$\begin{aligned}\varepsilon\Phi C_\alpha H_\beta O_\gamma N_\delta + 0.21O_2 + 0.79N_2 \rightarrow\ & \upsilon_1 CO_2 \\ & + \upsilon_2 H_2O + \upsilon_3 N_2 + \upsilon_4 O_2 + \upsilon_5 CO + \upsilon_6 H_2 \\ & + \upsilon_7 H + \upsilon_8 O + \upsilon_9 OH + \upsilon_{10} NO + \upsilon_{11} N + \upsilon_{12} C(s) \\ & + \upsilon_{13} NO_2 + \upsilon_{14} CH_4 + \ldots\end{aligned} \tag{6.19}$$

While the computational time involved in full equilibrium program is substantial, the simple equilibrium combustion products programs, such as ECP, have been developed. The species of importance because of dissociation are O, H, OH, and NO, when equivalence ratio is less than 3. The species in Eq. (6.19) can be reduced to 10 species for equilibrium combustion products simulation, described in Eq. (6.20). This limited set of species has been found to be sufficiently accurate for engine burned gas calculations [10].

Reproduced with permission of the copyright owner. Further reproduction prohibited without permission.

$$\varepsilon\Phi C_\alpha H_\beta O_\gamma N_\delta + 0.21O_2 + 0.79N_2 \rightarrow \upsilon_1 CO_2 + \upsilon_2 H_2O + \upsilon_3 N_2 + \upsilon_4 O_2 + \upsilon_5 CO + \upsilon_6 H_2 + \upsilon_7 H + \upsilon_8 O + \upsilon_9 OH + \upsilon_{10} NO \tag{6.20}$$

Atom balancing yields the following four equations:

C balance: $$\varepsilon\Phi\alpha = (y_1 + y_5)N \tag{6.21}$$

H balance: $$\varepsilon\Phi\beta = (2y_2 + 2y_6 + y_7 + y_9)N \tag{6.22}$$

O balance: $$\varepsilon\Phi\gamma + 0.42 = (2y_1 + y_2 + 2y_4 + y_5 + y_8 + y_9 + y_{10})N \tag{6.23}$$

N balance: $$\varepsilon\Phi\delta + 1.58 = (2y_3 + y_{10})N \tag{6.24}$$

$$N = \sum_{i=1}^{10} \upsilon_i \tag{6.25}$$

Where N is the total number of moles. By definition, the following can be written

$$\sum_{i=1}^{10} y_i - 1 = 0 \tag{6.26}$$

Introduction of the following six equilibrium constants and Eq. (6.26) will yield eleven equations for the ten unknown mole fractions y_i and the number of moles N.

$$\frac{1}{2}H_2 \Leftrightarrow H \qquad K_1 = \frac{y_7 P^{1/2}}{y_6^{1/2}} \tag{6.27}$$

$$\frac{1}{2}O_2 \Leftrightarrow O \qquad K_2 = \frac{y_8 P^{1/2}}{y_4^{1/2}} \tag{6.28}$$

$$\frac{1}{2}H_2 + \frac{1}{2}O_2 \Leftrightarrow OH \qquad K_3 = \frac{y_9}{y_4^{1/2} y_6^{1/2}} \tag{6.29}$$

$$\frac{1}{2}O_2 + \frac{1}{2}N_2 \Leftrightarrow NO \qquad K_4 = \frac{y_{10}}{y_4^{1/2} y_3^{1/2}} \tag{6.30}$$

Reproduced with permission of the copyright owner. Further reproduction prohibited without permission.

$$H_2 + \frac{1}{2}O_2 \Leftrightarrow H_2O \qquad K_5 = \frac{y_2}{y_4^{1/2} y_6 P^{1/2}} \tag{6.31}$$

$$CO + \frac{1}{2}O_2 \Leftrightarrow CO_2 \qquad K_6 = \frac{y_1}{y_5 y_4^{1/2} P^{1/2}} \tag{6.32}$$

This method is simple when considering the restricted species as the present case. With the compositions known, the computations of thermodynamic properties in ECP subroutine, such as enthalpy, entropy, specific volume, specific heats, and internal energy, can be executed subsequently.

6.2 Thermodynamic Engine Cycle Simulations

6.2.1 Ferguson Models

The governing equations for Ferguson models [2] are based on the first law. The simulations do not include availability calculations, but other thermodynamic properties, such as pressure, temperature, specific internal energy, specific enthalpy, and specific entropy calculations. These models include: air cycle and fuel/air cycle simulations.

- **Air Cycle Simulation**

The study of air cycle models for internal combustion engines is to illustrate some of the basic but crucial parameters which influence engine performance. Simple constant volume Otto cycle or constant pressure Diesel cycle models do not match the actual engine pressure and temperature data. A more realistic air cycle model, namely as arbitrary (finite) heat release model, is built in to simulate heat release process. By modeling combustion process as a heat release process, the analysis is simplified so that details of the physics and chemistry of combustion will not be required. The Air cycle simulations include (1) Arbitrary Heat Release (AHR), where there is heat addition described as a function of crank angle; (2) Arbitrary Heat Release with Heat Loss (AHR-HL), where the total heat transfer is interpreted as the heat addition due to combustion and heat loss by in-cylinder gases due to convection; (3) Arbitrary Heat Release with

Reproduced with permission of the copyright owner. Further reproduction prohibited without permission.

Heat Loss and Mass Loss (AHR-HML), where both heat loss and mass leakage during compression, heat release and expansion processes are simulated.

- **Fuel/air Cycle Simulation**

The fuel/air cycle simulations combine the models of mass of fuel burned with the models of in-cylinder mixture properties (a frozen mixture for the unburned mixture and an equilibrium mixture for the burned mixture), and provide more quantitative information on engine operation. The Ferguson fuel/air cycle models include a four-stroke Otto fuel/air cycle simulation, with isentropic compression of in-cylinder mixtures, adiabatic and isometric combustion, isentropic expansion of equilibrium combustion products, and ideal intake and exhaust processes. The fuel/air cycle also includes fuel inducted SI engine and fuel injected CI engine simulations.

6.2.2 Current Models: Air Cycle Availability Simulation

- **Development of Governing Equations**

The air cycle thermomechanical availability simulation starts at the bottom dead center (-180°) where both the inlet and exhaust valves are closed, and ends at the bottom dead center (180°) where the exhaust valve begins to open. The whole cycle simulation includes the compression, heat release, and expansion processes. The simulated in-cylinder working content is air, which is viewed as an ideal gas within the simulation.

The equation of state for an ideal gas is

$$pV = mRT \tag{6.33}$$

For fixed rotational speed of the crankshaft, the time derivatives can be written in terms of the change in crank angle $d\theta$.

Reproduced with permission of the copyright owner. Further reproduction prohibited without permission.

As blowby happens, mass in the cylinder is no longer constant. Mass is transferred from the cylinder to the crankcase. Taking the logarithm of both sides of Eq. (6.33) and differentiating with respect to crank angle gives

$$\frac{1}{p}\frac{dp}{d\theta}+\frac{1}{V}\frac{dV}{d\theta}=\frac{1}{m}\frac{dm}{d\theta}+\frac{1}{T}\frac{dT}{d\theta} \tag{6.34}$$

For this air cycle simulation, it is convenient to assume that the specific heats of the cylinder contents are constant. Modification of specific heats changing with temperature for the air cycle simulation will be described in the following section. For both the air cycle and the fuel/air cycle simulations, kinetic and potential energies are neglected for SI engine development. Therefore, the first law of thermodynamics in a differential form gives

$$mc_v\frac{dT}{d\theta}+c_vT\frac{dm}{d\theta}=\frac{dQ}{d\theta}-p\frac{dV}{d\theta}-\frac{\dot{m}_l c_pT}{\omega} \tag{6.35}$$

Where ω is the engine speed in revolution per second (rad/s), $\dot{m}_l$ is the instantaneous leakage or blowby rate and is assumed to be always out of the cylinder and taking with it energy which can be characterized by enthalpy of the cylinder contents, c_pT.

Dividing the left-hand side by mRT and the right-hand side by PV, and rearranging Eq.(6.35) yields

$$\frac{1}{T}\frac{dT}{d\theta}+\frac{1}{m}\frac{dm}{d\theta}=(\gamma-1)\left(\frac{1}{pV}\frac{dQ}{d\theta}-\frac{1}{V}\frac{dV}{d\theta}-\frac{\dot{m}_l c_pT}{\omega pV}\right) \tag{6.36}$$

Combining the differential forms of ideal gas state equation Eq. (6.34) and first law of thermodynamics (6.36) gives

Reproduced with permission of the copyright owner. Further reproduction prohibited without permission.

$$\frac{dp}{d\theta} = -\gamma \frac{p}{V}\frac{dV}{d\theta} + \frac{(\gamma - 1)}{V}\frac{dQ}{d\theta} - \frac{\gamma \dot{m}_l}{\omega m} \tag{6.37}$$

The differential equation of continuity for mass conservation gives

$$\frac{dm}{d\theta} = -\frac{\dot{m}_l}{\omega} \tag{6.38}$$

Introducing constant C, $C = \dot{m}_l / m$. It is a strong function of ring design and varies considerably from engine to engine. The value of C is chosen as 0.8 /s in the simulation, so that it is about 2.5% of the charge is lost, consistent with the observation from real engine operations.

Both heat addition due to heat release into the system and heat loss by the in-cylinder mixture because of convection have been considered.

$$\frac{dQ}{d\theta} = Q_{in}\frac{dx}{d\theta} - \frac{dQ_l}{d\theta} \tag{6.39}$$

From the definition of heat transfer due to convection, the heat loss is expressed as:

$$\frac{dQ_l}{d\theta} = \mathbf{h}\, A_{surface}(T - T_w) \tag{6.40}$$

In practice, it is convenient to normalize the equations by the initial conditions.

$$\tilde{p} = p/p_1 \qquad \tilde{V} = V/V_1 \qquad \tilde{Q} = Q_{in}/p_1V_1$$

$$\tilde{T} = \frac{T}{T_1} \qquad \tilde{Q}_l = \frac{Q_l}{p_1V_1} \qquad \tilde{m} = \frac{m}{m_1}$$

$$\tilde{\mathbf{h}} = \frac{\mathbf{h}T_1(A_0 - 4V_0/b)}{p_1V_1\omega} \qquad \beta = \frac{4V_1}{b(A_0 - 4V_0/b)} \tag{6.41}$$

Reproduced with permission of the copyright owner. Further reproduction prohibited without permission.

The normalized volume V is simulated by an empirical function of compression ratio and crank angles.

$$\tilde{V} = \left[1 + \frac{r-1}{2}(1-\cos\theta)\right] \Big/ r \tag{6.42}$$

An empirical function is used to simulate heat release with parameters θ_s , θ_b and n, which are defined by curve fit to the experimental data.

$$x = 1 - \exp\left[-\left(\frac{\theta - \theta_s}{\theta_b}\right)^n\right] \tag{6.43}$$

Combining Eq. from (6.37 to (6.41) gives

$$\frac{d\tilde{p}}{d\theta} = -\gamma \frac{\tilde{p}}{\tilde{V}} \frac{d\tilde{V}}{d\theta} + \frac{(\gamma-1)}{\tilde{V}}\left[\tilde{Q}\frac{dx}{d\theta} - \tilde{\mathbf{h}}(1+\beta\tilde{V})(\tilde{p}\tilde{V}/\tilde{m} - \tilde{T}_w)\right] - \frac{\gamma C \tilde{p}}{\omega} \tag{6.44}$$

$$\frac{d\tilde{W}}{d\theta} = \tilde{p}\frac{d\tilde{V}}{d\theta} \tag{6.45}$$

$$\frac{d\tilde{Q}_l}{d\theta} = \tilde{\mathbf{h}}(1+\beta\tilde{V})(\tilde{p}\tilde{V}/\tilde{m} - \tilde{T}_w) \tag{6.46}$$

$$\frac{d\tilde{m}}{d\theta} = -\frac{C\tilde{m}}{\omega} \tag{6.47}$$

The Equations from (6.44) to (6.47) are a set of linear first-order differential equations, which can be simultaneously integrated for air cycle simulation.

Reproduced with permission of the copyright owner. Further reproduction prohibited without permission.

- **Development of Air Cycle Thermomechanical Availability Balance**

The thermomechanical availability calculations are added to the air cycle simulation programs, and explored in two different ways.

The availability balance equation can be developed from the energy and entropy balances. The differential forms of the energy and entropy equations are respectively

$$\frac{dU}{d\theta} = \frac{dQ}{d\theta} - \frac{dW}{d\theta} \tag{6.48}$$

$$\frac{dS}{d\theta} = \frac{1}{T}\frac{dQ}{d\theta} + \sigma' \tag{6.49}$$

Adding the term $p_0\, dV/d\theta$ to both sides of Eq. (6.48), multipying Eq. (6.49) by T_0, and subtracting the two resulting expressions give the thermomechanical availability in Eq. (6.50).

$$\frac{dU}{d\theta} + p_0\frac{dV}{d\theta} - T_0\frac{dS}{d\theta} = (1-\frac{T_0}{T})\frac{dQ}{d\theta} - (\frac{dW}{d\theta} - p_0\frac{dV}{d\theta}) - T_0\sigma' \tag{6.50}$$

- **Method I**

The objective of the Method I is to evaluate the theoretical maximum thermomechanical availability, without considering the irreversibilities effects, $T_0\sigma'$. In the Method I, thermomechanical availability is modified from the right hand side of Eq. (6.50).

For the current air cycle simulations for SI engines, the in-cylinder contents at the beginning of compression process have been viewed as a control mass, because both intake and exhaust valves are closed and there is no mass exchange. If the control mass is in any state other than the restricted dead state, it is able to change its condition

Reproduced with permission of the copyright owner. Further reproduction prohibited without permission.

spontaneously toward the restricted dead state through heat and /or work interactions with the environment.

Whether the control mass is heated or cooled from its initial dead state, its final state has associated with it a positive value for availability, because its temperature differs from that of the environment. Thus, an increase in availability is realized by heating to increase temperature from T_0 to T, or by cooling to decrease the temperature from T_0 to T. The differential form for the flow of availability associated with the heat transfer at the final state is given as follows.

$$\frac{dA_Q}{d\theta} = (1 - \frac{T_0}{T}) \cdot \frac{dQ}{d\theta} \tag{6.51}$$

To evaluate availability associated with work interaction, a convenient choice is an adiabatic process. Thus, the differential form of availability transfer associated with work of the combined system can be expressed as follows:

$$\frac{dA_W}{d\theta} = -(\frac{dW}{d\theta} - p_0 \frac{dV}{d\theta}) \tag{6.52}$$

Normalizing Eq. (6.51) and Eq. (6.52) by inputting Eq. (6.41) and defining the following terms:

$$\tilde{A} = A/p_i V_i \qquad \tilde{T}_0 = T_0/T_i \qquad \tilde{p}_0 = p_0/p_i \tag{6.53}$$

Therefore, the normalized maximum thermomechanical availability, which is the sum of the heat and work interaction terms, is expressed in the following differential equation form:

$$\frac{d\tilde{A}}{d\theta} = (1 - \frac{\tilde{T}_0}{\tilde{T}}) \frac{d\tilde{Q}}{d\theta} - (\frac{d\tilde{W}}{d\theta} - \tilde{p}_0 \frac{d\tilde{V}}{d\theta}) \tag{6.54}$$

Reproduced with permission of the copyright owner. Further reproduction prohibited without permission.

- **Method II**

In the Method II, the thermomechanical availability is calculated from the left hand side of Eq. (6.50). The differential form is shown here.

$$\frac{dA}{d\theta}=\frac{dU}{d\theta}+p_0\frac{dV}{d\theta}-T_0\frac{dS}{d\theta} \tag{6.55}$$

Since the ideal gas model has been used in this air cycle analysis, the two constant ideal gas specific heats can be derived from the universal gas constant and the specific heat ratio.

$$c_v=\frac{R}{\gamma-1} \qquad\qquad c_p=\frac{\gamma R}{\gamma-1} \tag{6.56}$$

Therefore, the thermomechanical availability is as follows:

$$\frac{dA}{d\theta}=c_v\frac{dT}{d\theta}+R\frac{dT}{d\theta}-T_0\left(\frac{c_p}{T}\frac{dT}{d\theta}-\frac{R}{p}\frac{dp}{d\theta}\right) \tag{6.57}$$

The Method II takes into account both the availability transfers associated with heat and work interaction, and the availability destruction in engine cycle simulation.

Reproduced with permission of the copyright owner. Further reproduction prohibited without permission.

6.2.3 Current Models: Fuel/Air Cycle Availability Simulation

In the fuel/air cycle analysis, the combustion process is simulated as a fuel is burned to produce work, rather than addition heat being released. Therefore, thermomechanical and fuel chemical availability need to be simulated in the fuel/air cycle simulation.

The compression, combustion and expansion processes are studied in the fuel/air cycle simulation. The simulation begins at bottom dead center (-180°), where the intake and exhaust valves are both closed and the cylinder contains a homogeneous gas mixture of air, fuel and residual gases. The mixture is compressed until the initiation of combustion happens at a certain crank angle. Combustion results in the creation of a second zone that is assumed to consist of the equilibrium combustion products.

A two-zone combustion model is used so that the burned and unburned mixtures are analyzed separately. The burned zone consists of the equilibrium products of combustion, and the unburned zone contains a homogeneous gas mixture of air, fuel and residual gases. The rate at which mass is transferred from the unburned gas zone to the burned gas zone, the burning rate, is expressed as a sinusoidal function of crank angle, with parameters that allow to specify the sparking timing and combustion duration. Upon the completion of combustion, the product gases continue to expand to the bottom dead center (180°) till the exhaust valve opens.

The specific heats are simulated with respect to temperature in FARG and ECP subroutines, instead of fixing at constant values. As mentioned in the previous section, the specific heats for different components in fuel-air-residual gas mixture and equilibrium combustion products are curved fitted to polynomials functions. In addition, the simulations of specific internal energy, specific enthalpy, specific entropy, specific volume and mixture compositions will depend on the inputs of temperature, pressure, equivalence ratio, and residual gas fraction in the FARG and ECP programs.

Reproduced with permission of the copyright owner. Further reproduction prohibited without permission.

- **Development of Governing Equations**

Engine cycle simulation starts at bottom dead center, the cylinder is filled with homogeneous fuel, air and residual gas mixture. The whole engine cycle simulation includes compression, combustion and expansion processes.

A differential form of the energy conservation equation according to the first law is as follows:

$$m\frac{du}{d\theta}+u\frac{dm}{d\theta}=\frac{dQ}{d\theta}-p\frac{dV}{d\theta}-\frac{\dot{m}_l h_l}{\omega} \tag{6.58}$$

The in-cylinder mixtures in SI engines have internal energy, enthalpy, specific heats and entropy dependent upon temperature and pressure programmed into the subroutines FARG which is used for compression process simulation, and ECP which is used for combustion and expansion simulations.

The specific internal energy of the system is assumed to be

$$u=\frac{U}{m}=xu_b+(1-x)u_u \tag{6.59}$$

where x is the mass fraction of the cylinder contents which have been burned, u_b is the specific internal energy of the burned gas at a temperature T_b, and u_u is the specific internal energy of the unburned gas at a temperature T_u.

Likewise, the specific volume of the system is given by

$$v=\frac{V}{m}=xv_b+(1-x)v_u \tag{6.60}$$

Reproduced with permission of the copyright owner. Further reproduction prohibited without permission.

The state equation for ideal gases states that v_b is a function of T_b and p as

$$v_b = v_b(T_b, p) \tag{6.61}$$

The differential form of Eq. (6.61) with respect to crank angle is

$$\frac{dv_b}{d\theta} = \frac{\partial v_b}{\partial T_b}\frac{dT_b}{d\theta} + \frac{\partial v_b}{\partial p}\frac{dp}{d\theta} \tag{6.62}$$

The ECP subroutine is programmed to return the requisite partial derivatives in logarithmic form. Substitution of the logarithmic derivatives into Eq. (6.62) yields

$$\frac{dv_b}{d\theta} = \frac{v_b}{T_b}\frac{\partial \ln v_b}{\partial \ln T_b}\frac{dT_b}{d\theta} + \frac{v_b}{p}\frac{\partial \ln v_b}{\partial \ln p}\frac{dp}{d\theta} \tag{6.63}$$

By analogy

$$\frac{dv_u}{d\theta} = \frac{v_u}{T_u}\frac{\partial \ln v_u}{\partial \ln T_u}\frac{dT_u}{d\theta} + \frac{v_u}{p}\frac{\partial \ln v_u}{\partial \ln p}\frac{dp}{d\theta} \tag{6.64}$$

Likewise, u_b is a function of T_b and p as

$$u_b = u_b(T_b, p) \tag{6.65}$$

and

$$\frac{du_b}{d\theta} = \frac{\partial u_b}{\partial T_b}\frac{dT_b}{d\theta} + \frac{\partial u_b}{\partial p}\frac{dp}{d\theta} \tag{6.66}$$

Introducing the following equations

Reproduced with permission of the copyright owner. Further reproduction prohibited without permission.

$$\left(\frac{\partial u}{\partial T}\right)_P = c_P - \frac{pv}{T}\left(\frac{\partial \ln v}{\partial \ln T}\right)_P \tag{6.67}$$

$$\left(\frac{\partial u}{\partial p}\right)_T = -v\left[\left(\frac{\partial \ln v}{\partial \ln T}\right)_P + \left(\frac{\partial \ln v}{\partial \ln p}\right)_T\right] \tag{6.68}$$

The Eq. (6.66) leads to

$$\frac{du_b}{d\theta} = \left(c_{Pb} - \frac{pv_b}{T_b}\frac{\partial \ln v_b}{\partial \ln T_b}\right)\frac{dT_b}{d\theta} - v_b\left(\frac{\partial \ln v_b}{\partial \ln T_b} + \frac{\partial \ln v_b}{\partial \ln p}\right)\frac{dp}{d\theta} \tag{6.69}$$

Likewise for the unburned gas

$$\frac{du_u}{d\theta} = \left(c_{Pu} - \frac{pv_u}{T_u}\frac{\partial \ln v_u}{\partial \ln T_u}\right)\frac{dT_u}{d\theta} - v_u\left(\frac{\partial \ln v_u}{\partial \ln T_u} + \frac{\partial \ln v_u}{\partial \ln p}\right)\frac{dp}{d\theta} \tag{6.70}$$

The terms in energy equation Eq. (6.58) have been considered as follows. The first term on the left is developed from Eq. (6.59).

$$m\frac{du}{d\theta} = \left[x\frac{du_b}{d\theta} + (1-x)\frac{du_u}{d\theta} + (u_b - u_u)\frac{dx}{d\theta}\right]m \tag{6.71}$$

Eq. (6.71) can be rearrange by substituting Eq.(6.69) and (6.70) into Eq. (6.71) and gives:

$$\begin{aligned} m\frac{du}{d\theta} = {} & mx\left(c_{Pb} - \frac{pv_b}{T_b}\frac{\partial \ln v_b}{\partial \ln T_b}\right)\frac{dT_b}{d\theta} + m(1-x)\left(c_{Pu} - \frac{pv_u}{T_u}\frac{\partial \ln v_u}{\partial \ln T_u}\right)\frac{dT_u}{d\theta} \\ & - \left[mxv_b\left(\frac{\partial \ln v_b}{\partial \ln T_b} + \frac{\partial \ln v_b}{\partial \ln p}\right) + m(1-x)v_u\left(\frac{\partial \ln v_u}{\partial \ln T_u} + \frac{\partial \ln v_u}{\partial \ln p}\right)\right]\frac{dp}{d\theta} \\ & + m(u_b - u_u)\frac{dx}{d\theta} \end{aligned} \tag{6.72}$$

Reproduced with permission of the copyright owner. Further reproduction prohibited without permission.

The second term on the left-hand side of energy Eq. (6.58) is required to introduce the mass conservation and an algorithm to compute the blowby.

$$\frac{dm}{d\theta} = \frac{-\dot{m}_l}{\omega} = \frac{-Cm}{\omega} \tag{6.73}$$

The first term on the right-hand side of energy Eq. (6.58) is expressed in terms of the heat transfer from the in-cylinder burned and unburned mixtures to the cylinder walls, respectively.

$$\frac{dQ}{d\theta} = Q_{f\,tot}\frac{dx}{d\theta} - \frac{\dot{Q}_l}{\omega} = Q_{f\,tot}\frac{dx}{d\theta} - \frac{\dot{Q}_b + \dot{Q}_u}{\omega} \tag{6.74}$$

To express the heat loss terms requires the introduction of the heat transfer coefficient **h**. Constant heat transfer coefficient has been used in the simulation first, and instantaneous heat transfer coefficient will be expressed in details in Woshni correlation.

$$\dot{Q}_b = \mathbf{h}_b A_b (T_b - T_w) \tag{6.75}$$

$$\dot{Q}_u = \mathbf{h}_u A_u (T_u - T_w) \tag{6.76}$$

where A_b and A_u are the areas of burned and unburned gas in contact with the cylinder walls at a temperature T_w. To calculate the areas A_b and A_u, it is assumed that

$$A_b = \left(\frac{\pi b^2}{2} + \frac{4V}{b}\right) x^{1/2} \tag{6.77}$$

$$A_u = \left(\frac{\pi b^2}{2} + \frac{4V}{b}\right) 1 - x^{1/2} \tag{6.78}$$

Reproduced with permission of the copyright owner. Further reproduction prohibited without permission.

Equations (6.77) and (6.78) are empirical functions that have the correct limits in the case of a cylinder where $x \to 0$ and when $x \to 1$. The fraction of cylinder area contacted by burned gas is assumed to be proportional to the square root of the mass fraction burned. Because of the density difference between the burned and unburned gas, the burned gas occupies a larger volume fraction of the cylinder than the unburned gas.

In practice, the exponent on x may be left as a free parameter to be determined from experiments, or a more complicated scheme may be used based on an assumption about the flame shape.

Initially, it is assumed that $\mathbf{h}_u = \mathbf{h}_b = \mathbf{h} = \text{constant}$. Heat transfer coefficient **h** changes with crank angles will be expressed in the simulation for DaimlerChrysler V8 engine using the Woschni correlation.

The work term on the right-hand side of energy Eq.(6.58) requires no further explanation.

The last term on the right-hand side of energy Eq. (6.58), the enthalpy of the mass loss due to blowby, needs to be specified. Early in the combustion process, the unburned gas leaks past the rings. During the combustion process, the burned gas leaks past the rings. In the spirit of being conceptually correct while deviating from what might be in practice, it is assumed that

$$h_l = (1 - x^2)h_u + x^2 h_b \tag{6.79}$$

which has the correct limits and recognizes that a larger portion of unburned gas will be leaking than the unburned mass fraction.

Finally, to complete Eq.(6.79), the equation of state must include

Reproduced with permission of the copyright owner. Further reproduction prohibited without permission.

$$h_u = h_u(T_u, p) \tag{6.80}$$

$$h_b = h_b(T_b, p) \tag{6.81}$$

which are respectively computed by subroutines FARG and ECP.

In summary, the examination of all the terms of energy Eq.(6.58) discussed above reveals the following derivatives in the equation

$$\frac{dp}{d\theta}, \frac{dT_b}{d\theta}, \frac{dT_u}{d\theta}, \frac{dV}{d\theta}, \frac{dx}{d\theta} \tag{6.82}$$

and the following variables

$$p, T_b, T_u \tag{6.83}$$

$$u_b, u_u, v_b, v_u, h_b, h_u \tag{6.84}$$

$$\frac{\partial \ln v_b}{\partial \ln T_b}, \frac{\partial \ln v_u}{\partial \ln T_u}, \frac{\partial \ln v_b}{\partial \ln p}, \frac{\partial \ln v_u}{\partial \ln p}, c_{Pb}, c_{Pu} \tag{6.85}$$

$$m, V, x \tag{6.86}$$

$$C, \omega, \mathbf{h}, b \tag{6.87}$$

The variables in (6.87) are all constants which are specified according to the engine type and the operating characteristics.

The variables in Eq. (6.86) are all known as functions of crank angle.

The mass at any crank angle integrating from Eq. (6.73) is

$$m = m_1 \exp[-C(\theta - \theta_1)/\omega] \tag{6.88}$$

The initial mass m_1 at $\theta = \theta_1$ (start of combustion) is specified from the volumetric efficiency and the residual gas fraction.

Reproduced with permission of the copyright owner. Further reproduction prohibited without permission.

The cylinder volume is simulated as an empirical function of compression ratio r, volume at TDC, and ε = S/2l (S = stroke, l = rod length).

$$V = V_0\left\{1+\frac{r+1}{2}\left\{1-\cos\theta+\frac{1}{\varepsilon}\left[1-\left(1-\varepsilon^2\sin^2\theta\right)^{1/2}\right]\right\}\right\} \tag{6.89}$$

The mass fraction burned is simulated from the empirical burning law.

$$x = \begin{cases} 0 & (\theta < \theta_s) \\ \frac{1}{2}\left\{1-\cos\left[\frac{\pi(\theta-\theta_s)}{\theta_b}\right]\right\} & (\theta_s < \theta < \theta_s+\theta_b) \\ 1 & (\theta > \theta_s+\theta_b) \end{cases} \tag{6.90}$$

All the variables in the lists of (6.84) and (6.85) are the thermodynamic properties and can be calculated from ECP and FARG subroutines by inputting the initial p, T_b, T_u, and f.

The derivatives $dV/d\theta$ and $dx/d\theta$ in Eq. (6.82) are known by differentiating (6.89) and Eq. (6.90) respectively.

Therefore, the energy equation (6.58) is thus seen to be a relationship among three derivatives, their integrals, and a parameter (crank angle) dependent upon the integrals. In other words, we have an energy equation of the following form:

$$f\left(\theta, \frac{dp}{d\theta}, \frac{dT_b}{d\theta}, \frac{dT_u}{d\theta}, p, T_b, T_u\right)=0 \tag{6.91}$$

Reproduced with permission of the copyright owner. Further reproduction prohibited without permission.

If two more equations can be found, three equations can be rearranged into a standard form used to numerically integrate a set of ordinary differential equations, as shown below.

$$\frac{dp}{d\theta} = f_1(\theta, p, T_b, T_u) \tag{6.92}$$

$$\frac{dT_b}{d\theta} = f_2(\theta, p, T_b, T_u) \tag{6.93}$$

$$\frac{dT_u}{d\theta} = f_3(\theta, p, T_b, T_u) \tag{6.94}$$

It is also convenient to integrate equations simultaneously for the work output, heat loss, and enthalpy loss calculations.

$$\frac{dW}{d\theta} = f_4(\theta, p) \tag{6.95}$$

$$\frac{dQ_l}{d\theta} = f_5(\theta, p, T_b, T_u) \tag{6.96}$$

$$\frac{dH_l}{d\theta} = f_6(\theta, p, T_b, T_u) \tag{6.97}$$

One of the requisite equations can be derived from Eq. (6.60) for the specific volume of the system. Differentiating it and incorporating Eq. (6.63) and (6.64) yield

$$\begin{aligned}
\frac{1}{m}\frac{dV}{d\theta} - \frac{V}{m^2}\frac{dm}{d\theta} &= x\frac{dv_b}{d\theta} + (1-x)\frac{dv_u}{d\theta} + (v_b - v_u)\frac{dx}{d\theta} \\
\frac{1}{m}\frac{dV}{d\theta} + \frac{VC}{m\omega} &= x\frac{v_b}{T_b}\frac{\partial \ln v_b}{\partial \ln T_b}\frac{dT_b}{d\theta} + (1-x)\frac{v_u}{T_u}\frac{\partial \ln v_u}{\partial \ln T_u}\frac{dT_u}{d\theta} \\
&\quad + \left[x\frac{v_b}{P}\frac{\partial \ln v_b}{\partial \ln P} + (1-x)\frac{v_u}{P}\frac{\partial \ln v_u}{\partial \ln P}\right]\frac{dP}{d\theta} + (v_b - v_u)\frac{dx}{d\theta}
\end{aligned} \tag{6.98}$$

Reproduced with permission of the copyright owner. Further reproduction prohibited without permission.

The remaining equation comes from introducing the unburned gas entropy into the analysis. Treating the unburned gas as an open system losing mass via leakage and combustion, it can be shown that

$$-\dot{Q}_u = \omega m(1-x)T_u \frac{ds_u}{d\theta} \tag{6.99}$$

To utilize Eq. (6.99), the equation of state relating entropy to the temperature and pressure must be introduced.

$$s_u = s_u(T_u, p) \tag{6.100}$$

From which it follows

$$\frac{ds_u}{d\theta} = \left(\frac{\partial s_u}{\partial T_u}\right)\frac{dT_u}{d\theta} + \left(\frac{\partial s_u}{\partial p}\right)\frac{dp}{d\theta} \tag{6.101}$$

$$\frac{ds_u}{d\theta} = \left(\frac{c_{Pu}}{T_u}\right)\frac{dT_u}{d\theta} - \frac{v_u}{T_u}\frac{\partial \ln v_u}{\partial \ln T_u}\frac{dp}{d\theta} \tag{6.102}$$

Eliminating of $ds_u/d\theta$ between Eq.(6.99) and (6.102) gives

$$c_{Pu}\frac{dT_u}{d\theta} - v_u\frac{\partial \ln v_u}{\partial \ln T_u}\frac{dP}{d\theta} = \frac{-h\left(\frac{\pi b^2}{2} + \frac{4V}{b}\right)}{\omega m}\frac{(1-x^{1/2})}{(1-x)}(T_u - T_w) \tag{6.103}$$

Therefore, the three equations, which are Eq. (6.58), (6.98), and (6.103), are used to solve Eq. (6.92) through (6.94).

For convenience, the following variables are defined in the engine cycle simulation:

Reproduced with permission of the copyright owner. Further reproduction prohibited without permission.

$$A = \frac{1}{m}\left(\frac{dV}{d\theta} + \frac{VC}{\omega}\right) \tag{6.104}$$

$$B = \mathbf{h}\frac{\left(\frac{\pi b^2}{2} + \frac{4V}{b}\right)}{\omega m}\left[\frac{v_b}{c_{Pb}}\frac{\partial \ln v_b}{\partial \ln T_b}x^{1/2}\frac{T_b - T_w}{T_b} + \frac{v_u}{c_{Pu}}\frac{\partial \ln v_u}{\partial \ln T_u}(1-x^{1/2})\frac{T_u - T_w}{T_w}\right] \tag{6.105}$$

$$C = -(v_b - v_u)\frac{dx}{d\theta} - v_b\frac{\partial \ln v_b}{\partial \ln T_b}\frac{h_u - h_b}{c_{Pb}T_b}\left[\frac{dx}{d\theta} - \frac{(x-x^2)C}{\omega}\right] \tag{6.106}$$

$$D = x\left[\frac{v_b^2}{c_{Pb}T_b}\left(\frac{\partial \ln v_b}{\partial \ln T_b}\right)^2 + \frac{v_b}{p}\frac{\partial \ln v_b}{\partial \ln p}\right] \tag{6.107}$$

$$E = (1-x)\left[\frac{v_u^2}{c_{Pu}T_u}\left(\frac{\partial \ln v_u}{\partial \ln T_u}\right)^2 + \frac{v_u}{p}\frac{\partial \ln v_u}{\partial \ln p}\right] \tag{6.108}$$

Finally, the six equations to be integrated are:

$$\frac{dp}{d\theta} = \frac{A+B+C}{D+E} \tag{6.109}$$

$$\frac{dT_b}{d\theta} = \frac{-\mathbf{h}\left(\frac{\pi b^2}{2} + \frac{4V}{b}\right)x^{1/2}(T_b - T_w)}{\omega m c_{Pb} x} + \frac{v_b}{c_{Pb}}\frac{\partial \ln v_b}{\partial \ln T_b}\left(\frac{A+B+C}{D+E}\right) + \frac{h_u - h_b}{xc_{Pb}}\left[\frac{dx}{d\theta} - (x-x^2)\frac{C}{\omega}\right] \tag{6.110}$$

$$\frac{dT_u}{d\theta} = \frac{-\mathbf{h}\left(\frac{\pi b^2}{2} + \frac{4V}{b}\right)(1-x^{1/2})(T_u - T_w)}{\omega m c_{Pu}(1-x)} + \frac{v_u}{c_{Pu}}\frac{\partial \ln v_u}{\partial \ln T_u}\left(\frac{A+B+C}{D+E}\right) \tag{6.111}$$

$$\frac{dW}{d\theta} = p\frac{dV}{d\theta} \tag{6.112}$$

$$\frac{dQ_l}{d\theta} = \frac{\mathbf{h}}{\omega}\left(\frac{\pi}{2}b^2 + \frac{4V}{b}\right)\left[x^{1/2}(T_b - T_u) + (1-x^{1/2})(T_u - T_w)\right] \tag{6.113}$$

$$\frac{dH_l}{d\theta} = \frac{Cm}{\omega}\left[(1-x^2)h_u + x^2 h_b\right] \tag{6.114}$$

Reproduced with permission of the copyright owner. Further reproduction prohibited without permission.

A set of ordinary differential equations, describing the rates of change of pressure, temperature, mass, work, and heat loss with respect to crank angle, are derived. Simultaneously integrating these equations from the start of compression to the end of expansion processes, the pressure-volume diagram, the indicated efficiency, indicated mean effective pressure, power, torque and indicated specific fuel consumption can be determined.

- **Development of Availability Equation**

Figure 6.2 shows a system at temperature T and pressure p that contains various species with different chemical potential μ_k. The system is to be enclosed completely in a reference environment at temperature T_0, and pressure p_0. The chemical potentials are μ_k^0 for the environmental components. In general, some species present in the system are also present in the reference environment, but some are not. During compression, combustion and expansion processes, the in-cylinder mixture can be considered as a control mass.

Heat and work interactions can take place between the control mass and the environment, but only work interaction is permitted across the control surface of the combined system. Although the volumes of the control mass and environment can vary, the total volume remains constant: $\Delta(V+V^0)=0$.

As the control mass passes from some given state to the dead state, the work derived from the combined system is determined from an energy balance equation of the combined system as

$$W_C = -\Delta E_C \tag{6.115}$$

ΔE_C is the energy change of the combined system: the sum of the energy changes for control mass and environment. (where potential and kinetic energy are ignored)

$$\Delta E_C = (U_0 - U) + \Delta U^0 \tag{6.116}$$

Reproduced with permission of the copyright owner. Further reproduction prohibited without permission.

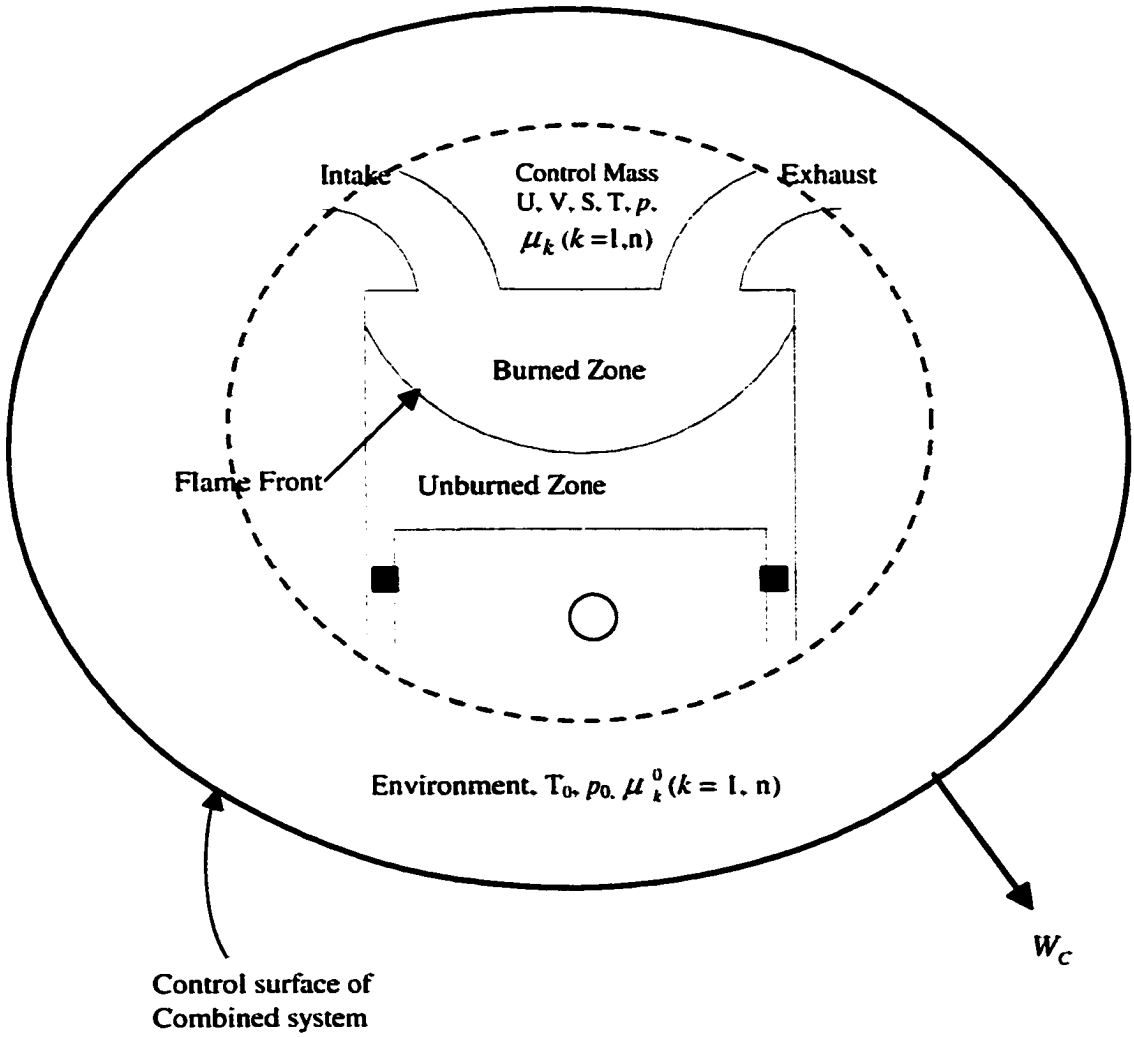

Figure 6.2 Schematic diagram of the two-zone model and the combined system for determining availability in fuel/air cycle analysis.

Initially, the entropy of the combined system is $S^0 + S$, the volume is $V^0 + V$, and the internal energy is $U^0 + U$, where U^0 is given as

Reproduced with permission of the copyright owner. Further reproduction prohibited without permission.

$$U^0 = T_0 S^0 - p_0 V^0 + \sum_{k=1}^{n} N_k^0 \mu_k^0 \tag{6.117}$$

At equilibrium the energy of the combined system is

$$U^0 + U = T_0(S^0 + S + \sigma) - p_0(V^0 + V) + \sum_{k=1}^{n}(N_k^0 + N_k)\mu_k^0 \tag{6.118}$$

The term σ accounts for the entropy produced due to irreversibilities. Term $(V^0 + V)$ is used because there is no change in total volume of the combined system, and term $(N_k^0 + N_k)$ is used because the amount of each species present is conserved.

Collecting Eqs (6.115) to (6.118)

$$W_C = (U + p_0 V - T_0 S - \sum_{k=1}^{n} N_k \mu_k^0) - T_0 \sigma \tag{6.119}$$

Since $\sigma \geq 0$, it follows that

$$W_C \leq U + p_0 V - T_0 S - \sum_{k=1}^{n} N_k \mu_k^0 \tag{6.120}$$

Thus, the maximum work of the combined system is

$$(W_C)_{max} = U + p_0 V - T_0 S - \sum_{k=1}^{n} N_k \mu_k^0 \tag{6.121}$$

The maximum is obtained only when the process of the combined system is in every respect internally reversible. By definition, the availability equals $(W_C)_{max}$. That is

$$A = U + p_0 V - T_0 S - \sum_{k=1}^{n} N_k \mu_k^0 \tag{6.122}$$

Reproduced with permission of the copyright owner. Further reproduction prohibited without permission.

The term availability is used in this thesis. It also has been referred to in the literature by other names, such as essergy (essence of energy) and exergy.

For the engine cycle simulation it is convenient to consider the availability, described in Eq. (6.122), as the sum of two contributions, the thermomechanical availability and the chemical availability.

$$A = A^{th} + A^{ch} \tag{6.123}$$

As described before, thermomechanical availability is associated with work that could be obtained from the combined system by allowing only thermal and mechanical interactions between the system and environment. The combined system achieves a restricted dead state condition when the system temperature is T_0, and the system pressure is p_0. No additional potential exists for developing work from the combined system without mass exchange between the system and the reference environment.

The chemical availability is defined as the maximum work that could be developed by the combined system going from the restricted dead state to the dead state. This additional work can be obtained by two means.

First, the chemical availability can be exploited from the chemical potential differences associated with species present in the system at the restricted dead state and those in the reference environment at the same time. In engine operation, it is usually neglected to consider such chemical availability, due to their relatively small amounts of work produced and practical difficulties of implementing such potential energy.

Second, species such as a fuel not present in the reference environment could be allowed to enter into chemical reactions with species from the reference environment to produce environmental species. The tables for different fuel chemical availability can be found in Moran's Availability Analysis [5] and Fundamentals of Engineering Thermodynamics [11].

Reproduced with permission of the copyright owner. Further reproduction prohibited without permission.

When the equivalence ratio is no larger than 1, the mixture is at lean or stoichiometric. It is assumed that the original fuel chemical availability is completely consumed in such lean or stoichiometric condition. When the equivalence ratio is larger than 1, the fuel chemical availability will not be entirely used. The equilibrium combustion products include CO and H_2, which carry certain amount of fuel chemical availability. Such waste of fuel availability is taken into account into the fuel/air cycle fuel chemical availability simulation with respect to crank angle.

The availability balance equation allows for a detailed accounts of the availability inputs in terms of availability transfer with work, availability transfer with heat, availability transfer with exhaust to the surroundings, availability destruction due to combustion, and availability destruction due to other reasons such as inlet mixing, mechanical losses and so forth.

As described in the previous section, to obtain the thermomechanical availability equation, the entropy balance is multiplied by T_0 and subtracted from the energy balance. Then, the term $p_0 \frac{dV}{d\theta}$ is added to each side of the resulting equation to give

$$\frac{dU}{d\theta} + p_0 \frac{dV}{d\theta} - T_0 \frac{dS}{d\theta} = (1 - \frac{T_0}{T}) \cdot \frac{dQ}{d\theta} - (\frac{dW}{d\theta} - p_0 \frac{dV}{d\theta}) - T_0 \sigma' \qquad (6.124)$$

The total irreversibilities changing with crank angle term is expressed as $T_0\sigma'$, which consists of irreversible processes such as combustion (chemical reaction), heat transfer through a finite temperature difference, inlet mixing, and friction in SI engine operations. Only the combustion destruction is simulated with respect to crank angle in the current study, labeled as I_c.

The combustion destruction is simulated from entropy production, labeled as σ_c. The entropy production is simulated from entropy change, heat transfer, and temperature in a two-zone combustion model, expressed in Eq. (6.127). The simple and convenient

Reproduced with permission of the copyright owner. Further reproduction prohibited without permission.

assumption for the final entropy calculation is related to mass fraction burn and illustrated in Eq. (6.126). Therefore, solving Eq. (6.125) to Eq. (6.127) gives the combustion destruction, I_c.

$$I_c = T_0 \sigma_c \tag{6.125}$$

$$s = x \cdot s_b + (1-x) \cdot s_u \tag{6.126}$$

$$\Delta s = -\int \frac{x \cdot Q_l}{T_b} - \int \frac{(1-x) \cdot Q_l}{T_u} + \sigma_c \tag{6.127}$$

The availability destruction due to inlet mixing and friction in SI engines are in small amounts, compared with availability destruction due to combustion and heat transfer. For instance, Caton [4] predicted that destruction due to inlet mixing is around 1%. R.J. Primus and P.F. Flynn [12] showed that mechanical friction destruction is around 3-4%. In the current study, destructions due to inlet mixing and friction are ignored in the final availability balance analysis. It is assumed that total irreversibilities include only destruction due to combustion and destruction due to heat transfer, which is expressed in Eq. (6.128). As mentioned before, combustion destruction comes from a simulation model, while the destruction due to heat transfer can be captured by the total availability distribution in the availability balance.

$$I_{total} = I_c + I_{heat\ transfer} \tag{6.128}$$

The final form of the availability balance in differential forms is shown in Eq.(6.129).

$$\frac{dA}{d\theta} = (1 - \frac{T_0}{T}) \cdot \frac{dQ}{d\theta} - (\frac{dW}{d\theta} - p_0 \frac{dV}{d\theta}) + \frac{m_f}{m} \cdot \frac{dx}{d\theta} \cdot a_f^{ch} - I_c^{'} - I^{'}_{heat\ transfer} \tag{6.129}$$

1 2 3 4 5 6

The numbered terms in Eq.(6.129) can be interpreted as the following availability quantities:

Reproduced with permission of the copyright owner. Further reproduction prohibited without permission.

Term 1: The change of total availability

Terms 2: The availability transfer with heat

Term 3: The availability transfer with work

Term 4: The fuel chemical availability

Term 5: The availability destruction due to combustion

Term 6: The availability destruction due to heat transfer

- **Simulated Engine Parameters**

The simulated engine parameters have been chosen to follow the referenced Ferguson model [2] and listed in Table 6-3. These baseline engine simulation parameters are used for gasoline, CNG and methanol fueled SI engine cycle simulations.

Table 6-3 SI Engine parameters for simulation

Bore (mm)	10.0
Stroke (mm)	80
Half of stroke to connecting rod ratio	0.25
Compression ratio	10 : 1
Engine speed, rpm	2000
Heat transfer coefficient ($W/m^2 \cdot K$)	500
Blowby coefficient	0.8
Equivalence ratio	0.8
Residual gas fraction	0.1
Initial pressure (kPa)	101.35
Initial temperature (K)	350
Wall temperature (K)	420
Start of combustion (°BTDC)	-35
Combustion duration (°CA)	60

- **Simulated CNG and Methanol fueled SI engines**

The effort of simulation is made to investigate and identify the potential of alternative fuels operations in SI engines from a second law efficiency point of view, compared with the traditional gasoline operation.

Reproduced with permission of the copyright owner. Further reproduction prohibited without permission.

As discussed before, natural gas reserves are the world's most readily available and abundant gaseous fuel resources. Natural gas consists chiefly of methane, ranging anywhere from 75% to 99% by volume. Charging preparation is somewhat simplified in that methane is already a vapor, a benefit when cold-starting an engine. One hundred cubic feet of methane gas is approximately equal to one gallon of gasoline in terms of stored chemical energy content, but operation with methane does require ignition timing adjustments because of its lower flame speeds. Methane has a high octane number and is easily ignited and has a higher ignition temperature than gasoline. Alcohol is another resource that has been used as an SI engine fuel. In Canada, methanol can be produced from natural gas and coal. This strongly suggests that alcohol be a reasonable choice for the future mix of worldwide SI fuel options.

Both CNG and methanol are good SI engine fuels due to their high octane ratings. For both fuels, compression ratio can be raised to increase the engine performance and output.

Calorific values, fuel chemical availability at the environmental temperature and pressure, and stoichiometric air-fuel ratio are presented in the Table 6-4, for gasoline, methane, and methanol fuels in the engine cycle simulations.

Table 6-4 Calorific value, fuel chemical availability, air/fuel ratio for three different fuels

Fuel	CV (kJ/g)	a_f^{ch} (kJ/g)	(AFR)stoich
Gasoline C_8H_{18}	44.651	47.713	14.7
Methane CH_4	50.031	52.085	17.2
Methanol CH_3OH	21.104	22.572	6.4

Reproduced with permission of the copyright owner. Further reproduction prohibited without permission.

6.2.4 Current Models: DaimlerChrysler 4.7 Liter V8 Engine Simulation

The operating parameters for the DaimlerChrysler CNG fueled port injection 4.7 Liter V8 engine are inputted to the simulation. The availability computation follows the same procedure used in the previous fuel/air cycle availability analysis. The mass fraction burned rate is simulated and compared with the experimental data[3]. Heat transfer coefficient is modified according to the Woschni correlation. Finally, the simulated pressure results are validated and compared with the experimental pressure data at wide open throttle and engine speed at 4000 rpm.

- **V8 Engine Parameters Used in Simulation**

Table 6-5 shows the major engine simulation parameters used in simulation for engine operating conditions at WOT, 4000 rpm. More detailed information on DaimlerChrysler 4.7Liter V8 Engine can be found in the reference [13].

Table 6-5 Baseline case for 4.7 Liter V8 SI engine model

Engine Geometry

Bore	93 mm
Stroke	86.5 mm
Connecting Rod	155.4 mm
Crank Radius	43.25 mm
Compression Ratio	9.3
Blowby Coefficient	0.8

Initial Fuel/Air Mixture Condition and Reference Environment

Crank angle	-180° before TDC
Fuel/air Temperature	300 K

[3] The experimental data was obtained from the University of Windsor/DaimlerChrysler Automotive Research and Development Center.

Reproduced with permission of the copyright owner. Further reproduction prohibited without permission.

Wall Temperature	420 K
Pressure	101.35 kPa
Equivalence Ratio	1.05
Residual Gas Fraction	0
Air Composition	21 % O_2
	79 % N_2

Fuel

CNG	Modeled as CH_4

Engine Operating Condition

Wide Open Throttle
4000 rev/min

- **Case of simulated and measured mass burn fraction**

The mass fraction burned curve with respect to crank angle can be predicted from an empirical burning law and the measurements of pressure data. The experimental cylinder pressures for V8 engine at wide open throttle and engine speed 4000 rev/min are used to assist the simulation. More specifically, the experimental p-V and log (p/p_0)-log (V/V_0) diagrams are helpful for the analysis of the mass fraction burned simulation.

The experimental log (p/p_0)-log (V/V_0) diagram can help to define the start of combustion and the combustion duration. In the log (p/p_0)-log (V/V_0) diagram shown in Fig. 6.3 (b), the compression process is a straight line of slope 1.33, while the expansion process is also a straight line of slope 1.21. Since the compression of the unburned mixture and the expansion of the burned gases following the end of combustion are close to isentropic processes, the observed behavior with constant specific heat ratio during compression and expansion processes is as expected. The start of combustion can be identified by the

Reproduced with permission of the copyright owner. Further reproduction prohibited without permission.

departure of the curve from the straight line in the compression process. The end of combustion can be located approximately in similar fashion from the straight line in the expansion process.

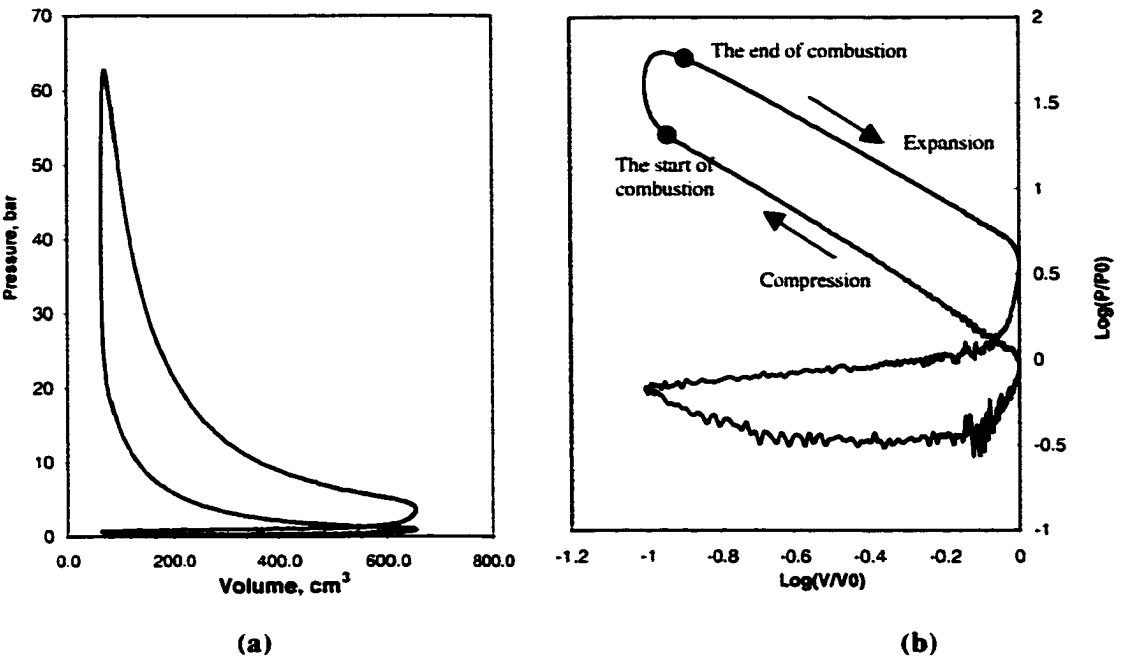

Figure 6.3 (a) Experimental Pressure-volume diagram at WOT, 4000rpm for V8 engine; (b) Experimental log (p/p_0)-log (V/V_0) plot at WOT, 4000 rpm for V8 engine.

The cycle-averaged experimental mass fraction burned data is directly used to define the start of combustion in the current study, shown in Figure 6.4. The experimental mass fraction burned curve is obtained from the cycle averaged experimental data. If mass fraction burned is less than 0.001, the cylinder consists of only the unburned fuel/air mixture. If mass fraction burned is over 0.001, it is assumed that combustion starts. The experimental data shows that mass fraction burned reaches 0.001 around 20° before TDC. Therefore, the start of combustion is defined as at 20° before TDC. This is used as a simulation input, but the combustion model in the current study does not capture the ignition delay. Considering the ignition delay, 10°, the actual spark advance timing is expected around 30° before TDC.

Reproduced with permission of the copyright owner. Further reproduction prohibited without permission.

The experimental log (p/p_0)-log (V/V_0) diagram does not provide the profile of the mass fraction burned. Eq.(6.130) represents an empirical burning law and is used for mass fraction burned simulation in the current study.

$$x = \frac{1}{2}\left(1 - \cos\left(\frac{\pi(\theta - \theta_s)}{\theta_b}\right)\right) \tag{6.130}$$

Another functional form often used to represent the mass fraction burned versus crank angle is the Wiebe function, expressed in Eq.(6.131).

$$x = 1 - \exp\left[-a\left(\frac{\theta - \theta_s}{\theta_b}\right)^n\right] \tag{6.131}$$

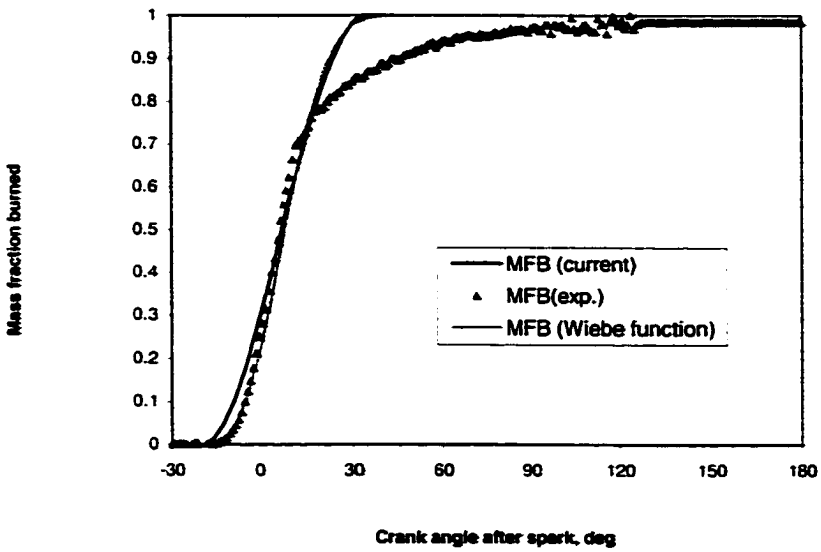

Figure 6.4 Predicted and measured mass fraction burned (MFB) versus crank angles at WOT, 4000 rpm for V8 engine.

Eq.(6.130) and Eq.(6.131) both assume a 100% combustion efficiency. The mass fraction burned curve approximated by the Wiebe function is almost the same as the current combustion model (see Figure 6.4). There seems to be a better fit for the Wiebe function with the experimental mass fraction burned curve before TDC. However, there is a bigger

Reproduced with permission of the copyright owner. Further reproduction prohibited without permission.

departure from experimental data past TDC and the Wiebe function does not help at large crank angles. In order to maintain consistency, the current study uses Eq. (6.130) for mass fraction burned simulation. The comparison of the current mass fraction burned model and the Wiebe function for the distributions of the fuel energy and fuel availability will be shown in the end of Chapter 7.

The combustion duration is taken to be 55° in order to obtain good agreement with the experimental mass fraction burned during most of the burn duration. As discussed above, there are differences between experimental and simulated curves. The experimental mass fraction burned curve shows the prolonged combustion duration, which is not captured in the simulation. This is mainly because that the combustion model assumes 100% combustion efficiency. There are other factors which affect mass fraction burn of real engine. The major factors are heat transfer loss, and crevices loss which are present in the real case and could not be presented in the current combustion model and the Wiebe function. There is also a possibility that this particular experimental data set used in this work exhibits abnormally long combustion periods. In fact more recent data [29] from the same engine shows that a crank angle for 50% mass fraction burned only at about 30° from the start of combustion. If one assumes symmetry in a combustion process, it would lead to 60° crank angles for combustion duration. This value is much shorter than the 120° crank angles combustion duration suggested by experimental data in Figure 6.4.

- **Instantaneous Spatial Average Heat Transfer Coefficient Simulation**

Solving engine heat transfer problems is one of the major design tasks. The peak burned gas temperature in the cylinder of an internal combustion engine is the order of 2500K. In regions of high heat flux, thermal stress must be kept below levels which would cause fatigue cracking, 400°C for cast iron and 300°C for aluminum alloys. The gas-side surface of the cylinder wall must be kept below about 180°C to prevent deterioration of the lubricating oil film [10]. Spark plug and valves must be kept cool to avoid knock and pre-ignition problems which result from overheated spark plug electrodes or exhaust valves. On the contrary, heat transfer affects engine performance, efficiency and

Reproduced with permission of the copyright owner. Further reproduction prohibited without permission.

emissions. High heat transfer to the combustion chamber walls will lower the average combustion gas temperature and pressure, and then reduce the work per cycle transferred to the piston. Changes in gas temperature due to the heat transfer also impact on emission formation processes in the engine cylinder and the exhaust system.

The overall heat transfer process is from the gases within the cylinder through the combustion chamber wall to the coolant flow. The heat flux into the wall has in general both a convective and a radiation component. Then the heat flux is conducted through the wall and then convected from the wall to the coolant.

For the current DaimlerChysler V8 engine simulation, only heat transferred by convection, from the in-cylinder mixture to the gases-side cylinder walls, is considered. More specifically, it is between the in-cylinder mixture and the cylinder head, valves, cylinder walls, and piston during the compression, combustion and expansion processes. Radiation is not included in the current study because of the low value of the emissivity coefficient, the short optical path length, and no-soot present in the CNG operations.

While the overall time-averaged heat transfer is used for the previous fuel/air cycle simulation, the instantaneous heat flux simulation during the engine cycle is necessary for the realistic cycle calculations. Thus, the Woschni correlation [10] is introduced for simulating the instantaneous spatial average heat transfer coefficient.

Woschni assumed a Nusselt number correlation as

$$\mathrm{Nu} = 0.035\mathrm{Re}^{m} \tag{6.132}$$

where

$$\mathrm{Nu} = \frac{\mathbf{h} \cdot L}{k} \tag{6.133}$$

$$\mathrm{Re} = \frac{\rho\, wL}{\mu} \tag{6.134}$$

Reproduced with permission of the copyright owner. Further reproduction prohibited without permission.

With the cylinder bore b taken as the characteristic length, with w as a local average gas velocity in the cylinder, and assuming $k \propto T^{0.75}$, $\mu \propto T^{0.62}$, and $p = \rho RT$.

The mean temperature is expressed as follows:

$$T = x \cdot T_b + (1 - x) \cdot T_u \tag{6.135}$$

The Woschni correlation can be written

$$\mathbf{h} = Cb^{m-1} p^m w^m T^{0.75-1.62m} \tag{6.136}$$

During the compression process, the Woschni correlation suggests the average gas velocity be proportional to the mean piston speed, $\overline{U}_p$.

During the combustion and expansion processes, the Woschni correlation also uses piston speed but introduces a factor to account for gas motion induced by combustion. Thus the gas velocity induced by combustion is assumed to be proportional to the pressure rise due to combustion. The term $(p - p_m)$ was introduced (p_m is the motored cylinder pressure) to express the gas velocity used in the current study.

Therefore, the average cylinder gas velocity w for the compression, combustion and expansion processes is expressed as follows:

$$w = \left[C_1 \overline{U}_p + C_2 \frac{V_d T_r}{p_r V_r} (p - p_m) \right] \tag{6.137}$$

Where V_d is the displaced volume, p is the instantaneous cylinder pressure, p_r, V_r, T_r are the cylinder mixture pressure, volume, and temperature at some reference state, such as

Reproduced with permission of the copyright owner. Further reproduction prohibited without permission.

the point of inlet valve closing or the start of combustion, and p_m is the motored cylinder pressure at the same crank angle as p.

For compression process: $C_1 = 2.28, \quad C_2 = 0$

For combustion and expansion processes: $C_1 = 2.28, \quad C_2 = 3.24 \times 10^{-3}$

With the exponent in Eq.(6.136) equal to 0.8 and the average cylinder gas velocity w defined above, the Woschni correlation can be summarized as:

$$\mathbf{h}\,(\mathrm{W/m^2 \cdot K}) = 3.26 b\,(\mathrm{m})^{-0.2}\, p(\mathrm{kPa})^{0.8} T(\mathrm{K})^{-0.55}\, w(\mathrm{m/s})^{0.8} \qquad (6.138)$$

Figure 6.5 illustrates the instantaneous and time-averaged heat transfer coefficient for a engine operating condition. The instantaneous heat transfer coefficient is used in the DaimlerChrysler V8 enigne cycle simulation, according to Eq.(6.138).

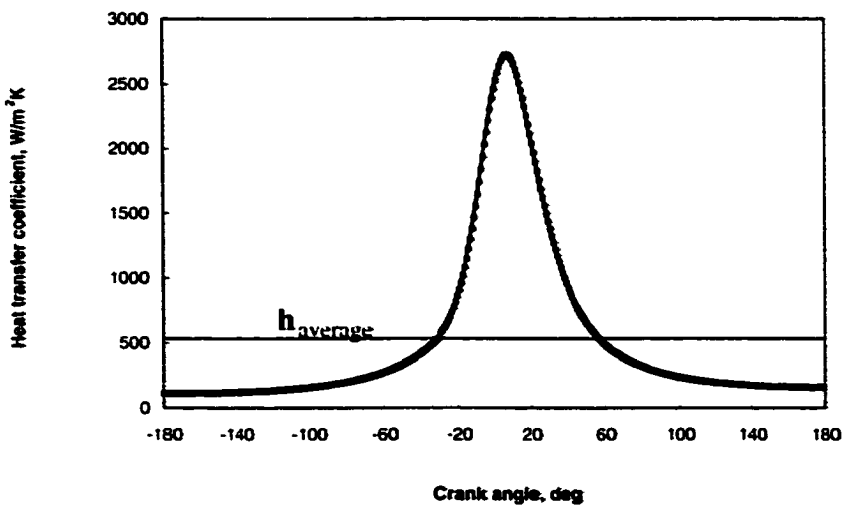

Figure 6.5 Heat transfer coefficient changes with crank angles at WOT, 4000 rpm, equivalence ratio (1.1), start of combustion (-30°), combustion duration (70°), and residual gas fraction (0).

Reproduced with permission of the copyright owner. Further reproduction prohibited without permission.

CHAPTER 7 RESULTS AND DISCUSSIONS

7.1 Air Cycle Thermomechanical Availability Results

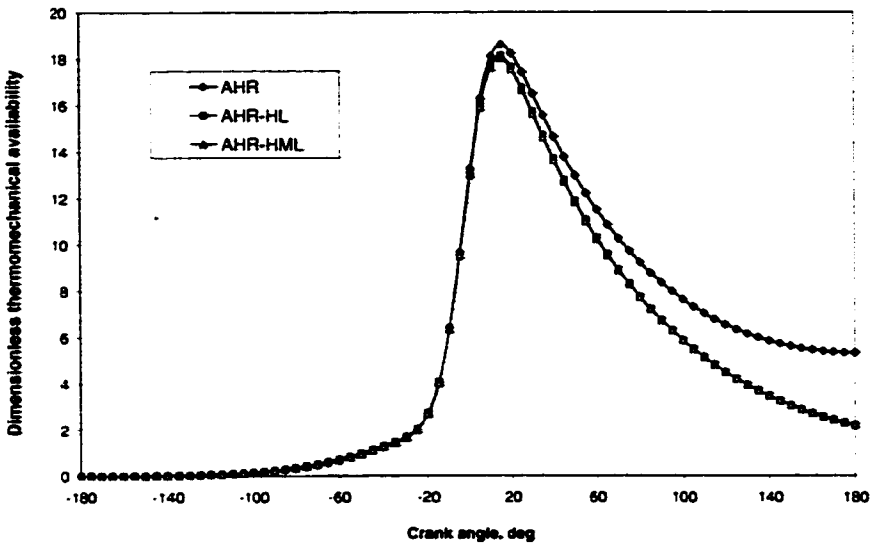

Figure 7.1 Air cycle thermomechanical availability from Method I for arbitrary heat release (AHR), arbitrary heat release with heat loss (AHR-HL), and arbitrary heat release with heat and mass losses (AHR-HML).

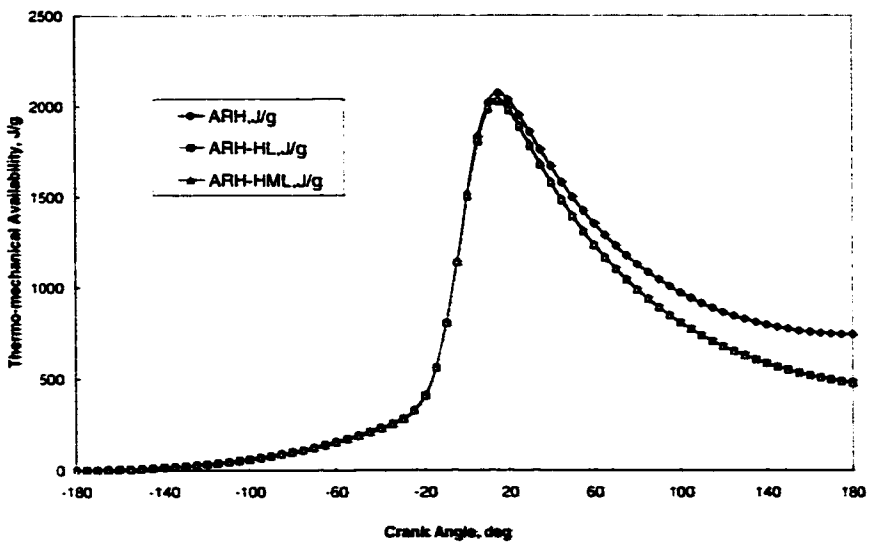

Figure 7.2 Air cycle thermomechanical availability from Method II for arbitrary heat release (AHR), arbitrary heat release with heat loss (AHR-HL), and arbitrary heat release with heat and mass losses (AHR-HML).

Reproduced with permission of the copyright owner. Further reproduction prohibited without permission.

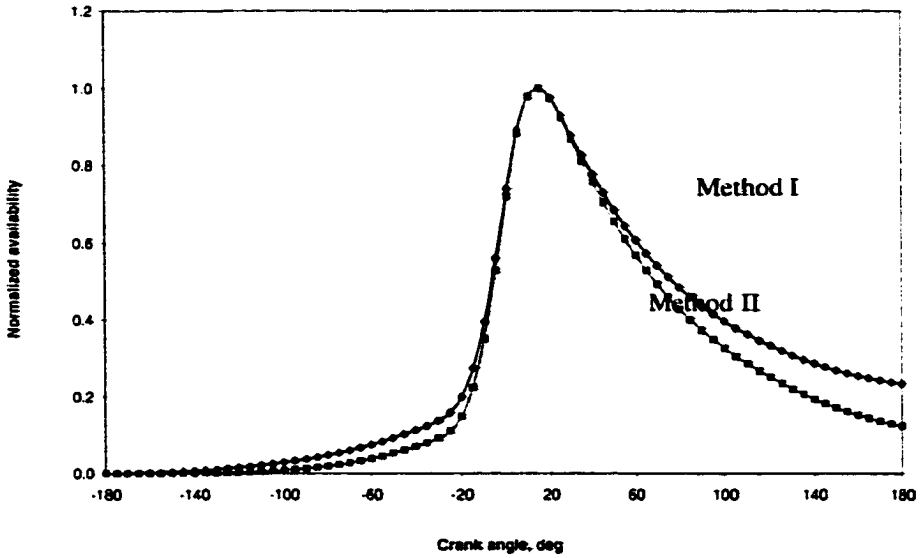

Figure 7.3 Air cycle arbitrary heat release with heat and mass losses (AHR-HML) from Method I & II.

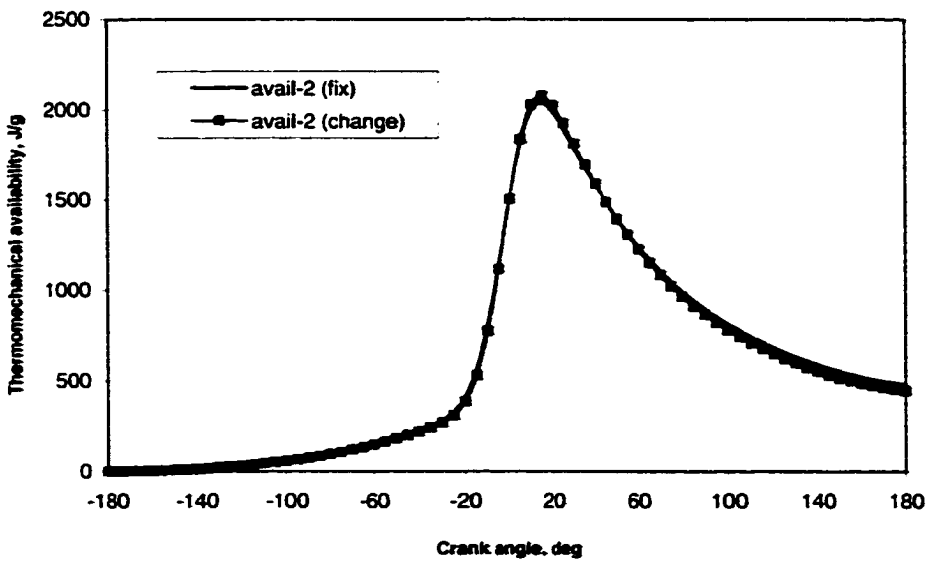

Figure 7.4 Effects of constant and changing specific heat on air cycle thermomechanical availability simulation for arbitrary heat release with heat and mass losses (AHR-HML).

Reproduced with permission of the copyright owner. Further reproduction prohibited without permission.

7.2 Discussion of Air Cycle Availability Results

Fig.7.1 and Fig.7.2 show the thermomechanical availability results for the air cycle arbitrary heat release models using the Method I & II. The results from both methods follow the same trend, and the comparison is shown in Fig. 7.3. The difference shown in Fig. 7.3 is due to the fact that only the Method II considers irreversibilities. The value of the Method I is to predict the maximum thermomechanical availability. For the purpose of comparing the two methods, Method II is normalized by the maximum thermomechanical availability in Fig. 7.3.

Fig. 7.4 shows the effects of specific heat on air cycle thermomechanical availability simulation. Fig 7.5(a) shows the pressure and temperature trend in the simulation. The specific heat has been modified with respect to temperature, shown in Fig. 7.5 (b). It is assumed that air consists of 79% N_2 and 21% O_2.

$$c_p = 0.79(c_p)_{N_2} + 0.21(c_p)_{O_2}$$

The coefficients of the specific heat for nitrogen and oxygen are listed in the Appendix B. As shown in Fig. 7.4, the modified specific heat has little effect on the air cycle thermomechanical availability calculation.

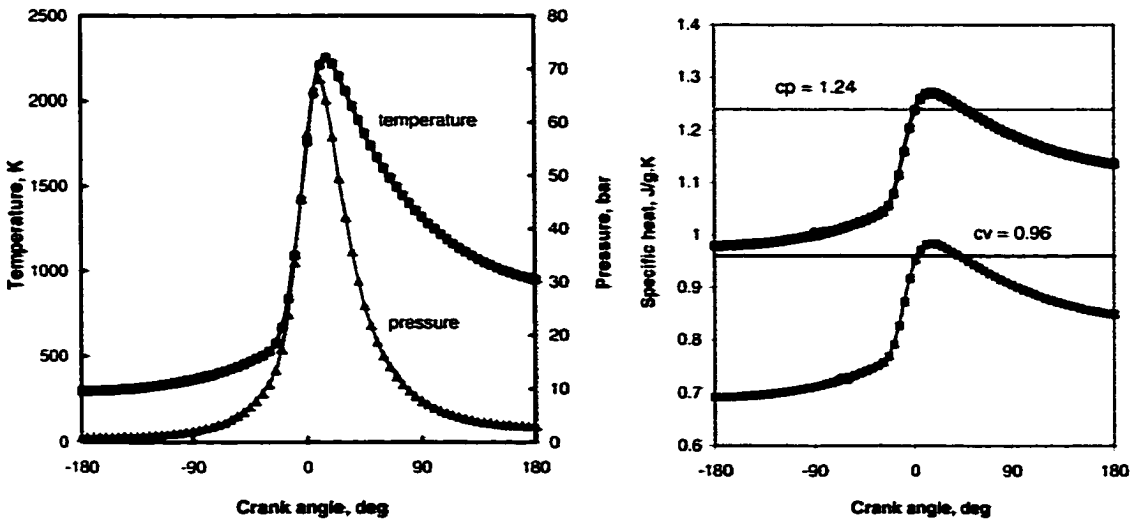

(a) (b)

Figure 7.5 (a) Pressure and temperature versus crank angles for air cycle arbitrary heat release with heat and mass losses (AHR-HML). (b) Constant and varying specific heats for air cycle arbitrary heat release with heat and mass loss (AHR-HML).

Reproduced with permission of the copyright owner. Further reproduction prohibited without permission.

7.3 Fuel-Air Cycle Thermomechanical & Fuel Chemical Availability Results

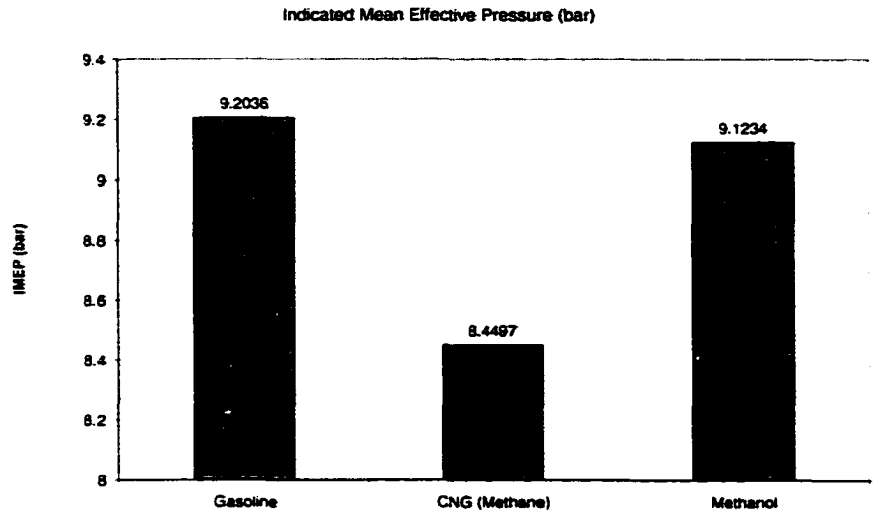

Figure 7.6 Fuel/air cycle indicated mean effective pressure (IMEP) for gasoline, CNG and methanol.

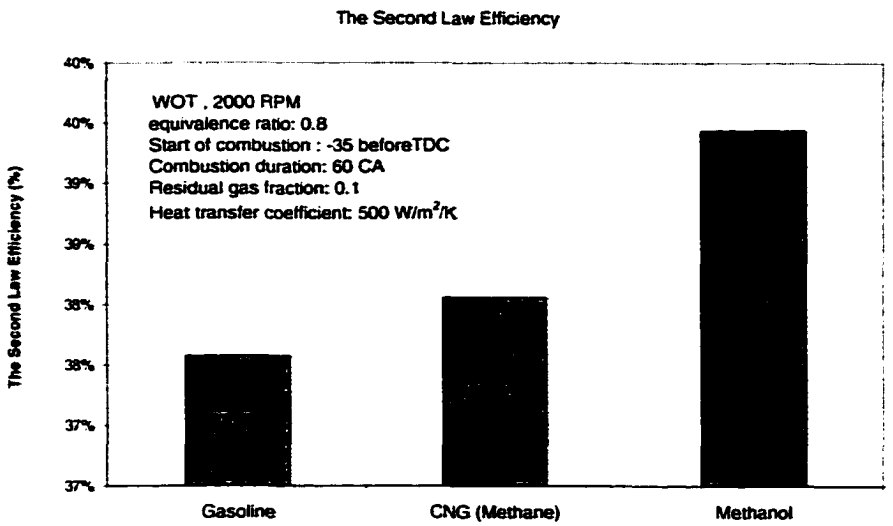

Figure 7.7 Fuel/air cycle second law efficiency for gasoline, CNG and methanol.

Reproduced with permission of the copyright owner. Further reproduction prohibited without permission.

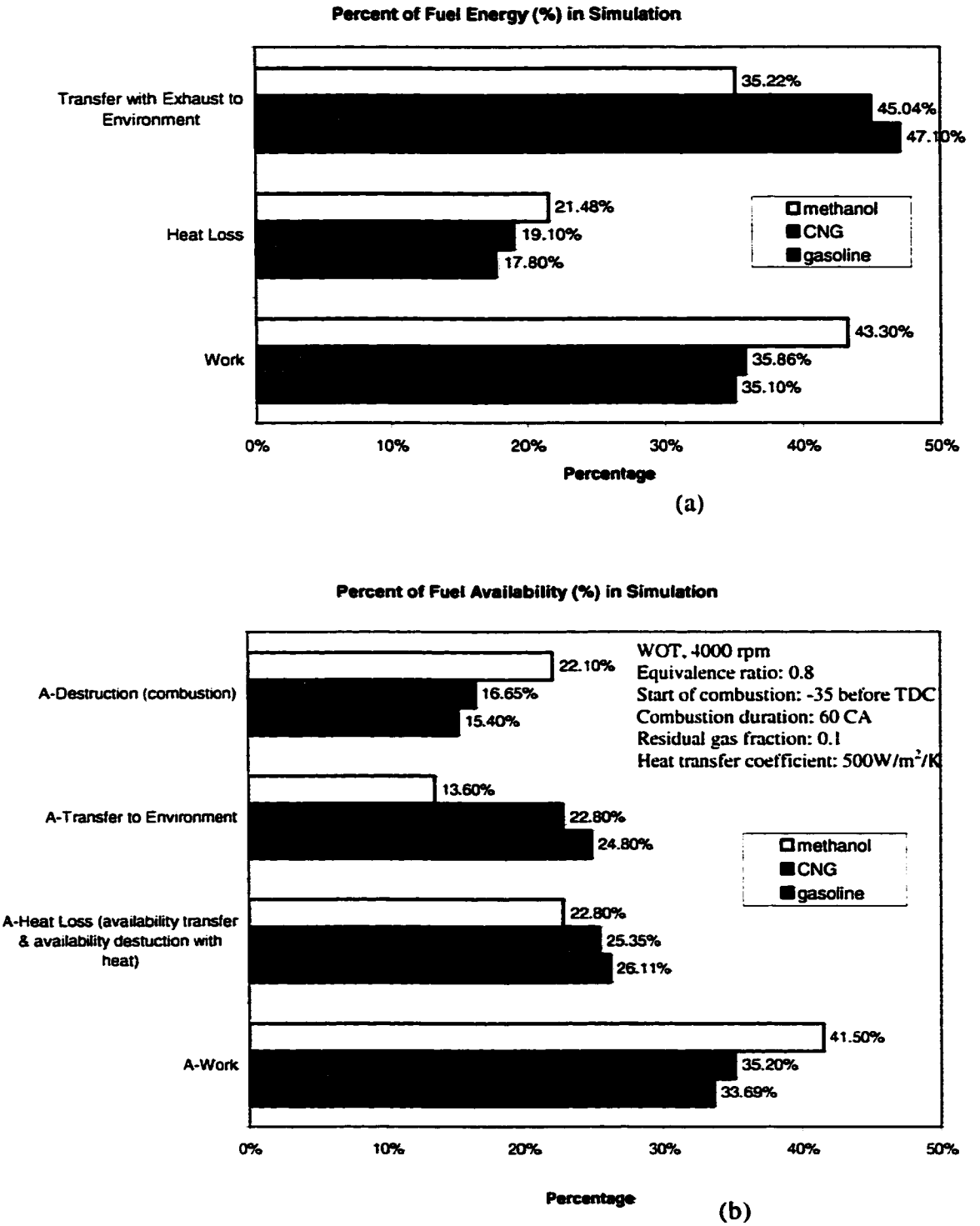

Figure 7.8 The distributions of fuel energy and fuel availability (I) in engine cycle processes for gasoline, CNG and methanol at Φ=0.8.

Reproduced with permission of the copyright owner. Further reproduction prohibited without permission.

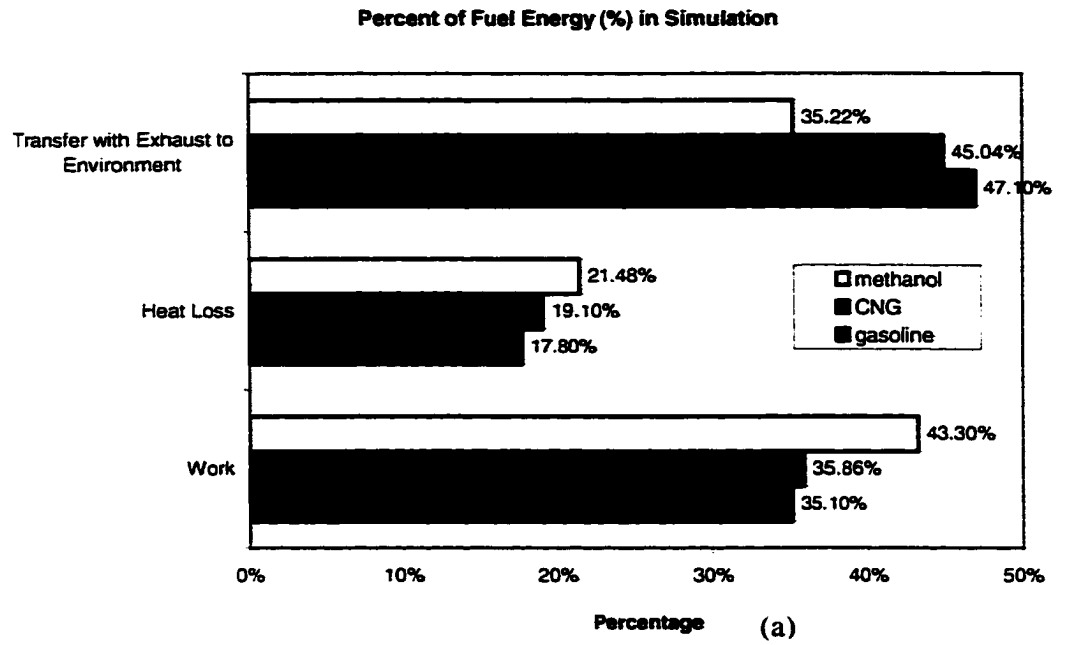

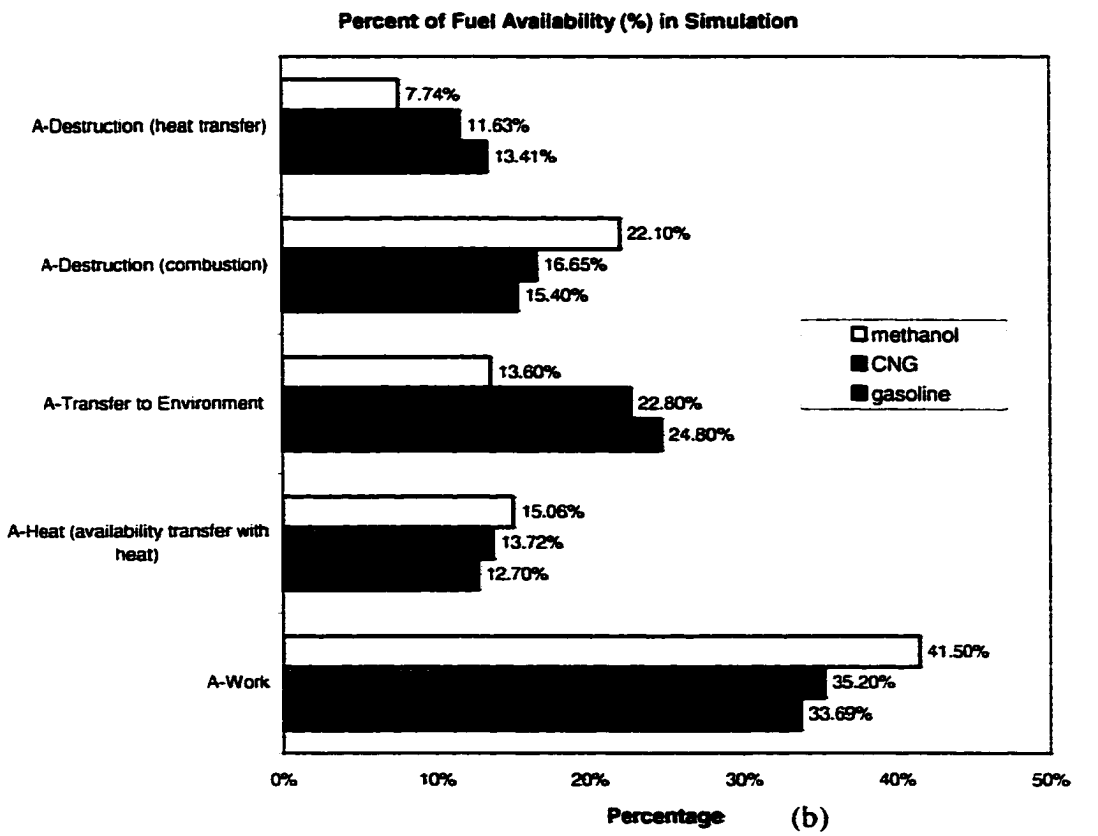

Figure 7.9 The distributions of fuel energy and fuel availability (II) in engine cycle processes for gasoline, CNG and methanol at Φ=0.8.

Reproduced with permission of the copyright owner. Further reproduction prohibited without permission.

7.4 Discussion of Fuel-Air Cycle Availability Results

7.4.1 Indicated Mean Effective Pressure & Second Law Efficiency

Three different fuels, namely gasoline, CNG and methanol, are simulated at the same engine conditions, which are at wide open throttle, 2000 rpm, compression ratio as 10, equivalence ratio as 0.8, start of combustion as 35°bTDC, combustion duration as 60°, residual gas fraction as 0.1, and constant heat transfer coefficient as 500 $W/m^2/K$. The indicated mean effective pressure and the second law efficiency bring us different perspectives.

At the same engine operating conditions, natural gas and methanol have lower calorific values and lower fuel chemical availability than gasoline. The total mass of in-cylinder fuel/air mixture, total calorific values, and initial fuel chemical availability per unit of the in-cylinder mixture are listed in Table 7.1. The engine outputs of CNG and methanol fueled SI engines, reflected in the indicated mean effective pressure in Fig 7.6, are lower than that of gasoline fueled engines. However, Fig. 7.7 indicates that the second law efficiencies of CNG and methanol are higher than that of gasoline at the same engine operating conditions. It exhibits better energy utilization in CNG and methanol fueled SI engines. Higher proportional of total fuel availability can be converted to useful work for CNG and methanol operations.

Table 7-1 Total in-cylinder mass, calorific value, and total specific availability per unit of the in-cylinder mixture for three different fuels

Fuels	Total In-cylinder mass (g)	Calorific Value (J)	Fuel chemical availability (J/g)
Gasoline	0.714	1645.72	2458.1
CNG	0.668	1480.92	2314.9
Methanol	0.696	1322.17	2031.2

In order to illustrate the concept of the second law efficiency, consider a system at steady-state for which energy and availability can be written, respectively, as

Energy in = Energy out (as work) + Energy loss (a)

Reproduced with permission of the copyright owner. Further reproduction prohibited without permission.

Availability in = Availability out (as work) + Availability transfer +
Availability destruction (b)

The energy-based efficiency is

$$\eta = \frac{Energy\ out\ (as\ work)}{Energy\ in} = 1 - \frac{Energy\ loss}{Energy\ in}$$

The second law efficiency makes a clear distinction between energy losses to the environment and internal irreversibilities to the process.

$$\varepsilon = \frac{Availability\ out\ (as\ work)}{Availability\ in} = 1 - \frac{Availability\ transfer + Availability\ destruction}{Availability\ in}$$

The second law efficiency gives a finer understanding of performance than energy-based efficiency. The second law efficiency stresses that both availability transfer losses and internal availability destruction due to irreversibilities need to deal with to improve performance. It is the irreversibilities that are most significant and the more difficult to dealt with.

7.4.2 Distributions of Fuel Energy and Fuel Availability Analyses

The distributions of the fuel energy and availability for gasoline, CNG and methanol were shown in Figure 7.8 and Figure 7.9, using first law and second law analyses. The first law of thermodynamics is the basis for energy accounting in which heat, work and energy transfer with exhaust are balanced. Figure 7.8(a) and Figure 7.9(a) indicate that over 1/3 of the fuel energy (gasoline 47.10%, CNG 45.04%, and methanol 35.22%) is exhausted to the environment.

However, comparison of energy quantities from the first law alone can be misleading. The combined use of the first and second laws makes it possible to distinguish energy which is recoverable (available) from which is unrecoverable (destroyed) in real processes. Figure 7.8(b) and Figure 7.9(b) catalog such differences. The fuel availability

Reproduced with permission of the copyright owner. Further reproduction prohibited without permission.

transferred to the environment for gasoline is 24.80%, CNG 22.80%, and methanol 13.60%, which is almost half of the values predicted from the first law. This amount of fuel availability transferred to the environment is still recoverable from the second law point of view. The simulation captures the availability destruction due to combustion with respect to crank angles. The fuel availability destroyed due to combustion process for gasoline is 15.40%, CNG 16.65%, and methanol 22.10%. This amount of energy destroyed during combustion and other processes cannot be recovered any more. In order to have a general picture of availability with heat loss, Figure 7.8(b) shows the percentages of availability with heat loss. It is 26.11% for gasoline, 25.35% for CNG, 22.80% for methanol. Figure 7.9(b) separately listed the percentages of availability transfer with heat, which is recoverable energy, and availability destruction with heat, which is unrecoverable energy.

7.5 Parametric Study on DaimlerChysler V8 Engine Performance

The major operating variables that affect SI engine performance, efficiency, and emissions at any given load and engine speed are: spark timing, combustion duration, equivalence ratio, and residual gas fraction that are recycled mainly for NO_x emission control. The effects of these variables have been reviewed in the following.

7.5.1 Spark Timing and Combustion Duration

The combustion process should be properly adjusted relative to the top dead center, in order to obtain the maximum torque. If ignition is too early, there will be too much pressure rise before the end of the compression stroke, which is as a waste and does not contribute to the engine output. Also, the peak pressure and temperature may be sufficient to cause knock, due to the early ignition. Conversely, if ignition is too late, the work done by the piston during the compression stroke is reduced. So is the work done on the piston during the expansion stroke, since the pressures including the peak pressure during the cycle are reduced. Therefore, the ignition timing has to be optimized and controlled accurately for maximum engine torque at fixed engine speed and equivalence ratio. It is often called MBT, minimum advance for best torque. Timing which is

Reproduced with permission of the copyright owner. Further reproduction prohibited without permission.

advanced or retarded from this optimal point gives lower torque. The definition of MBT timing is somewhat arbitrary. As the maximum torque is fairly flat the ignition timing is usually arranged to occur on the late side of the maximum [14].

The effects of sparking timing on the unburned and burned mixture temperatures are shown in Figure 7.10. With advancing the sparking timing, both unburned and burned mixture temperatures increase. This is because combustion occurs when the cylinder mixtures are compressed. The unburned and burned mixture temperatures decrease as the spark timing is retarded, because combustion occurs when cylinder pressures are lower.

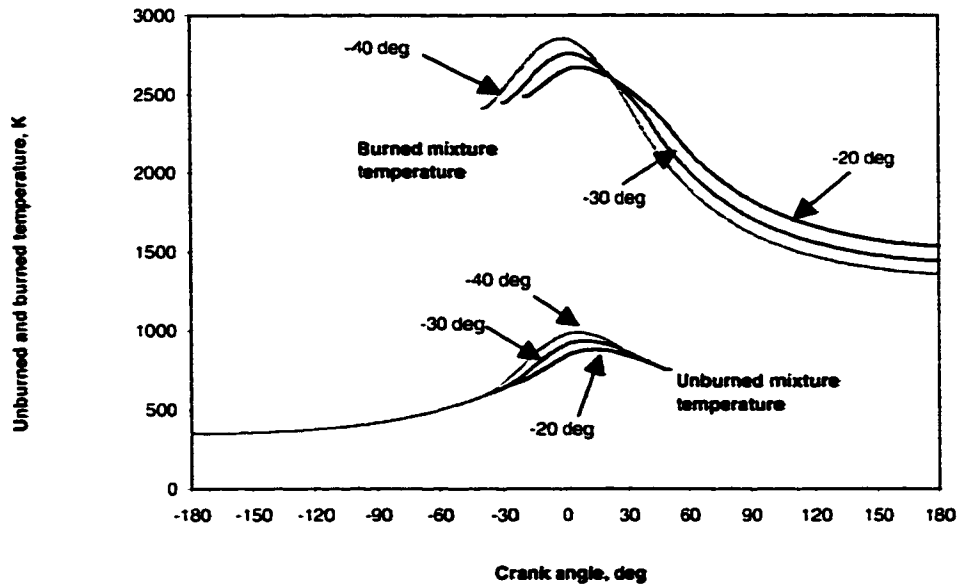

Figure 7.10 Effects of sparking timing on unburned and burned mixtures temperature, for V8 engine at equivalence ratio (1.1), residual gas fraction (0.0), combustion duration (70°), WOT, and 4000 rpm.

The optimum spark setting will depend on the rate of flame development and propagation, the length of the flame travel path across the combustion chamber, and the details of the flame termination process after it reaches the wall. These depend on engine design and operating conditions, and the properties of the fuel, air and burned gas mixture. MBT timing also depends on engine speed. As engine speed increases the spark timing must be advance to maintain optimum timing. Optimum spark timing depends on engine load as well. As load and intake manifold pressure are decreased, the spark timing

Reproduced with permission of the copyright owner. Further reproduction prohibited without permission.

must be further advanced to maintain optimum engine performance. The simulated pressure versus crank angle curves shown Fig. 7.11 allow us to understand why torque varies as spark timing is varied relative to TDC.

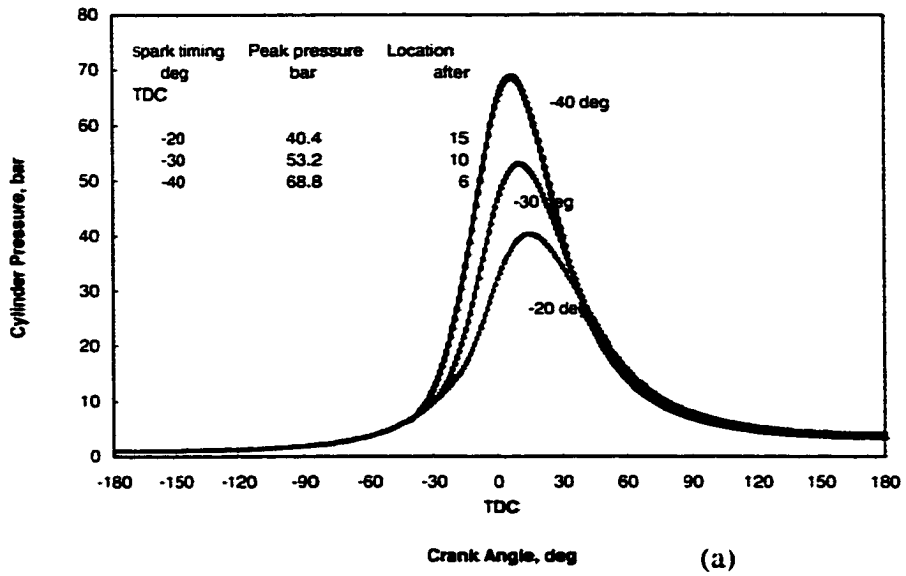

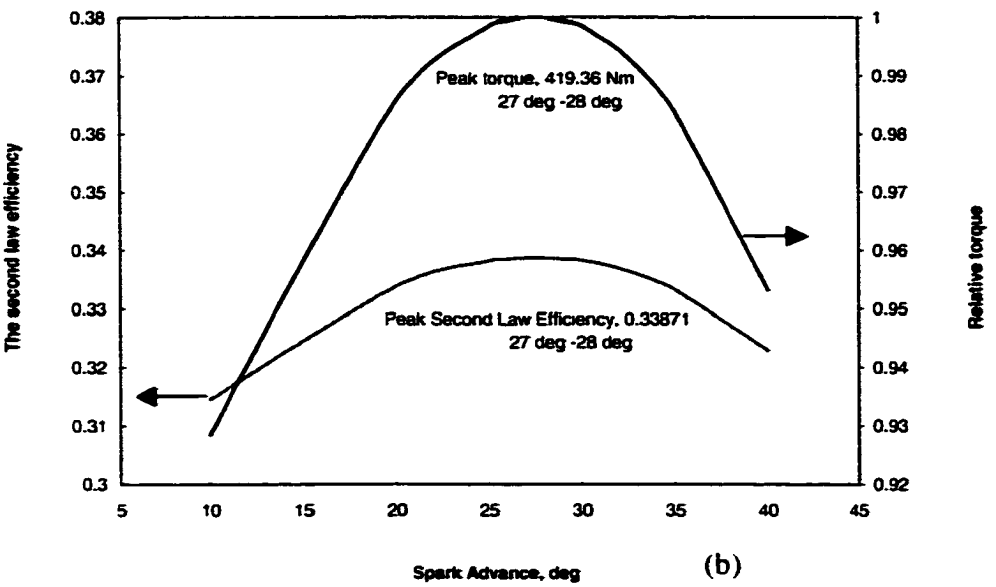

Figure 7.11 (a) V8 engine simulated cylinder pressure versus crank angle for overadvanced spark timing (40°), MBT timing (30°), and retarded timing (20°). (b) Effects of spark advance on indicated torque and the second law efficiency for V8 engine at combustion duration (70°), equivalence ratio (1.1), residual gas fraction (0.0), WOT and 4000rpm.

Reproduced with permission of the copyright owner. Further reproduction prohibited without permission.

For the V8 engine CNG operation, Fig. 7.12(a) shows the availability transfer with work is the best for MBT timing (30° before TDC). Fig 7.12(b) shows the effects of combustion duration on availability transfer with work. Extending the combustion duration decreases the amount of work that can be extracted from the expansion process. It is due to the fact that the cylinder pressure decreases faster during expansion and the late burning mixtures are not expanded to do useful work effectively.

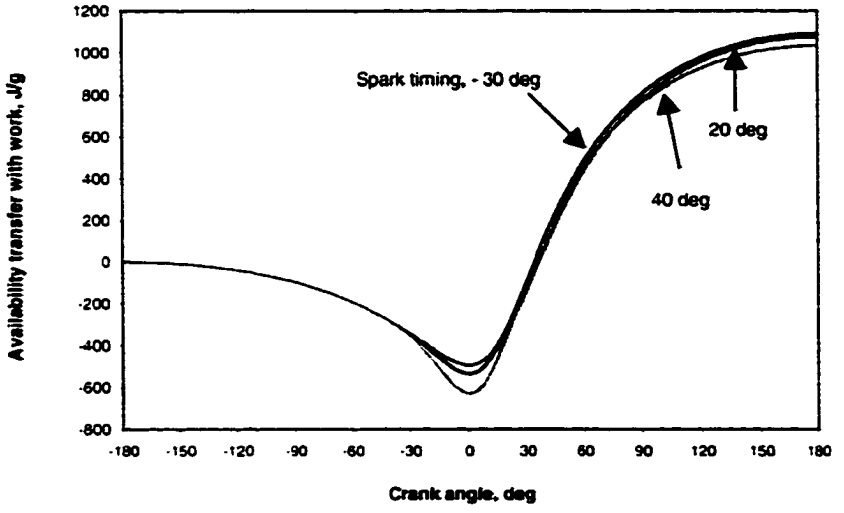

Figure 7.12(a) Effects of spark timing on availability transfer with work for V8 engine at combustion duration (70°), equivalence ratio (1.1), residual gas fraction (0.0), WOT and 4000rpm.

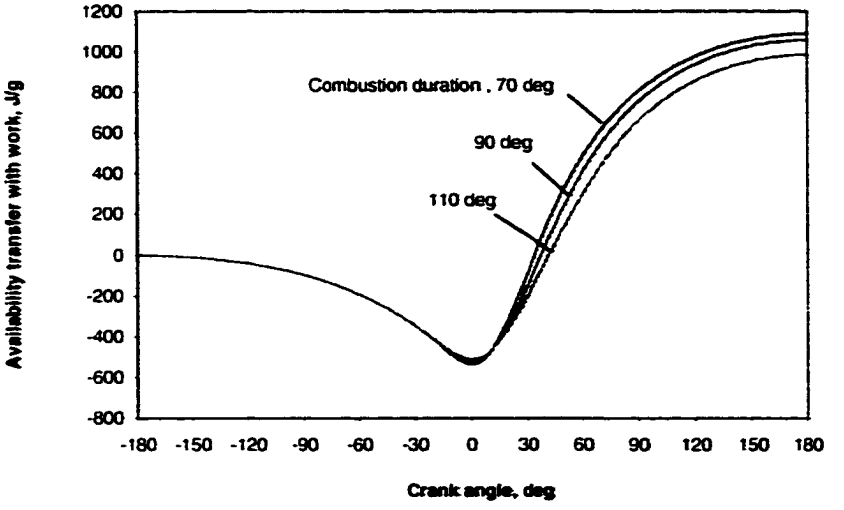

Figure 7.12(b) Effects of combustion duration on availability transfer with work for V8 engine at spark timing (- 30° before TDC), equivalence ratio (1.1), residual gas fraction (0.0), WOT and 4000 rpm.

Reproduced with permission of the copyright owner. Further reproduction prohibited without permission.

Figure 7.13 shows the availability destruction due to combustion changing with spark timing. As the spark timing is retarded, the start point of combustion destruction moves toward TDC. The results show that the spark timing has little effect on the fuel availability destruction and the rate of availability destruction is the same for all spark timing. However, the MBT timing (- 30° before TDC) does have relatively small combustion destruction. The final level is reached faster for over advanced spark timing (- 40° before TDC) due to the rapidly decreasing temperature after combustion shown in Figure 7.10 and higher heat loss shown in Figure 7.14. Since the final burned gas temperature at - 40° before TDC is relatively lower, its combustion destruction is relatively smaller.

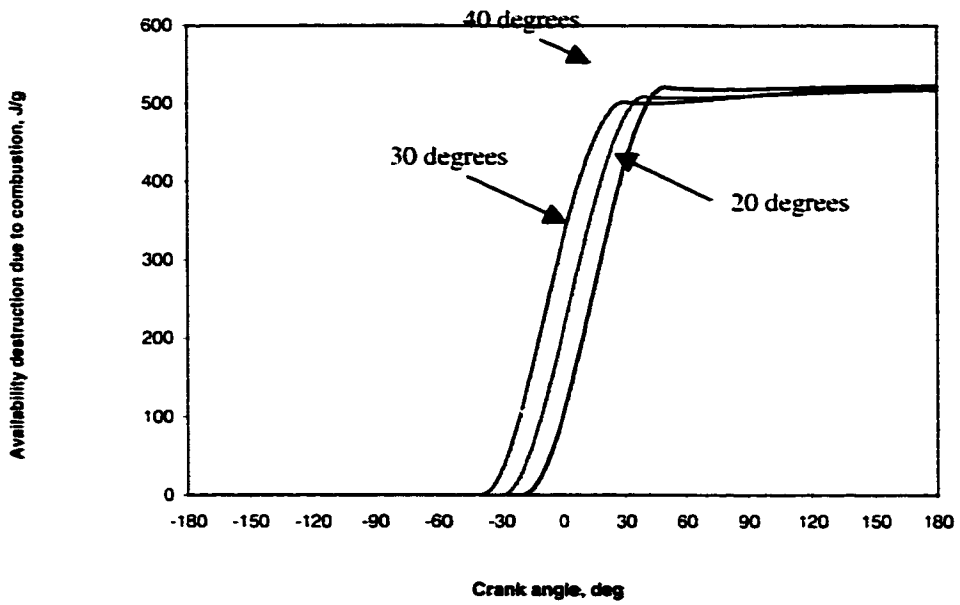

Figure 7.13 Effects of spark timing on availability destruction due to combustion for V8 engine at combustion duration (70°), equivalence ratio (1.1), residual gas fraction (0.0), WOT and 4000rpm.

Figure 7.15 shows the availability destruction due to combustion changing with combustion duration. As the combustion duration decreases from 110° to 90° , the combustion destruction decreases but the slope of availability destruction increases. The prolonged combustion duration results in poor combustion in SI engines and higher

Reproduced with permission of the copyright owner. Further reproduction prohibited without permission.

temperature in the expansion process, which could overheat the engine and further deteriorate the volumetric efficiency of the engine operation.

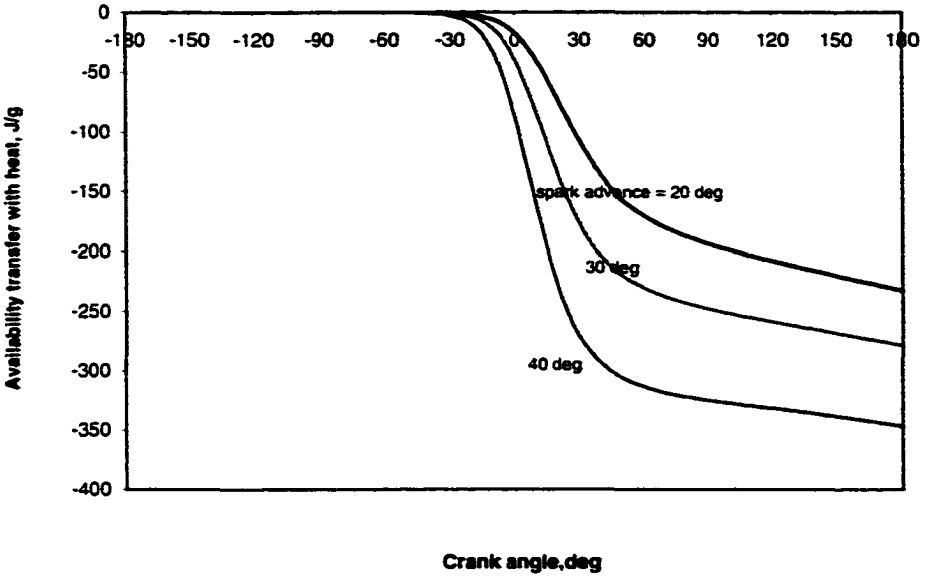

Figure 7.14 Effects of spark timing on availability with heat transfer for V8 engine at combustion duration (70°), equivalence ratio (1.1), residual gas fraction (0.0), WOT and 4000rpm.

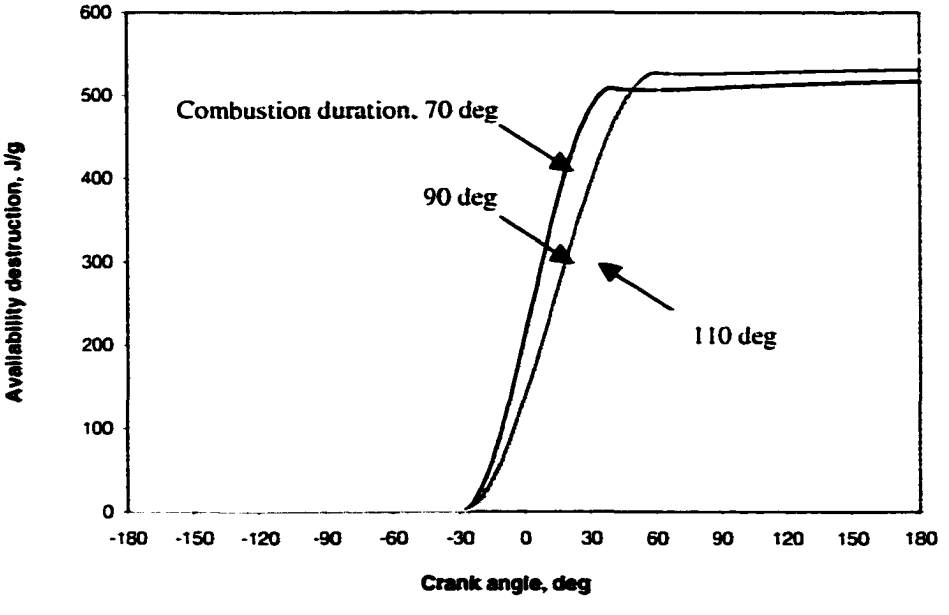

Figure 7.15 Effects of combustion duration on the availability destruction due to combustion for V8 engine at spark timing (-30° before TDC), equivalence ratio (1.1), residual gas fraction (0.0), WOT and 4000 rpm.

Reproduced with permission of the copyright owner. Further reproduction prohibited without permission.

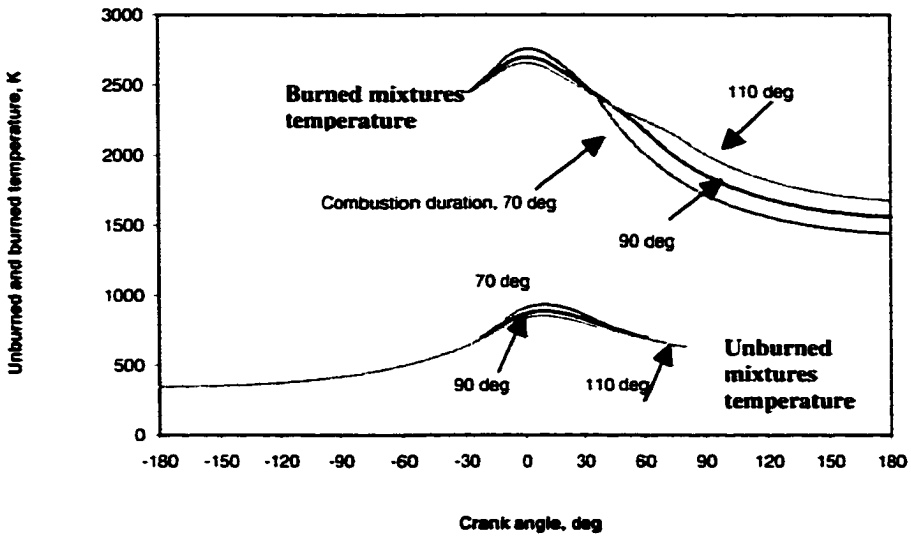

Figure 7.16 Effects of combustion duration on unburned and burned mixtures temperature for V8 engine at spark timing (-30° before TDC), equivalence ratio (1.1), residual gas fraction (0.0), WOT and 4000 rpm.

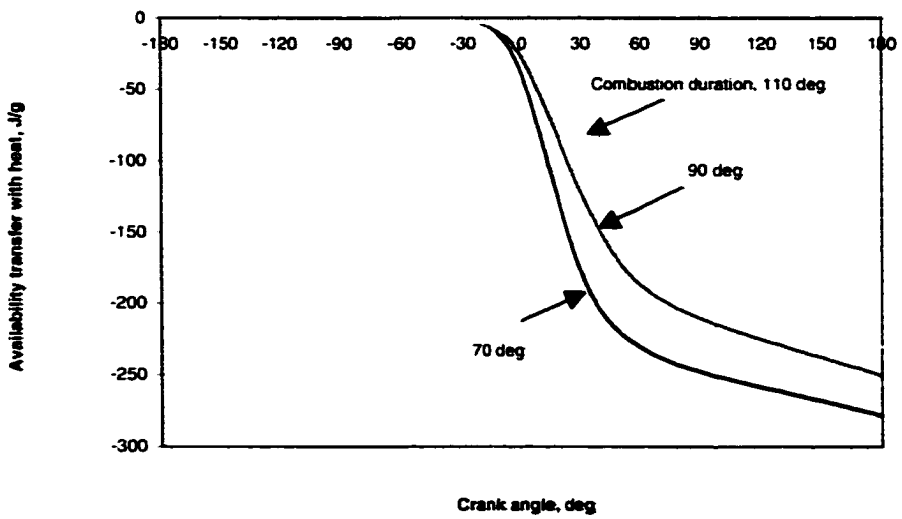

Figure 7.17 Effects of combustion duration on availability with heat for V8 engine at spark timing (-30° before TDC), equivalence ratio (1.1), residual gas fraction (0.0), WOT and 4000 rpm.

The final burned mixture temperature of the prolonged combustion duration (110°) is highest in Figure 7.16, which also reflects the higher combustion destruction in Figure 7.15. The lower availability transfer with heat for 110° combustion duration in Figure 7.17 is mainly due to its corresponding lower peak temperature.

Reproduced with permission of the copyright owner. Further reproduction prohibited without permission.

7.5.2 Equivalence Ratio

The unburned mixture in the engine cylinder consists of CNG fuel, air and residual gases. The residual gases together with recycled exhaust can be used for NO_x control for SI engine operation. Mixture composition during combustion is critical, since it determines the development of the combustion process which governs engine operating characteristics.

The effects of equivalence ratio on the second law efficiency and the indicated mean effective pressure are shown in Figure 7.18 and Fig. 7.19, respectively. The maximum second law efficiency occurs on the lean side, while the maximum indicated mean effective pressure is on the rich side at $\Phi = 1.1$.

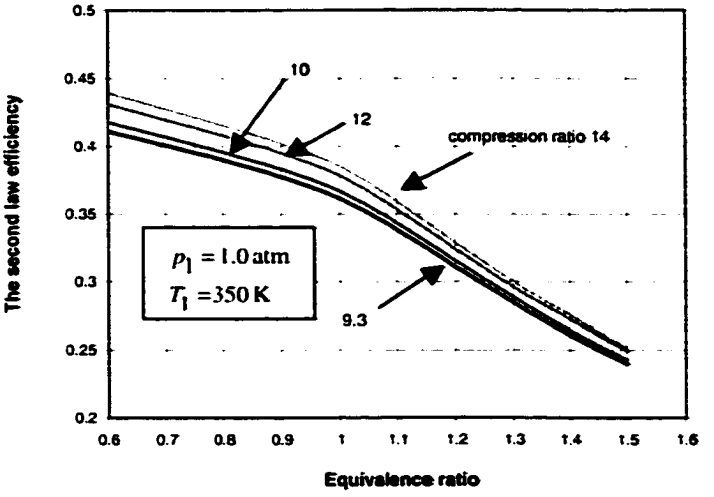

Figure 7.18 Fuel/air cycle simulation results for the second law efficiency as a function of equivalence ratio and compression ratio at spark timing (- 30° before TDC), combustion duration (70°), residual gas fraction (0.0), WOT and 4000 rpm.

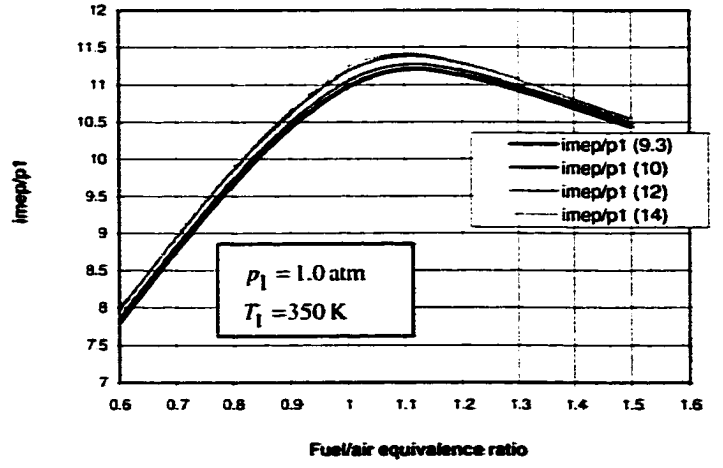

Figure 7.19 Fuel/air cycle simulation results for indicated mean effective pressure as a function of equivalence ratio and compression ratio at spark timing (- 30° before TDC), combustion duration (70°), residual gas fraction (0.0), WOT and 4000 rpm.

Reproduced with permission of the copyright owner. Further reproduction prohibited without permission.

The temperature and pressure increase while equivalence ratio changes from lean to rich mixture at 1.1, which delivers increased power and imep. As the mixture is enriched above equivalence ratio 1.1, the imep decreases, due to the decreasing combustion efficiency.

For lean mixtures, the second law efficiency increases almost linearly as fuel/air equivalence ratio increases. Combustion of mixtures leaner than stoichiometric produces combustion products at lower temperature, and with less dissociation of the molecules CO_2 and H_2O. A greater fraction of the fuel's energy is transferred as work to the piston during expansion. In other words, the second law efficiency increases, and the fraction of the fuel chemical availability rejected to the exhaust system, availability destruction due to combustion and availability with heat lost decrease. For rich mixtures, the second law efficiency decreases from its stoichiometric value, due to the incomplete combustion and the deterioration of the fuel availability utilization.

Figure 7.20 shows the indicated specific fuel consumption and the indicated mean effective pressure of V8 spark ignition engine at the wide-open throttle and 4000 rpm.

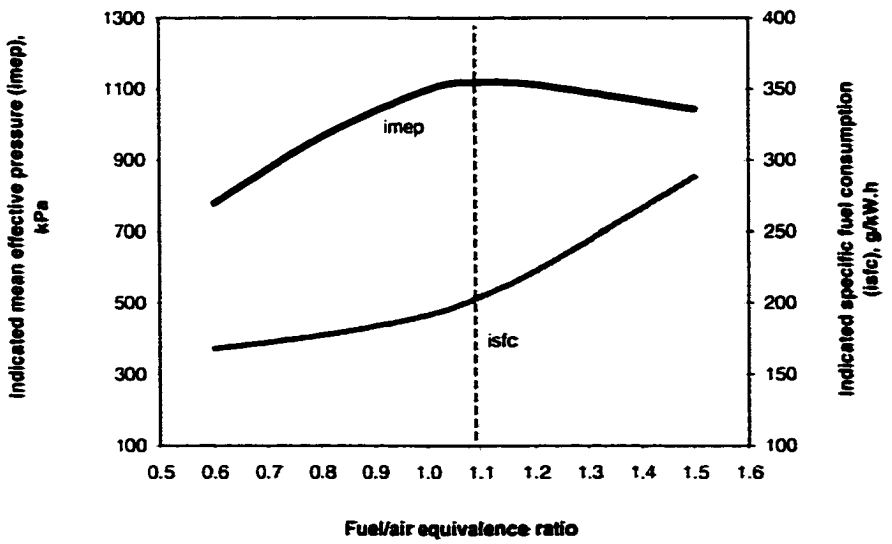

Figure 7.20 Effects of the fuel/air equivalence ratio variations on indicated mean effective pressure, and specific fuel consumption for V8 engine at spark timing (-30° before TDC), combustion duration (70°), residual gas fraction (0.0), WOT and 4000 rpm.

Reproduced with permission of the copyright owner. Further reproduction prohibited without permission.

At the wide open throttle, the objective is to obtain maximum power. Increases in power can be obtained by increasing the equivalence ratio. Therefore, the mixture is enriched to obtain the maximum power at WOT, with corresponding equivalence ratio at $\Phi = 1.1$.

For part load operation, the equivalence ratio is usually set close to achieve a minimum fuel consumption while avoiding partial burning or misfire in one or more cylinders. At very light load, the mixture is rich to compensate for slower flame speeds at lower mixture density and increased residual fraction.

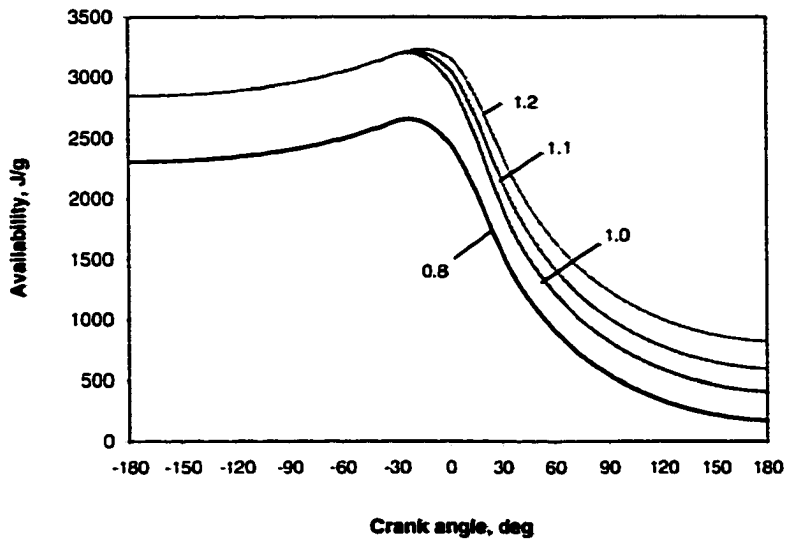

Figure 7.21 Effects of equivalence ratio on the total availability for V8 engine at spark timing (- 30° before TDC), combustion duration (70°), residual gas fraction (0.0), WOT and 4000 rpm.

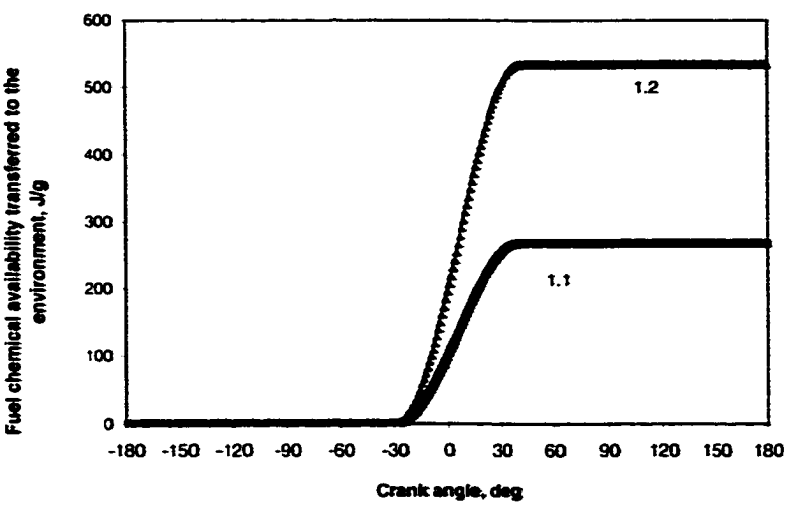

Figure 7.22 Effects of equivalence ratio on the fuel chemical availability transferred to the environment for V8 engine at spark timing (-30° before TDC), combustion duration (70°), residual gas fraction (0.0), WOT and 4000 rpm.

Reproduced with permission of the copyright owner. Further reproduction prohibited without permission.

When the equivalence ratio is increased from 0.8 to 1.2, the total availability, including thermomechanical and fuel chemical availability, increase as shown in Figure 7.21. This reflects the increasing amount of fuel present, but as equivalence ratio is increased beyond stoichiometric condition, the total usable or available fuel chemical availability is equal to the same amount which is at stoichiometric condition. The extra fuel chemical availability for rich mixture cannot be utilized during the combustion process, and is transfer to the environment. Figure 7.22 demonstrates the transferred fuel chemical availability to the environment, which cannot be converted to combustion products.

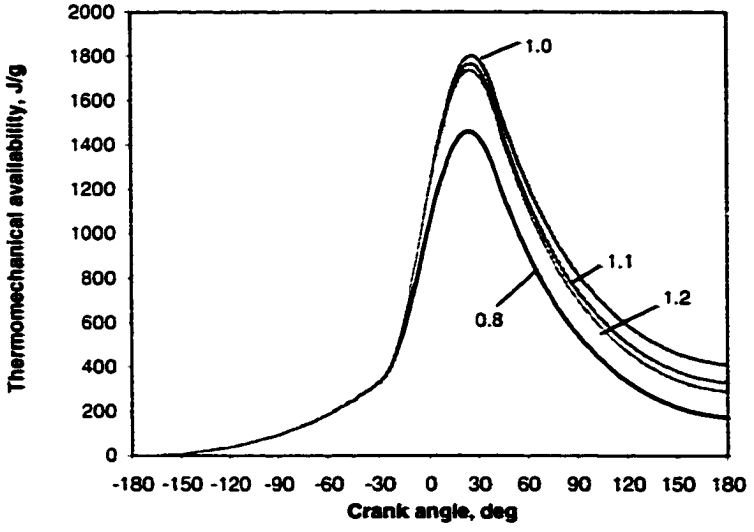

Figure 7.23 Effects of equivalence ratio on the thermomechanical availability for V8 engine at spark timing (- 30° before TDC), combustion duration (70°), residual gas fraction (0.0), WOT and 4000 rpm.

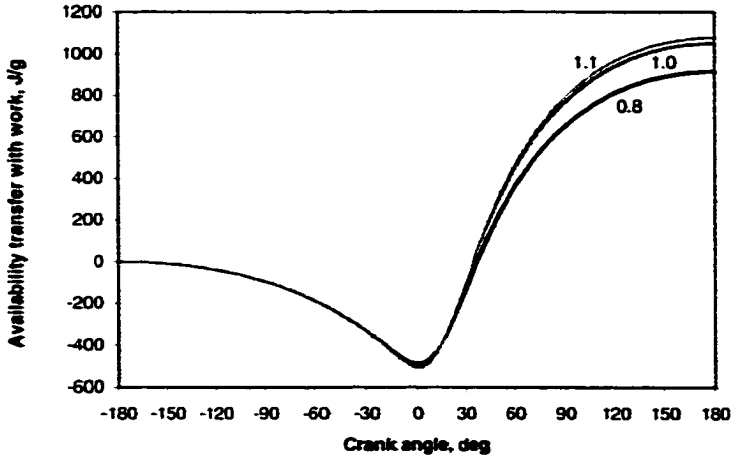

Figure 7.24 Effects of equivalence ratio on availability transfer with work for V8 engine at spark timing (- 30° before TDC), combustion duration (70°), residual gas fraction (0.0), WOT and 4000 rpm.

Reproduced with permission of the copyright owner. Further reproduction prohibited without permission.

When the equivalence ratio is at stoichiometric, the temperature is at maximum. Thus, it has maximum thermomechanical availability shown in Figure 7.23. However, because equivalence ratio of 1.1 gives the maximum indicated mean effective pressure, it has the highest availability transfer with work, shown in Figure 7.24. Figure 7.25 shows how the combustion destruction increases while equivalence ratio increases. This corresponds to the second law efficiency decrease as the equivalence ratio increases from 0.8 to 1.2.

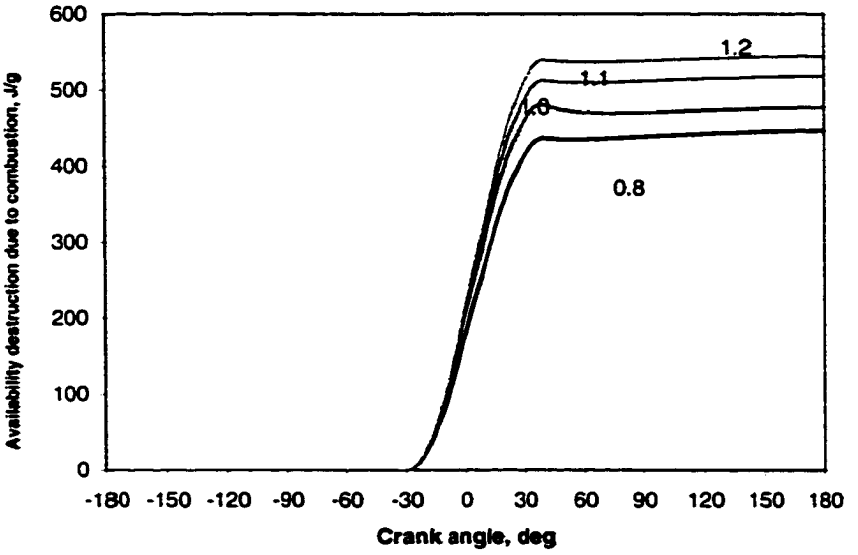

Figure 7.25 Effects of equivalence ratio on availability destruction due to combustion in V8 engine simulation for V8 engine at spark timing (-30° before TDC), combustion duration (70°), residual gas fraction (0.0), WOT and 4000 rpm.

7.5.3 Residual Gas Fraction

The magnitude of the residual gas fraction in the cylinder during the compression process affects the volumetric efficiency and engine performance directly, and efficiency and emissions through its effect on thermodynamic properties of the engine mixture. The residual gas fraction used in the current program is simply defined as the fraction of in-cylinder mass at the end of the blowdown process to the in-cylinder mass at the beginning of the blowdown process in the expansion stroke. In fact, the residual gas

Reproduced with permission of the copyright owner. Further reproduction prohibited without permission.

fraction is primarily a function of inlet and exhaust pressures, speed, compression ratio, valve timing, and exhaust system dynamics.

The thermomechanical availability, shown in Figure 7.26, is significantly affected by the residual gas fraction, because the residual gas displaces the unburned fuel air mixture and thus decreases the amount of combustible mixture in the cylinder. The decrease in thermomechanical availability is essentially in proportion to the amount of fuel air mixture displaced. The availability transfer with work, shown in Fig. 7.27, also shows that it increases with reducing residual gas fraction.

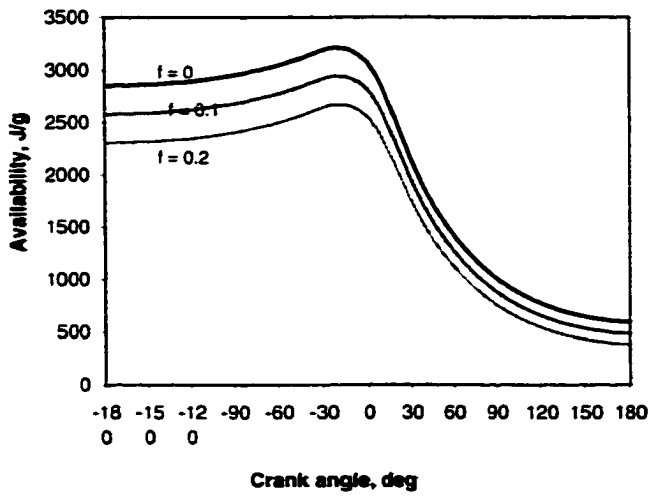

Figure 7.26 Effects of residual gas fraction on the total availability for V8 engine at spark timing (-30° before TDC), combustion duration (70°), equivalence ratio (1.1), WOT and 4000 rpm.

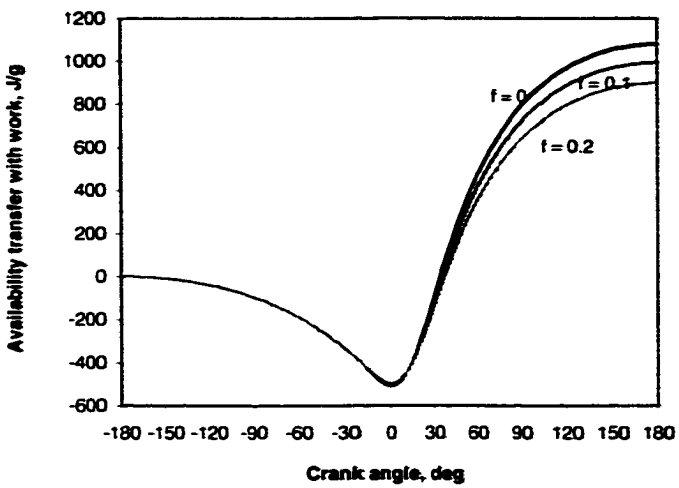

Figure 7.27 Effects of residual gas fraction on the availability transfer with work for V8 engine at spark timing (-30° before TDC), combustion duration (70°), equivalence ratio (1.1), WOT and 4000 rpm.

Reproduced with permission of the copyright owner. Further reproduction prohibited without permission.

Figure 7.28 shows that the combustion destruction decreases with increasing residual gas fraction. As certain amount of residual gas replace the initial fresh fuel and air mixture, combustion destruction decreases due to the low combustion temperature in the cylinder.

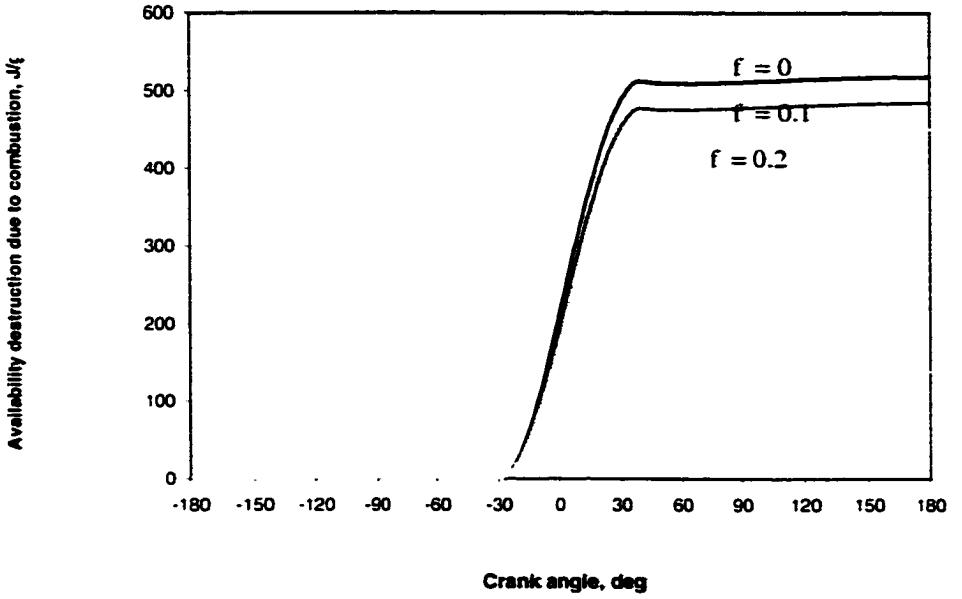

Figure 7.28 Effects of residual gas fraction on availability destruction due to combustion for V8 engine at spark timing (-30° before TDC), combustion duration (70°), equivalence ratio (1.1), WOT and 4000 rpm.

7.5.4 Compression Ratio

The Otto cycle efficiency increases continuously with compression ratio. However, in an actual engine, some processes, such as combustion rate and stability, heat transfer, and mechanical friction which influence engine performance and efficiency, vary with changes in compression ratio. While the geometric compression ratio (the ratio of maximum to minimum cylinder volume) is well defined, the actual compression and expansion processes in engines depend on valve timing details. The intake valve opening typically occurs 10° to 25° before TDC, while the intake valve closing usually falls in the range of 40° to 60° after BDC, in order to bring in enough fresh charge while cylinder pressure is below the intake manifold pressure. Exhaust valve opening occurs at 50° to

Reproduced with permission of the copyright owner. Further reproduction prohibited without permission.

60° before BDC to achieve effective removal of combustion products. Exhaust valve closing, which ends the exhaust process and determines the duration of the valve overlap period, typically falls in the range 8° to 20° after TDC. Furthermore, the ability to increase the compression ratio is limited by the octane number of fuels used in SI engines and knock. CNG can be operated at a compression ratio of 11-13, which is greater than gasoline fueled engines.

The effect of compression ratio on SI engine performance and efficiency over a wide range of compression ratio is examined. Figure 7.29 shows results obtained at wide-open throttle at 4000 rpm. The peak indicated mean effective pressure is at the compression ratio range from 12 to 15. The maximum second law efficiency is at the compression ratio of about 17. Further increasing the compression ratio, the second law efficiency and indicated mean effective pressure decrease. It is mainly due to the increasing surface/volume ratio and slower combustion. In a real engine, friction loss will reduce gains due to higher compression ratio.

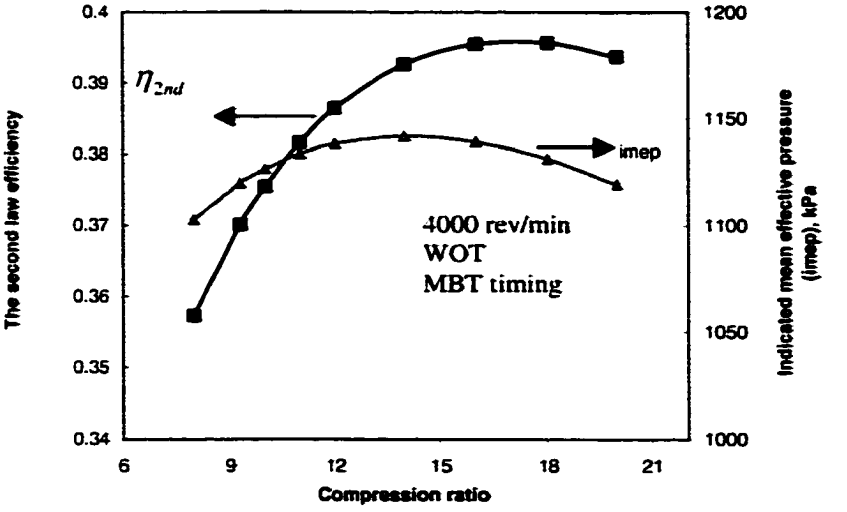

Figure 7.29 Effects of compression ratio on indicated mean effective pressure and the second law efficiency at spark timing (-30° before TDC), combustion duration (70°), equivalence ratio (1.1), residual gas fraction (0.0), WOT and 4000 rpm. Equivalence ratio and spark timing are set for maximum torque and indicated mean effective pressure.

Reproduced with permission of the copyright owner. Further reproduction prohibited without permission.

Figure 7.30 illustrates the effects of compression ratio on the availability destruction due to combustion. As compression ratio increases, the combustion destruction increases slightly. However, at the end of expansion process, it almost reaches the same level. This illustrates that increasing compression ratio has little negative effect on the availability destruction due to combustion.

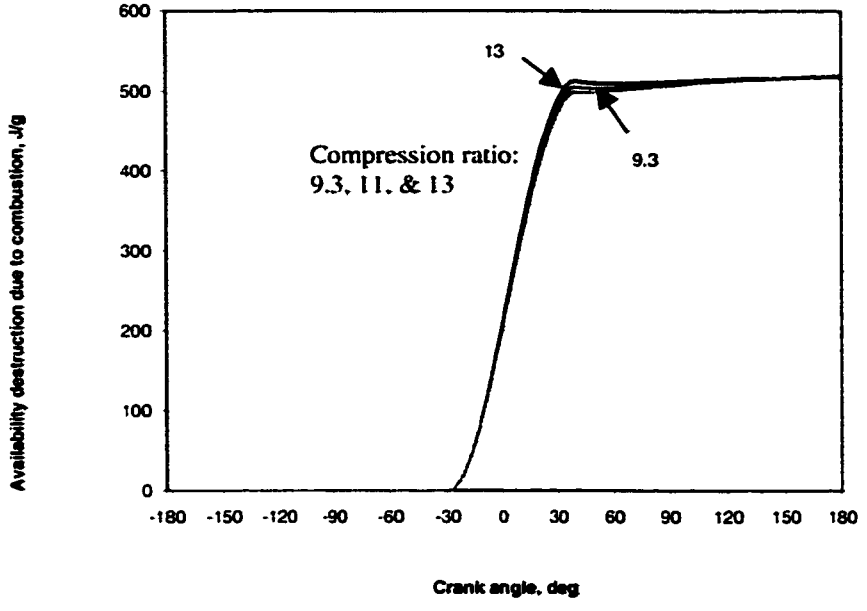

Figure 7.30 Effects of compression ratio on the availability destruction due to combustion at spark timing (-30° before TDC), combustion duration (70°), equivalence ratio (1.1), residual gas fraction (0.0), WOT and 4000 rpm.

7.6 Comparison of Optimized CNG and Gasoline Fueled SI engine operations

The optimal operating conditions for DaimlerChrysler V8 engine are researched throughout the range of engine parameters of interest. The spark timing range is varied from 20° to 50° before TDC, the combustion duration between 80° and 110°, the residual gas from 0 to 0.2, and the fuel/air equivalence ratio changes from lean to rich mixture, 0.8 to 1.2.

As discussed in the parametric studies, MBT timing for V8 engine is 30° before TDC. Its associated optimal combustion duration is simulated as 70° crank angle. Although the

Reproduced with permission of the copyright owner. Further reproduction prohibited without permission.

maximum second law efficiency occurs at lean mixture with equivalence ratio around 0.8, the peak indicated mean effective pressure occurs at rich mixture with equivalence ration of 1.1. The residual gas fraction has been selected as 0 in order to maintain a high availability transfer with useful work. Therefore, V8 engine's optimal wide open throttle maximum best torque conditions are set as follows: spark timing as 30° before TDC, combustion duration as 70° crank angle, equivalence ratio as 1.1, and residual gas fraction as 0, while keeping the original compression ratio of 9.3. Based on the high octane number for CNG, the compression ratio for CNG SI engine operation could be 12:1. Although this increase in compression ratio could increase engine output, it might not contribute significantly due to simultaneously increasing friction (mechanical) losses.

The second law efficiency still remains at a relative high value, while choosing a slight rich condition at wide open throttle. In addition, such engine operation condition is optimal for emission control by using catalytic converter in SI engine.

Optimization is further investigated by assuming gasoline fueled version of the same engine. The optimal engine conditions for gasoline operation are investigated following the same way as described in the parametric studies for CNG operation. As mentioned, the crucial point is to find out the MBT timing and its corresponding combustion duration for gasoline operation. The optimal sparking timing is 25° before TDC, and combustion duration is 60° crank angle, while optimal equivalence ratio is 1.2. The optimal residual gas fraction is set to 0. The same compression ratio of 9.3 is used in the gasoline case.

Figure 7.31 displays the terms[4] in availability balance with respect to crank angles for CNG optimal operating conditions. During the compression stroke, A_w increases negatively and A^{th} increases. Combustion starts at -30° before TDC. There is a corresponding rise in A^{th}, as temperature and pressure increase by burning the fuel. A_Q increases negatively due to the increasing gas temperature. The irreversibility curve

[4] A^{total}—Total availability (including both thermomechanical and fuel chemical availability), $A^{f,ch}$—Fuel chemical availability, A^{th}—Thermomechanical availability, A_W—Availability transfer associated with work, A_Q—Availability transfer associated with heat loss, A_I—Availability destruction due to combustion.

Reproduced with permission of the copyright owner. Further reproduction prohibited without permission.

traces the availability destruction (A_I) due to the combustion. It does not change with the crank angles after about 40°, because combustion has completed.

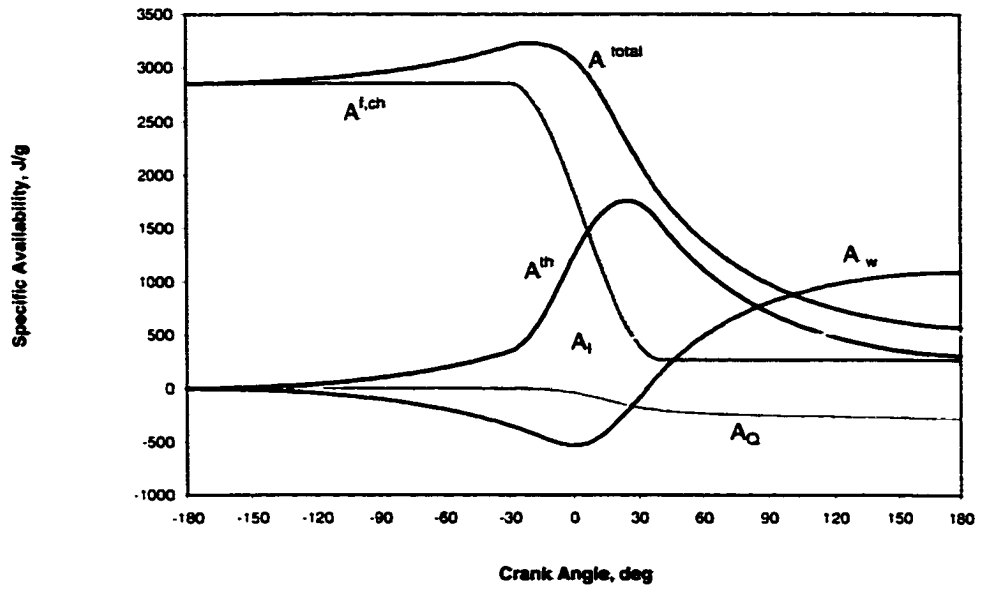

Figure 7.31 Availability simulation versus crank angles in the predicted optimum engine operation conditions: equivalence ratio (1.1), spark timing (-30°), combustion duration(70°), residual gas fraction (0.0) at WOT and 4000 rpm for DaimlerChrysler V8 engine fueled with CNG.

Figure 7.32 is the comparison of CNG and gasoline operations. At the same compression ratio (9.3), the same engine load (WOT), and the same engine speed (4000 rpm), gasoline fueled SI engine has the highest IMEP (12.7 bar), while CNG is 11.3 bar. The relevant engine operating conditions are listed in Figure 7.32. Although the IMEP values indicate that the gasoline fueled SI engine performs better than the CNG fueling, the second law efficiency and other related ratio bring out a different perspective. Figure 7.32 shows the second law efficiency (A_W / A_{ini}), the ratio of engine output to the initial total availability (W_i / A_{ini}), the ratio of availability transfer with work to the maximum availability, which takes into account of the effects of compression stroke on the initial total availability ($A_W / A_{tot,max}$), and the ratio of thermomechnaical availability to the maximum availability, which study the effects of rising pressure and temperature due to parametric design on the

Reproduced with permission of the copyright owner. Further reproduction prohibited without permission.

engine processes ($A_{th,max}$ / $A_{tot,\ max}$). As shown, CNG has higher values for these ratios, which means that CNG combustion has a higher potential to convert the initial fuel availability to do useful work eventually, even without taking advantage of its higher octane number rating. If the compression ratio is increased, CNG operation is expected to have better engine performance in terms of IMEP as well as better energy utilization.

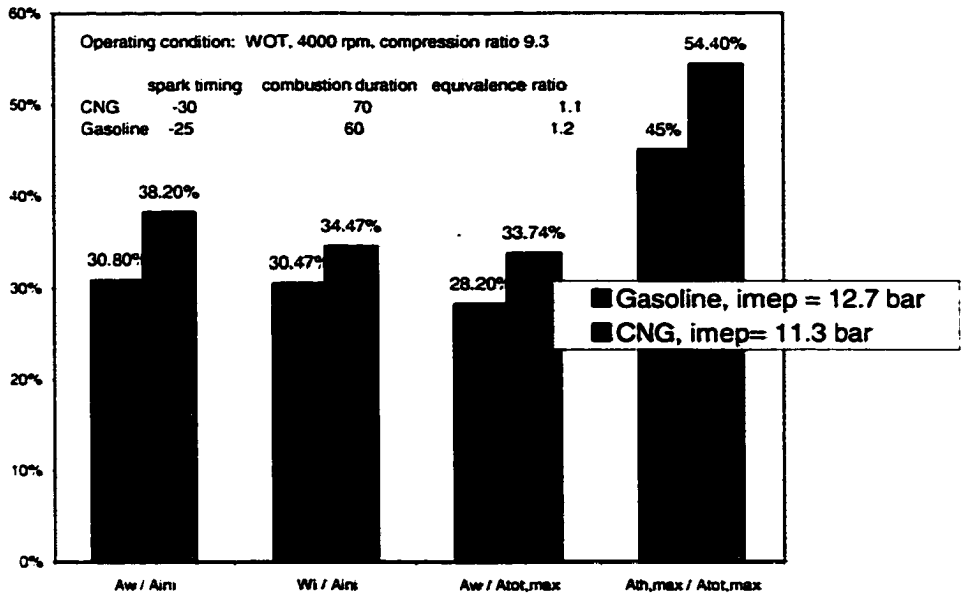

Figure 7.32 CNG and gasoline operations at the predicted optimal engine conditions for best indicated mean effective pressure (IMEP).

The operating conditions in Figure 7.32 are chosen to achieve best torque (or IMEP) for both engine performances. However, considering the gasoline fueling listed in Figure 7.32, the equivalence ratio of 1.2 is higher than usually used. Generally, conventional gasoline fueled SI engines will not run on such rich mixture, because it is beyond the catalytic converter operating range, so that exhaust emission will be high with an equivalence ratio of 1.2. Therefore, the simulation is performed again after adjusting the equivalence ratio to 1.1 for gasoline fueled SI engine simulations. Figure 7.33 shows that the gasoline operated IMEP is still higher than CNG. The relevant ratios have changed but indicated that CNG operation is still better than gasoline when the second law efficiency is considered.

Reproduced with permission of the copyright owner. Further reproduction prohibited without permission.

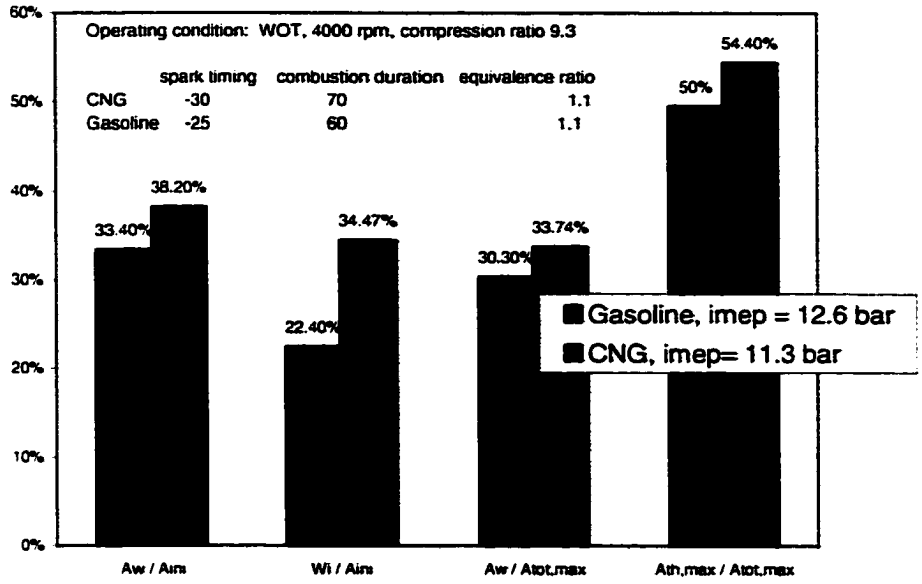

Figure 7.33 CNG and gasoline operations at the same equivalence ratio, $\Phi = 1.1$.

Figure 7.34(a) gives a general picture of availability losses to heat transfer. The availability with heat loss is lower with CNG (24%), while gasoline is 31%. It also shows that CNG facilitates higher availability transfer with work (38.20%) out of the combined system than gasoline operation (33.40%). The availability destruction due to combustion is about the same for CNG and gasoline.

Figure 7.34(b) further catalogs the percentage of availability destruction due to heat transfer and availability transfer with heat for gasoline and CNG operations. Availability transfers with work, heat, and exhaust to the environment belong to the recoverable availability. As shown, the first law analysis is obviously misleading. It predicts that percentages of fuel energy for work output, heat loss and waste to the environment are about the same for CNG and gasoline operation. Furthermore, it overpredicts the percentages of energy waste to the environment.

Reproduced with permission of the copyright owner. Further reproduction prohibited without permission.

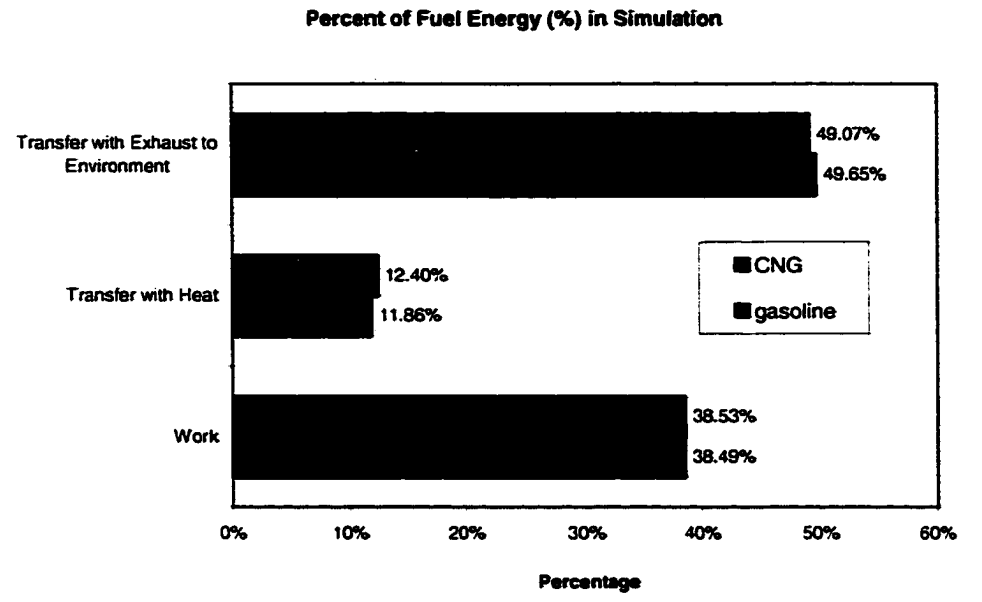

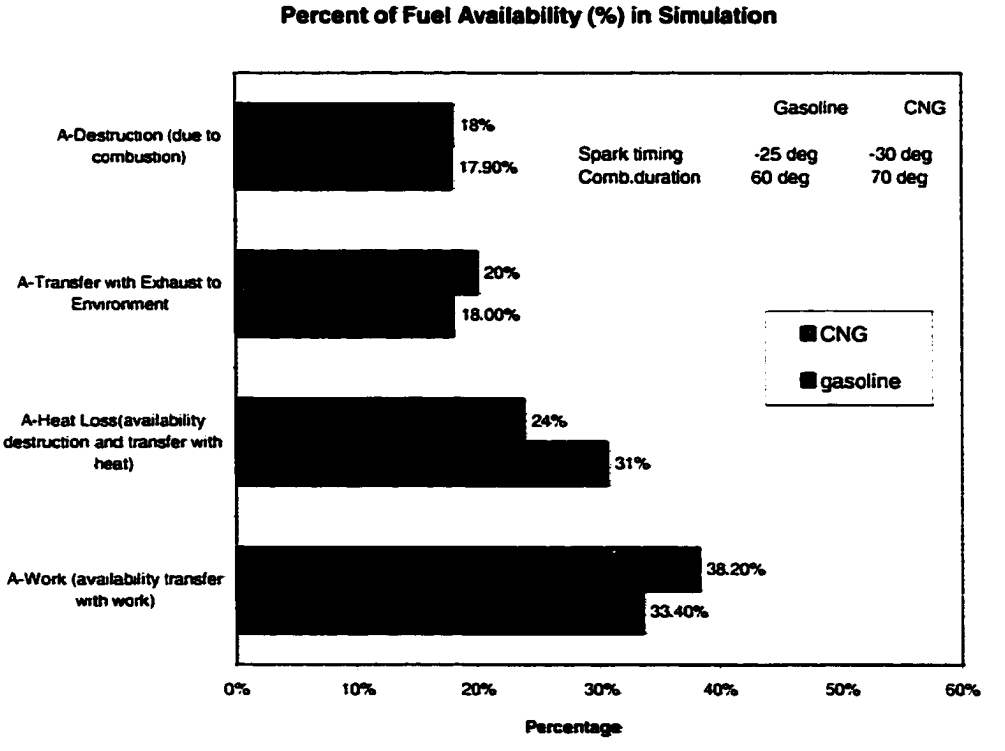

Figure 7.34 (a) The distributions of fuel energy and fuel availability of CNG and gasoline fueled SI engines at the same equivalence ratio, Φ=1.1.

Reproduced with permission of the copyright owner. Further reproduction prohibited without permission.

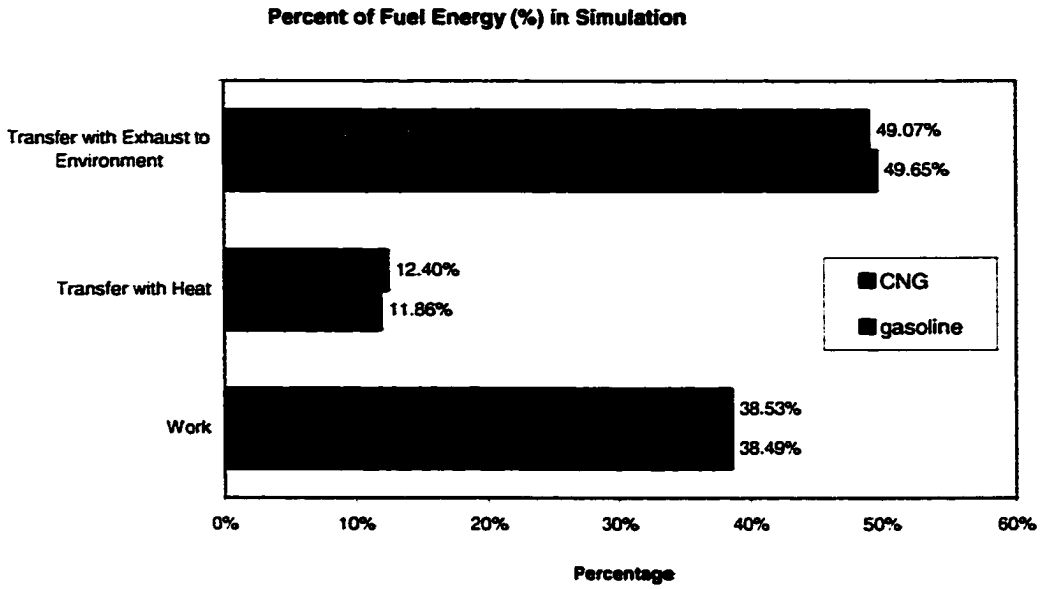

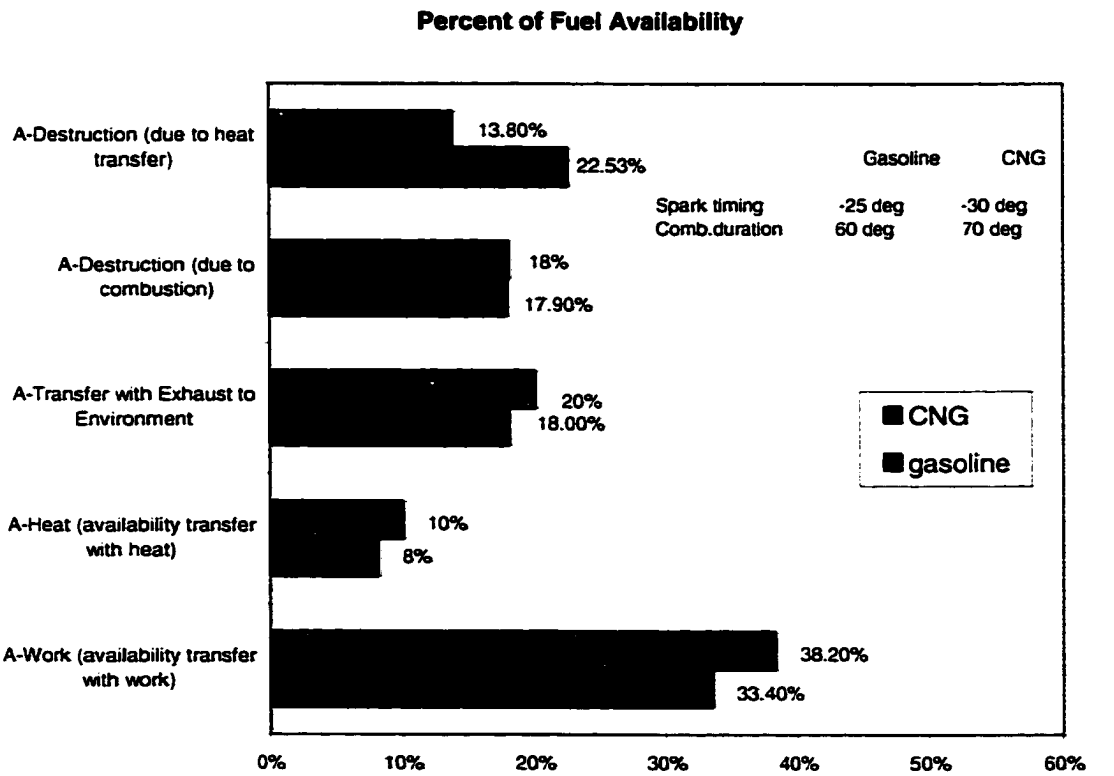

Figure 7.34 (b) The distributions of fuel energy and fuel availability of CNG and gasoline fueled SI engines at the same equivalence ratio, Φ=1.1.

Reproduced with permission of the copyright owner. Further reproduction prohibited without permission.

7.7 Thermodynamic Properties Studies for CNG Engine Simulation

The section shows how the relevant thermodynamic properties of in-cylinder mixtures change during the engine cycle simulation discussed in previous sections. Figure 7.35 shows the cylinder gas temperature as a function of the specific entropy of the in-cylinder contents for CNG optimal operation, as they occur in the engine simulation. Starting with the intake valve close (IVC), the mixtures temperature increases while the specific entropy remains nearly constants (close to a isentropic process). During the end of the compression process, the specific entropy decreases slightly as the hot gases lose energy to the cylinder walls. As combustion starts at 30 ° before TDC, the specific entropy increases mainly due to the increasing temperature, pressure, and combustion irreversibilities during the combustion process. During the expansion process, the specific entropy decreases as temperature decreases rapidly.

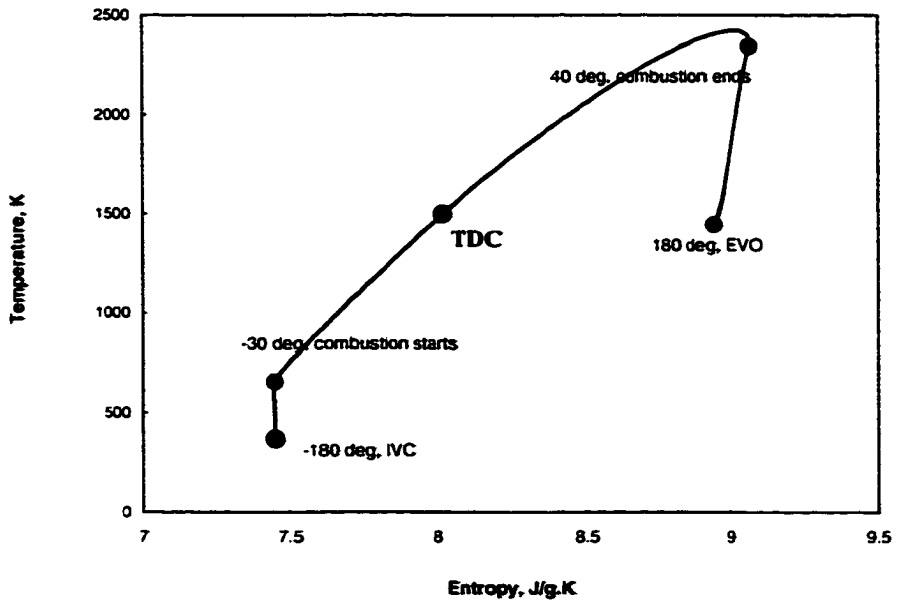

Figure 7.35 Entropy-temperature diagram at the predicted optimal conditions for CNG fueled V8 engine.

Figure 7.36 shows the specific internal energy of the in-cylinder fuel/air and combustion products mixtures as a function of temperature for CNG optimal operation. Starting with

Reproduced with permission of the copyright owner. Further reproduction prohibited without permission.

the intake valve close, the specific internal energy increases linearly with temperature until combustion starts at 30° before TDC. It continues to increase slowly to 3° after TDC due to the increasing temperature. Past this point, the specific internal energy starts to decrease mainly because the fuel/air mixture is gradually converted into the combustion products after TDC. At 40° after TDC, combustion ends, and the specific internal energy decrease steadily to the point of exhaust valve open (EVO), because temperature decreases during this period. For the first law point of view, the specific internal energy decreases during combustion and expansion processes, it is because work is being done and heat loss during this period.

The calculated values of the specific entropy, specific internal energy, and specific volume are used to determine the specific availability of the cylinder contents. Figure 7.36 shows the specific availability as a function of the gas temperature. Starting with the intake valve close, the specific availability increases slightly due to the addition of compression work. As combustion begins, the specific availability decreases due to the availability transfer with heat and the combustion irreversibilities. The specific availability continues to decrease after temperature has reached to the maximum point due to the availability transfer with work and heat transfer.

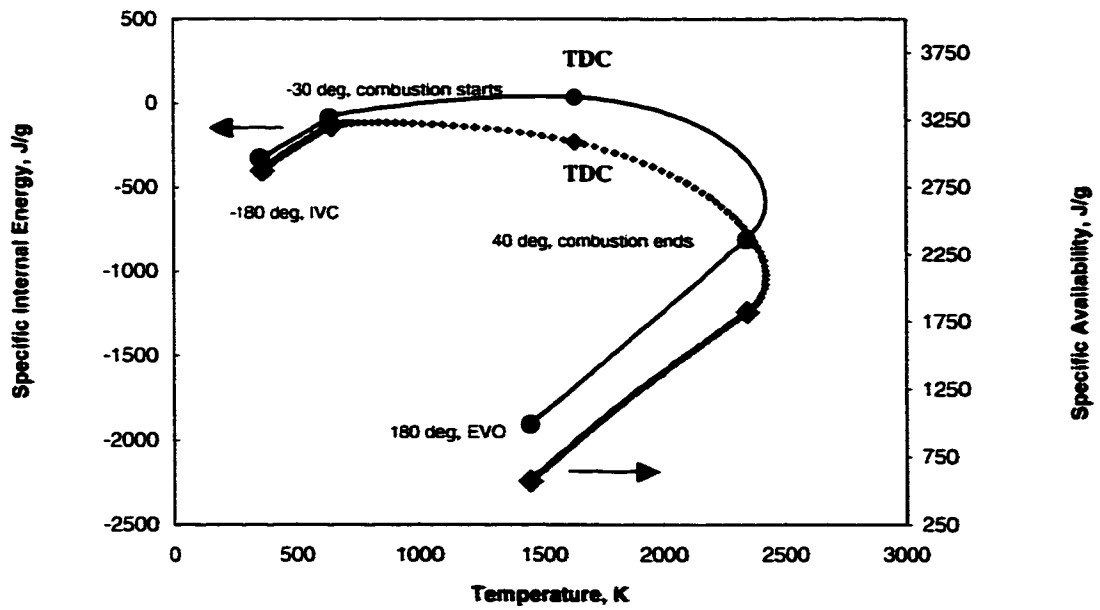

Figure 7.36 Specific availability and internal energy vs. temperature at the predicted optimal conditions for CNG fueled V8 engine.

Reproduced with permission of the copyright owner. Further reproduction prohibited without permission.

Changes of the compositions of the fuel-air-residual gas mixture and equilibrium combustion products are simulated with the crank angle. Figure 7.37 shows the mole fractions of the major species (O_2, CO_2, H_2O, and fuel) and the cylinder temperature with respect to crank angle for the CNG optimal operation conditions. As shown, the mole fractions of O_2 and fuel decrease, while the mole fractions of CO_2 and H_2O increase during the combustion process. For a rich mixture ($\Phi = 1.1$), water gas equilibrium reaction occurs, so eventually H_2O decreases and CO_2 increases slightly in the end of expansion process.

The water gas reaction for a rich mixture is:

$$CO + H_2O \Leftrightarrow CO_2 + H_2$$

Figure 7.38(a) and Figure 7.38(b) show the mole fractions of some of the minor species (CO, H_2, OH, NO, O and H) and the cylinder gas temperature as a function of crank angle. The mole fractions of CO, OH, NO and H_2 show higher peaks than the mole fractions of H and O atoms. The decrease of CO and increase of H_2 in the end of the expansion process are due to the water gas equilibrium reaction for the rich condition.

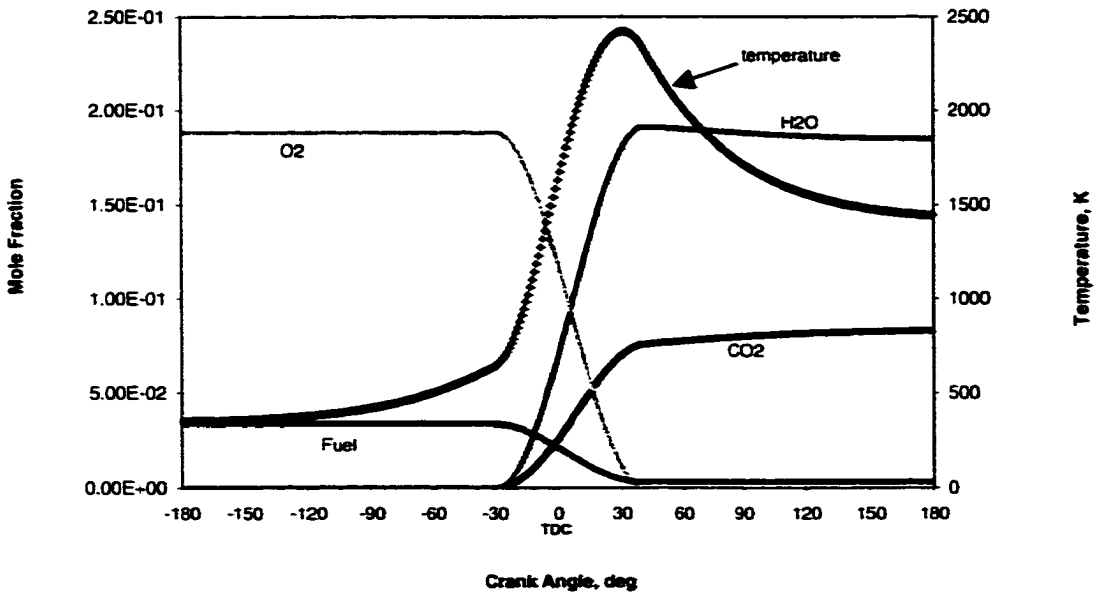

Figure 7.37 Major species and the cylinder mixtures temperature as a function of crank angles for CNG optimal operating conditions.

Reproduced with permission of the copyright owner. Further reproduction prohibited without permission.

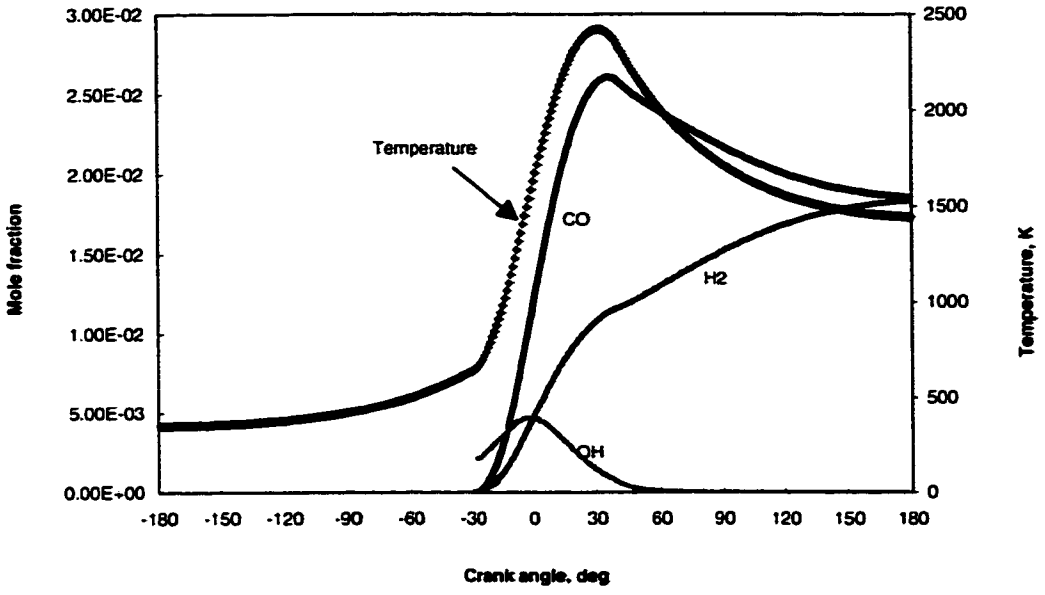

Figure 7.38(a) The mole fractions of minor species (CO, H_2, OH) and the cylinder mixtures temperature as a function of crank angles for CNG optimal operating conditions.

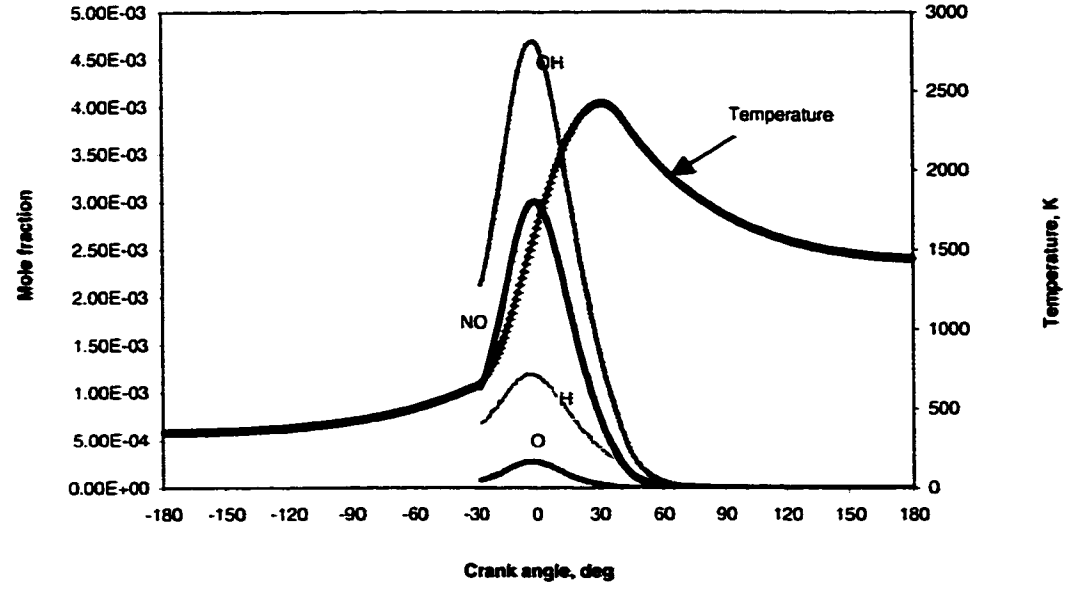

Figure 7.38(b) Minor species (OH, NO, O, H) and the cylinder mixtures temperature as a function of crank angles for CNG optimal operating conditions.

Reproduced with permission of the copyright owner. Further reproduction prohibited without permission.

The term "emission" refers primarily to pollutants in the engine exhaust. Examples of pollutants are carbon dioxide (CO_2) which is greenhouse gas, carbon monoxide (CO) which is toxic gas, various oxides of nitrogen (NO_x) which is the photochemical smog and ozone depletion agents and unburned hydrocarbons (UHC) which is appropriately organic emissions. Some of unburned hydrocarbons are highly reactive in the smog producing chemistry. In the current study, the emissions of major species such as CO_2, CO, H_2, and unburned CH_4 and minor species such as NO, H, O, and OH are examined particularly with varying fuel/air equivalence ratio.

Carbon monoxide (CO) is present with fuel-rich mixtures, as there will be incomplete combustion. Unburned hydrocarbon emissions (CH_4) can be reduced by fuel-lean mixtures. However, very lean mixtures will cause misfire. The formation of NO and other oxides of nitrogen increase very strongly with the increasing flame temperature, excess oxygen, and lower flame speed. NO formation is only significant when there is a high enough temperature and sufficient time. Low engine speed and lean mixtures provide a longer time for forming NO.

Figure 7.39 illustrates the exhaust gases compositions in terms of mole fractions for varying fuel/air equivalence ratio for CNG operation (WOT, 4000 rpm). As shown, for the fuel-lean mixtures, the exhaust gases contain mostly CO_2 and O_2, whereas for the fuel-rich mixtures, the exhaust gases contain CO, H_2, and UHC. CO_2 and H_2O are at the maximum levels at the equivalence ratio of 1.0, because combustion is most complete at the stoichiometric condition.

Figure 7.40 illustrates that the NO emission and minor species (OH, H, O) change with equivalence ratio at 30° after TDC, since peak temperature occurs around such a crank angle. The peak of NO occurs at the equivalence ratio of 0.8 (lean condition). The NO emission decreases for even leaner mixtures, due to lower flame temperature, and again NO emission decreases at rich mixtures, due to lacking of oxygen for their formation.

Reproduced with permission of the copyright owner. Further reproduction prohibited without permission.

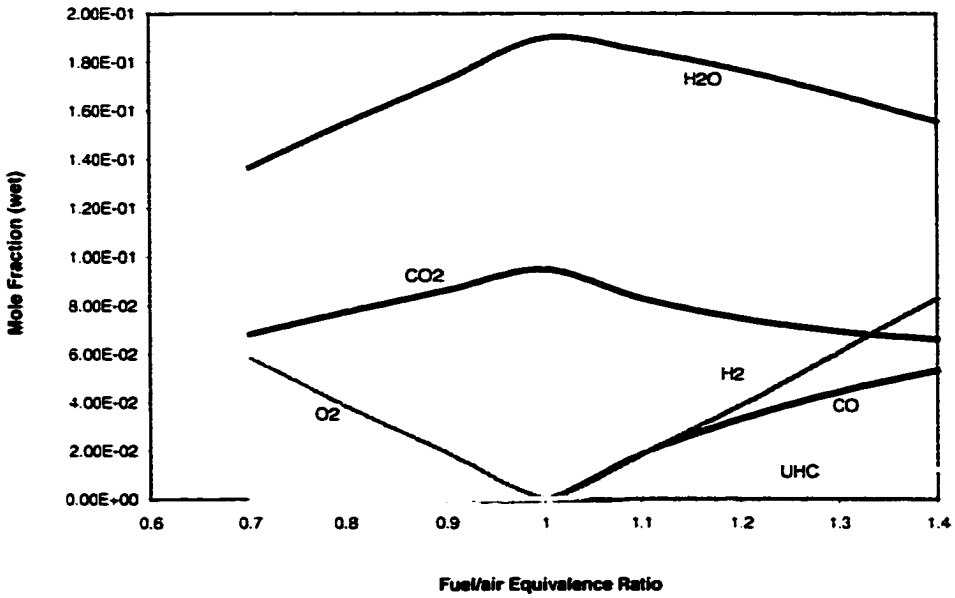

Figure 7.39 Wet exhaust gas compositions as a function of fuel/air equivalence ratio for CNG fuelled SI engine operations (at the end of the expansion stroke).

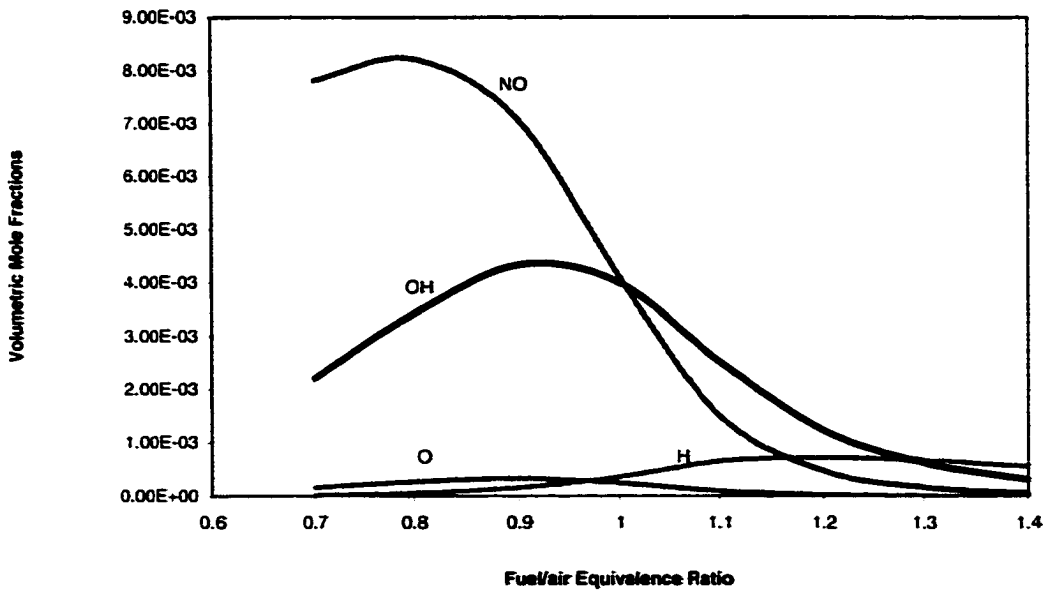

Figure 7.40 NO emission and minor species (OH, H, O) as a function of fuel/air equivalence ratio for CNG fuelled SI engine (30° after TDC).

Reproduced with permission of the copyright owner. Further reproduction prohibited without permission.

7.8 Comparison of Experimental with Simulated Pressure Data

Figure 7.41 compares the cylinder pressures as a function of cylinder volume with three cases: (1) air cycle constant properties simulations, (2) fuel/air cycle with variable thermodynamic properties simulation, (3) experimental pressure data.

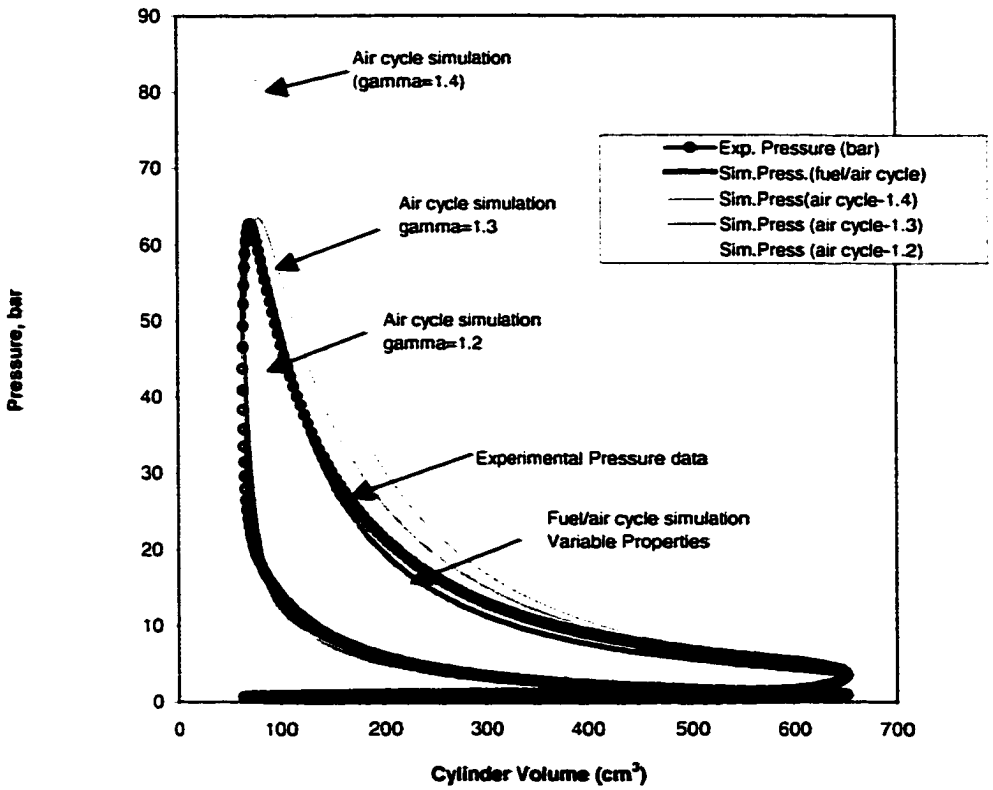

Figure 7.41 Pressure-Volume diagram for simulated (fuel/air cycle and air cycle) results and experimental data for V8 engine at WOT, 4000 rpm.

As shown above, fuel/air cycle with variable properties simulation is in good agreement with the experimental data. The agreement of air cycle simulations depends on the value of the ratio of specific heat. With the specific heat ratio of 1.3, the simple air cycle simulation results are in better agreement with the experimental pressures than the specific heat ratios of 1.2 and 1.4.

Reproduced with permission of the copyright owner. Further reproduction prohibited without permission.

The variable thermodynamic properties refer to the specific heat value and heat transfer coefficient changing with respect to temperature for fuel/air cycle simulations, which are used for a CNG fueled SI engine at WOT, 4000 rpm, with a equivalence ratio of 1.05.

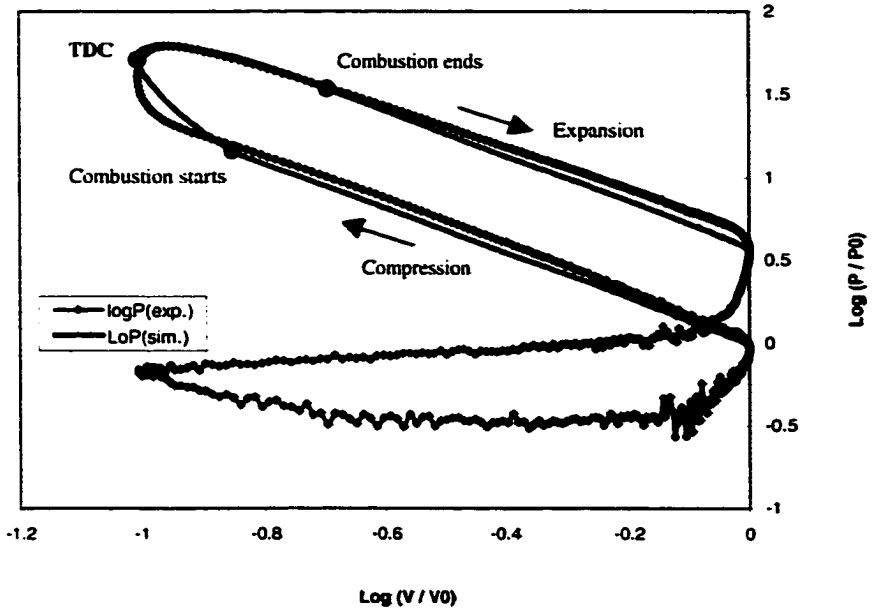

Figure 7.42 Log (p/p_0)-log (V/V_0) plot for simulated and experimental pressure data for V8 engine at WOT, 4000rpm, with the current mass fraction burned (MFB) model.

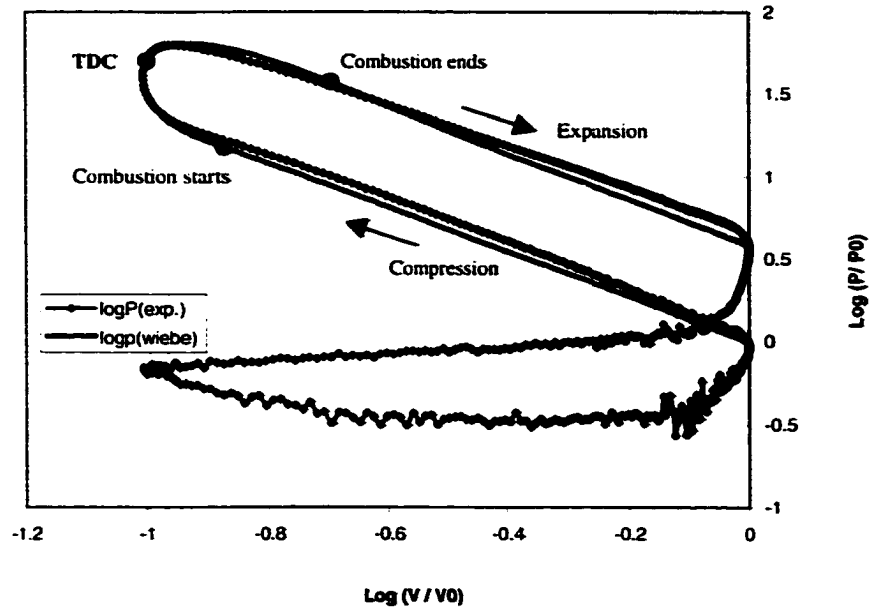

Figure 7.43 Log (p/p_0)-log (V/V_0) plot for simulated and experimental pressure data for V8 engine at WOT, 4000rpm, with the Wiebe function.

Reproduced with permission of the copyright owner. Further reproduction prohibited without permission.

Figure 7.42 further illustrate the differences between experimental and fuel/air cycle simulated pressures. One can notice several discrepancies between two curves, mostly during combustion period. The simulated specific heat ratio during the compression process Is 1.34, while the experimental specific heat ratio is 1.33. The simulated specific ratio in the expansion process is 1.36, which is higher than the experimental result (1.21). Because of the higher values of the simulated specific heat ratios, the predicted pressures are lower than the experimental pressures during the compression and expansion processes.

Figure 7.42 clearly shows the differences during combustion process with the current mass fraction burned (MFB) model. This initial difference between the pressure curves during the combustion period is because of the specific heat ratio during the compression stage. Even bigger difference, which occurs during the combustion before TDC, could be contributed to the failure of the applied mass fraction burned function to simulate the combustion process.

Figure 7.43 re-examines the Wiebe function in Log (p/p_0)-log (V/V_0) plot for comparing the simulated and experimental pressures. As shown, the Wiebe function shows better approximate for the initial stage of combustion. However, there is still bigger difference in the end of the combustion process. It is because that both the Wiebe function and the current mass fraction burned function could not match well the experimental mass fraction burn in the late stage of combustion process.

Figure 7.44 examines the distributions of the fuel energy and availability for CNG and gasoline fueled SI engines with the Wiebe function. The values in the brackets are the results from inputting the current MFB models, which are shown in Figure 7.34(b). One can notice, the percentages are close and follow the same trend. Especially for the availability destruction due to combustion, the Wiebe function predicts 17.96% for CNG and 17.80% for gasoline, while the current MFB model predicts 18% for CNG and 17.90% for gasoline; for the availability destruction due to heat transfer, the Wiebe function predicts 14.81% for CNG and 23.18% for gasoline, while the current MFB

Reproduced with permission of the copyright owner. Further reproduction prohibited without permission.

model predicts 13.8% for CNG and 22.53% for gasoline. Therefore, the comparison of the current MFB model and the Wiebe function further illustrates that a more realistic combustion model is required for accurately simulating the combustion process.

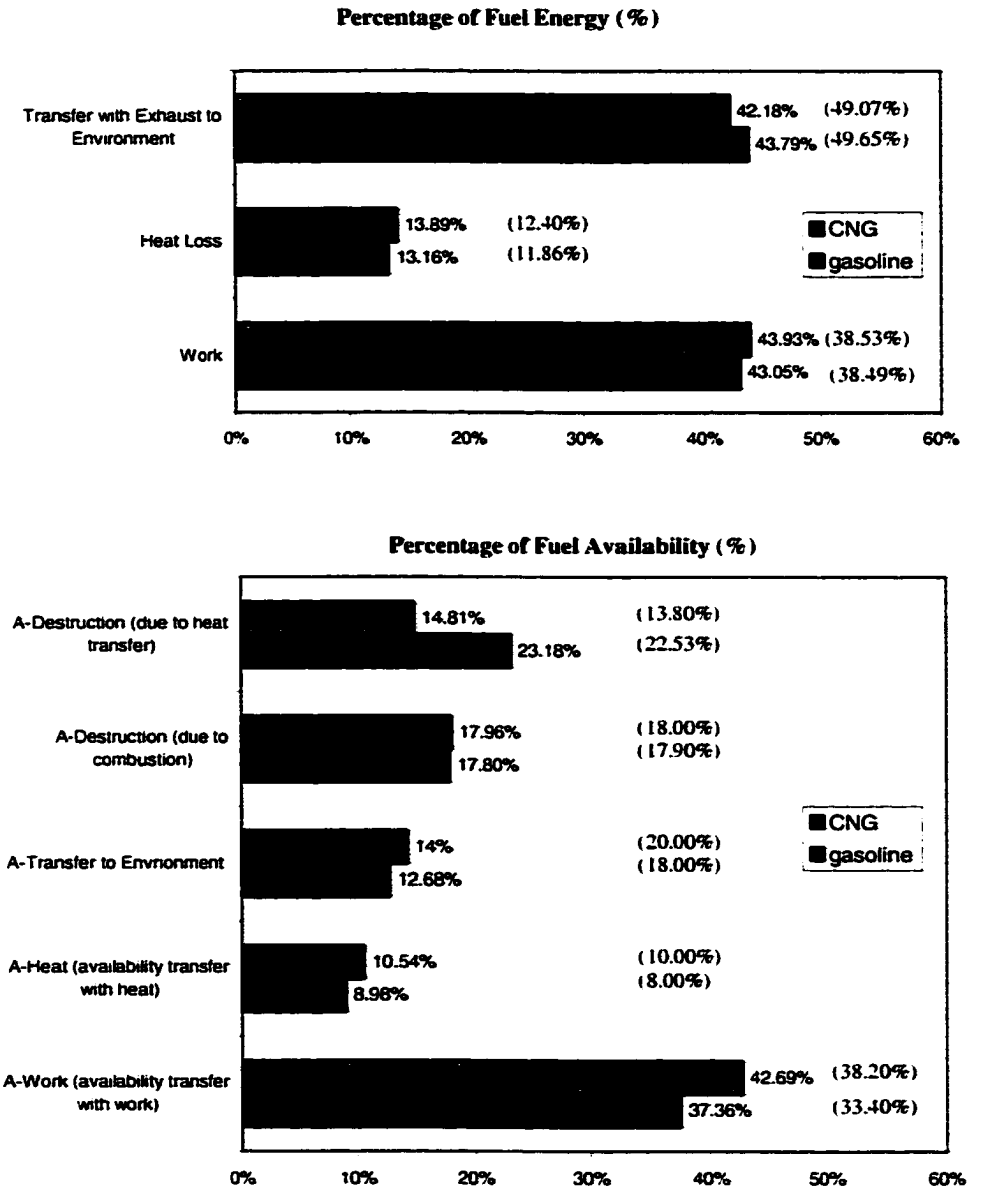

Figure 7.44 The distributions of fuel energy and fuel availability of CNG and gasoline fueled SI engines with the Wiebe function and the current MFB model.

Reproduced with permission of the copyright owner. Further reproduction prohibited without permission.

CHAPTER 8 SUMMARY, CONCLUSIONS AND RECOMMENDATIONS

8.1 Summary of the Approach

A comprehensive thermodynamic engine cycle modeling for SI engines fueled with alternative fuels was performed. The objective was to conduct an analysis based on the second law of thermodynamics and the related calculation of availability. The additional focus was on showing the potential advantages of engine fueling with alternative fuels as revealed by this type of analysis. An engine used for the experimental and computational results comparisons was a SI engine fueled with CNG. The major characteristics of the engine performance with respect to the second law were established.

The current practice of the modeling of engine processes reflects the understanding of the physics and chemistry of the internal combustion engines. For the processes which govern engine performance and emissions, two basic types of approaches can be developed, categorized as thermodynamic and fluid dynamic, depending on whether the equations giving the model its predominant structure are based on energy conservation or on a full analysis of the fluid motion.

The models in this thesis are the fundamental one-dimensional thermodynamic models, since in the absence of dimensions in this study, spatial features of the fluid motion cannot be predicted. Only the compression, combustion and expansion processes are studied extensively in the engine cycle simulations. In addition, the overall engine friction model and cycle-by-cycle variations are not considered in the current study.

The major assumptions and approximations used in the simulation include:

- In-cylinder species are assumed to obey ideal gas equation of state.
- Thermodynamic properties vary only with time (crank angles) and are spatially uniform.

Reproduced with permission of the copyright owner. Further reproduction prohibited without permission.

- The intake valve closes and the compression process starts at -180° before TDC and the expansion process ends at 180° after TDC at which the exhaust valve opens.
- Fuel is assumed to be completely vaporized and mixed with air at the beginning of the compression stroke.
- During the combustion process, the burned zone contains equilibrium products of combustion, while the unburned zone consists of a homogeneous mixture of air, fuel and residual gases.
- The equilibrium chemical compositions are obtained from generally accepted algorithms.
- The burning rate is expressed as a sinusoidal function of crank angle to represent the mass transformed from the unburned to the burned zone.
- The mass flow rates are determined from the one-dimensional mass conservation equation.
- The combustion efficiency and volumetric efficiency are assumed to be 100%.

8.2 Conclusions—Trends in Energy and Availability Changes with Engine Operating Variables

The total availability evolution during its cyclic process was studied as the outcome of the availability exchange and destruction through the processes of heat transfer, work and combustion.

- The major sources of the availability destruction in engine operations are irreversibilities associated with the combustion process and heat transfer. In fact, the availability analysis clearly identifies that energy expelled with the heat loss includes two components: energy which is still available, and energy irreversibly degraded.

- The availability analysis has shown that when engine operation is not optimized (to take into account such critical differences as higher octane number of

Reproduced with permission of the copyright owner. Further reproduction prohibited without permission.

alternative fuels, longer combustion time and different spark timing), the combustion irreversibilities are higher for alternative fuels. Concurrently, availability destruction due to heat transfer is higher for gasoline operation. These trends change when combustion parameters, such as spark timing and combustion duration and equivalence ratio, are properly adjusted. Based on the second law analysis, the availability destruction due to combustion is then comparable for gasoline and CNG operations.

- The availability destruction due to heat transfer is lower with CNG fueled engines at optimal engine conditions. This increases availability transfer with work and the second law efficiency for CNG operation.

- Trends in the availability losses, transfer and destruction predicted by the models follow the trends reported by other studies of similar nature for gasoline fueled SI engines.

- Engine performance characteristics predicted by fuel/air cycle model with variable properties are close to experimental data.

- The predicted pressures with the current mass fraction burned function matches well with the experimental data in the end of combustion process, while the predicted pressures with the Wiebe function matches well with the experimental data in the initial combustion process.

- Mass fraction burned function is critical for the accurate prediction of engine performance characteristic an availability balance. This indicates a need for a better model of mass fraction burn to accurately reflect this critical availability destruction process. With such a model a direct comparison of simulated availability balance with the availability balance of a real engine based on measured pressure, temperature and exhaust gas compositions could be attempted.

Reproduced with permission of the copyright owner. Further reproduction prohibited without permission.

- The availability analysis models provide a better understanding of interactions between engine cyclic processes and engine performance. This method shows not only how the energy is converted in engines, but also identifies and qualifies the unrecoverable degradation associated with chemical reactions and heat transfer across a finite temperature difference. The use of this type of analysis is also expected to find increasing application in the design process of future engine designs, as well as in the optimization of existing engines.

- The availability analysis makes it clear that SI engines fuelled with alternative fuels (CNG, methanol) present a better potential to obtain improved energy utilization, better engine performance and reduced emissions.

- Availability analysis programs developed in the current study offer a unique view of engine processes and constitute a valuable research and educational tool.

8.3 Recommendations for Future Work

The future work on engine availability analysis should include the following:

- The engine performance should be simulated at the different engine speed and engine loads.
- The realistic intake and exhaust valve timing (valve overlap) should be included in the availability study.
- Perturbation of mass burn rate could be introduced to study cycle-by-cycle variations.
- Completeness of combustion parameters could be introduced to improve mass burn rate simulation for cycle-by-cycle variations investigation.
- Availability analysis of a real engine based on the measured pressure, temperature and exhaust compositions and engine dynamometer performance should be accompanied with the availability analysis based on simulations.

Reproduced with permission of the copyright owner. Further reproduction prohibited without permission.

CHAPTER 9 REFERENCES

1 U.S. department of energy, sustainable energy strategy, "Still Seeing Growth in the Energy Sector", 1999.

2 Colin R. Ferguson and Allan T. Kirkpatrick, "Internal Combustion Engine Applied Thermosciences", John Wiley & Sons, Inc, 2000.

3 Canadian Gas Association, "Air Emissions From Natural Gas", CGA's environmental affairs department, October 1997.

4 J.A. Caton, "A Review of Investigations Which have Used the Second Law of Thermodynamics to Study Internal Combustion Engines", SAE Technical Paper Number 2000-01-1081, 2000.

5 M.J. Moran, "Availability Analysis—A Guide to Efficient Energy Use", Prentice-Hall, Inc, 1982.

6 Van Gerpen, J.H. and Shapiro, H.N., "Second-Law Analysis of Diesel Engine Combustion", 1987.

7 J.A. Caton, "Results From the Second—Law of Thermodynamics for a Spark-Ignition Engine Using an Engine Cycle Simulation", 1999 Fall Technical Conference of the ASME Internal Combustion Engine Division, 1999.

8 Howard N. Shapiro and Jon H. Van Gerpen, "Two Zone Combustion Models for Second Law Analysis of Internal Combustion Engines", SAE Technical Paper Number 890823, 1989.

9 J. A. Caton, "Operating Characteristics of a Spark-Ignition Engine Using the Second Law of Thermodynamics: Effects of Speed and Load", SAE Technical Paper Number 2000-01-0952, 2000.

10 John B. Heywood, "Internal Combustion Engine Fundamentals", McGraw-Hill, Inc. 1988.

11 Moran, M. J., Shapiro, H. N., "Fundamentals of Engineering Thermodynamics", John Wiley & Sons, Inc., 1995.

12 R.J.Primus and P.F.Flynn, "The Assessment of Losses in Diesel Engines Using Second Law Analysis", 1986.

13 Robert Eugene Lee, "The New 4.7L V-8 Engine From DaimlerChrysler Corporation", SAE Technical Paper Number 1999-01-1258, 1999.

14 Stone, Richard, "Introduction to Internal Combustion Engines", Society of Automotive Engineers, Inc., 1999.

15 P.F.Flynn, K.L.Hoag, M.M.Kamel, and R.J.Priums, "A New Perspective on Diesel Engine Evaluation Based on Second Law Analysis", SAE Technical Paper Number 840032, 1984.

16 Alkidas, A.C., "The Application of Availability and Energy Balances to a Diesel Engine", Journal of Engineering for Gas Turbines and Power, Vol.110/469, 1988.

17 A.C.Alkidas, "The Use of Availability and Energy Balances in Diesel Engines", SAE Technical Paper Number 890822, 1989.

18 S.V.Kumar, W.J.Minkowycz, and K.S.Patel, "Thermodynamic Cycle Simulation of the Diesel Cycle: Exergy As a Second Law Analysis Parameter", International Journal of Heat Mass Transfer, vol.16, pp.335-346, 1989.

Reproduced with permission of the copyright owner. Further reproduction prohibited without permission.

19 Lipkea, W.H. and Dejoode, A.D., "A Comparison of the Performance of Two Direct Injection Diesel Engines From a Second Law Perspective", SAE Technical Paper Number 890824, 1989.

20 Waldyr Luiz Ribeiro Gallo and Luiz Fernando Milanez, "Exergetic Analysis of Ethanol and Gasoline Fueled Engines", SAE Technical Paper Number 920809, 1992.

21 Rakopoulos, C.D. "Evaluation of A Spark Ignition Engine Cycle Using First and Second Law Analysis Techniques", Energy Convers. Mgmt., Vol. 34. No.12, pp.1299-1314, 1993.

22 Rakopoulos, C.D., Andritsakis, E.C. and Kyritsis, D.K., "Availability Accumulation and Destruction in a DI Diesel Engine with Special Reference to the Limited Cooled Case", Heat Recovery Systems & CHP, Vol. 13, NO.3, pp.261-276, 1993.

23 C.D.Rakopoulos and F.G.Giakoumis, "Speed and Load Effects on the Availability Balances and Irreversibilities Production in a Multi-Cylinder Turbocharged Diesel Engine", Applied Thermal Engineering Vol.17, No.3, pp.299-313, 1997.

24 Anderson, M.K., and Assanis, D.N, and Filipi, Z.S., "First and Second Law Analyses of a Naturally—Aspirated, Miller Cycle, SI Engine with Late Intake Valve Closure", SAE Technical Paper Number 980990, 1998.

25 Caton, J.A.1999b, "An Evaluation of Time-Resoved Thermodynamic Properties for a Spark-Ignition Engine Using a Thermodynamic Cycle Simulation", The Combustion Institute 1999 Spring Technical Conference. Chemical and Physical Processes in Combustion, 1999.

26 Caton, J.A., "A Comparison of the Use of Constant or Variable Properties in a Thermodynamic Engine Cycle Simulation for a Spark Ignition Engine", The Combustion Institute 1999 Spring Technical Conference, Chemical and Physical Processes in Combustion, 1999.

27 Caton, J.A., "The Effect of Burn Rate Parameters on the Operating Attributes of a Spark-Ignition Engine as Determined from the Second Law of Thermodynamics", ICE-Vol. 34-2, 2000 Spring Technical Conference ASME 2000, Paper Number 2000-ICE-274, 2000.

28 Rakopoulos, C.D. and Kyritsis, D.C, "Parametric Study of the Availability Balance in an Internal Combustion Engine Cylinder", SAE Technical Paper Number 2001-01-1263, 2001.

29 Kevin J.Roth and Andrzej Sobiesiak, "In-Cylinder Pressure Measurements with Optical Fiber and Piezoelectric Pressure Transducers", SAE Technical Paper Number 2002-01-0745, 2002.

Reproduced with permission of the copyright owner. Further reproduction prohibited without permission.

CHAPTER 10 APPENDIXES

Appendix A

Computer Code (Fortran)—DaimlerChrylser CNG fueled 4.7 Liter V8 engine with variable properties simulation

```
      EXTERNAL RATES,ADODE,RKODE
      REAL IMEP, MNOT, M, N2,NO
      INTEGER O
      COMMON /ENGINE /R, B, S, EPS, RPM, H, C, THETAB, THETAS,
     +                PHI, F, P1, T1, TW, MNOT, OMEGA, UNOT, UFINAL
      DIMENSION Y1(6),Y2(10),Y(6),YO(6),QHR(360),ENW(360)
      DIMENSION AHRU(360),AHRB(360),AHLU(360),AHLB(360),AW(360),
     +       A(360),SATH(360),SAW(360),HTCO(360),LFA(360),XBURN(360)
      DIMENSION ACHFL(360),ATH(360),PRESS(360),TU(360),TB(360)
     +       ,AL(360),ACHF(360),UCOMPR(360),UCOMBU(360),TERNAL(360)
      DIMENSION VERI(360),SEN(360),SFUEL(360),SENN(360),EFA(360)
      DIMENSION QAINS(360),QHL(360),QLINS(360),AHL(360),DELTAP(360)
      DATA AO/52085./,FS/.058/,YO/1.,10000.,350.,0.,2*0./,
     +     N/6/, THETA/-180./, THETAE/-179./, TOL/.001/,
     +     PI/3.141593/,Y2/10*0.0/,Y1/6*0.0/
      DATA O/3/
      DATA QHRO/0.0/,QHLO/0.0/,CALR/50031./,LFO/0.0/
      DATA AWO/0.0/,ENWO/0.0/,AHRUO/0.0/,AHLUO/0.0/
     +       AHLBO/0.0/,AHRBO/0.0/,AHLO/0.0/,SAWO/0./
      DATA ACHO/52085./,AFRS/17.2/,ATHO/0.0/,SATHO/0.0/,LFAO/0.0/
      DATA ACHMOL/833364./,UINICOM/1000000000./
      DO 3 I=1,72
      QHR(I)=0.0
      QHL(I)=0.0
3     CONTINUE
      OPEN (UNIT=1,FILE='input.dat',STATUS='OLD')
      READ(1,*) R,B,S,EPS,RPM,C,THETAB,THETAS,PHI,F,P1,T1,TW
      CLOSE(1)
      CIMEPC=PI/4.*B**2.*S
      IF (PHI .LT. 0.5 .OR. PHI .GE.1.6) THEN
      WRITE(6,*)'equivalence ratio is out of range'
      STOP
      END IF

C
C     LABEL HEADER ON OUTPUT PAGE AND PRINT INITIAL CONDITIONS
C
      OMEGA = RPM*PI/30.
      CALL AUXLRY(THETA, V, X, EM)
      VO=V
      TEMPO=YO(3)
      PRESSO=YO(1)
      Y(1) = P1
      Y(3) = T1
      CALL FARG(Y(1), Y(3), PHI, F, HU, U, VU, SU, Y1, CP, DLVLT,
     +     DLVLP)
      SENO=SU
```


Reproduced with permission of the copyright owner. Further reproduction prohibited without permission.

```
      UINI=U
      MNOT = V/VU
      UNOT = MNOT*U
      AFRA=AFRS/PHI

      FMS=MNOT/((1.+FS*(1.-F))/(FS*(1.-F)))
      FMF=MNOT/((1.+PHI*FS*(1.-F))/(PHI*FS*(1.-F)))
      IF (PHI .GT. 0.5 .AND. PHI .LT. 1.0) THEN
      XFUELO=FMF/MNOT
      QIN=FMF*CALR
      AAO=FMF*ACHO
      ELSE
      ELSE IF (PHI .GE. 1.0 .AND. PHI .LT. 1.6) THEN
      XFUELO=FMS/MNOT
      QIN=FMS*CALR
      AAO=FMS*ACHO
      END IF
      SAO=XFUELO*ACHO
      VERIO=(SU-SENO)*300.
      TFCA=FMF/16.*ACHMOL
      OPEN(UNIT=20,FILE='PLOT.1',STATUS='UNKNOWN')
      OPEN(UNIT=30,FILE='PLOT.2',STATUS='UNKNOWN')
      OPEN(UNIT=40,FILE='PLOT.3',STATUS='UNKNOWN')
      OPEN(UNIT=50,FILE='PLOT.4',STATUS='UNKNOWN')
      OPEN(UNIT=60,FILE='PLOT.5',STATUS='UNKNOWN')
      OPEN(UNIT=70,FILE='MOLE',STATUS='UNKNOWN')

      WRITE(6,10)
      WRITE(20,10)
10    FORMAT(' THETA',5X,'VOL',3X,'X',4X,'PRESS',4X,
     +       'TB',4X,'T-UB',4X,'WORK',4X,'HL',4X,'MASS',4X,
     +       'H-LEAK',4X,'QHR',4X,'U.UB',4X,'U.B',4X,'int.energy',
     +        4X,'entropy')

      WRITE(6,15)
      WRITE(20,15)
15    FORMAT(' DEG ATDC',1X,'CM**3',2X,'--',4X,'BAR',6X,'K',
     +       6X,'K',8X,'J',6X,'J',4X,'GRAMS',4X,
     +       'J',8X,'J',4X,'J/g',4X,'J/g',4X,'J/g',4X,'J/g.K')

      WRITE(6,20) THETA, VO, X,
(YO(I),I=1,5),MNOT,YO(6),QHRO,UINI,UINICOM,
     +             UINI,SENO
      WRITE(20,20)
THETA,VO,X,(YO(I),I=1,5),MNOT,YO(6),QHRO,UINI,UINICOM,
     +               UINI,SENO

20    FORMAT(2X,F6.1,2X,F5.0,2X,F5.3,2X,F5.2,2X,F5.0,2X,F5.0,
     +       2X,F5.0,2X,F5.0,2X,F5.3,2X,F5.2,2X,F7.2,2X,F5.0,2X,F6.0,
     +       2X,F6.0,2X,F11.4)
C
C
C     INTEGRATE THE RATE EQUATIONS 4.80 - 4.85 AND PRINT ANSWERS
C     EVERY 10 DEGREES
C
      HTRIAL=THETAE-THETA
      OPEN(UNIT=1,FILE='pressure.dat',STATUS='OLD')
```


Reproduced with permission of the copyright owner. Further reproduction prohibited without permission.

```
      DO 21 I=1,360
21    READ(1,*)DELTAP(I)
      CLOSE(1)
      SPISTON=11.53

      DO 30 I = 1,360
      RAD=THETA*PI/180.

      STR=(155.4+43.25-43.25*COS(RAD)-
     +       (155.4**2.-43.25**2.*(SIN(RAD))**2.)**0.5)/10.
      V=PI*B**2.0*STR/4.+64.5
      PMOTOR=(R*587.5/(R-1.))**1.3/(V**1.3)

      IF (THETA .LT. THETAS) THEN
      VGAS=2.28*SPISTON
      ELSE
      VGAS=2.28*SPISTON+0.00324*TEMPO*587.5*
     +          (Y(1)-PMOTOR)/VO/PRESSO
      END IF

      IF (THETA .LT. THETAS) THEN
      HEATC=3.26*0.093**(-0.2)*(Y(1)*100.)**0.8*Y(3)**(-0.55)*
     +          VGAS**0.8
      ELSE IF (THETA .LT. THETAS+THETAB) THEN
      HEATCU=3.26*0.093**(-0.2)*(Y(1)*100.)**0.8*Y(3)**(-0.55)*
     +          VGAS**0.8
      HEATCB=3.26*0.093**(-0.2)*(Y(1)*100.)**0.8*Y(2)**(-0.55)*
     +           VGAS**0.8
      HEATC=X*HEATCB+(1.-X)*HEATCU
      ELSE
      HEATC=3.26*0.093**(-0.2)*(Y(1)*100.)**0.8*Y(2)**(-0.55)*
     +           VGAS**0.8
      END IF
C
C     input constant heat transfer coefficient
C
C     HEATC=529.67

      CALL  ADODE(O,N,RATES,THETA,THETAE,HEATC,YO,TOL,HTRIAL,Y,
     +     UCOMP,UCOMB,TEXP,PEX,VBEXP,CPEXP,CO2,H2O,N2,O2,CO,H2,
     +      HYD,OXY,OH,NO)
      WRITE(50,55)THETA,TEXP,PEX,VBEXP,CPEXP,HEATC,PMOTOR,Y(2)
55    FORMAT (8(2X,1PE11.4))

C     WRITE(70,56)CO2,H2O,N2,O2,CO,H2,HYD,OXY,OH,NO,FRFUEL

56    FORMAT(11(X,1PE10.3))

      UCOMPR(I)=UCOMP
      UCOMBU(I)=UCOMB
      CALL AUXLRY(THETAE, V, X, EM)

      IF (PHI .LE. 1.0) THEN
      FRFUEL=FMF*(1.-X)
      ELSE
      FRFUEL=FMS*(1.-X)+(FMF-FMS)*X
      END IF
```


Reproduced with permission of the copyright owner. Further reproduction prohibited without permission.

```
      WRITE(70,56)CO2,H2O,N2,O2,CO,H2,HYD,OXY,OH,NO,FRFUEL

      XBURN(I)=X
      M=EM*MNOT
      THETA = THETAE
      THETAE = THETA + 1.
      IF(THETAS .GE. THETA .AND. THETAS .LT. THETAE)
     +   CALL TINITL(Y(1),Y(3),PHI,F,Y(2))

      IF (THETA .GT. THETAS + THETAB) THEN
        Y(3) = 10000.
      UCOMPR(I)=10000000.
      ELSE IF (THETA .LT. THETAS) THEN
      UCOMBU(I)=10000000.
      ELSE IF (THETA .EQ. THETAS) THEN
      CALL ECP(Y(1),Y(2),PHI,HB,U,VB,S,Y2,CPB,DLVLTB,DLVLPB,IER)
      UCOMBU(I)= U
      ELSE IF (THETA .EQ. THETAS+1.) THEN
      CALL ECP(Y(1),Y(2),PHI,HB,U,VB,S,Y2,CPB,DLVLTB,DLVLPB,IER)
      UCOMBU(I)=U
      END IF
      QHR(I)=QIN*X
      QHL(I)=Y(5)
      IF (I .EQ. 1.) THEN
      QAINS(I)=QHR(I)-QHRO
      QLINS(I)=QHL(I)-QHLO
      ELSE
      QAINS(I)=QHR(I)-QHR(I-1.)
      QLINS(I)=QHL(I)-QHL(I-1.)
      END IF
      ENW(I)=1.0*10.**5*(VO-V)*10.**(-6)
      IF (THETA .LE. THETAS) THEN
      AHRB(I)=0.0
      AHLU(I)=Y(5)*(1.-300./Y(3))
      AHLB(I)=0.0
      CALL FARG(Y(1),Y(3),PHI,F,HC,UC,VC,SC,Y1,CP,DLVLT,DLVLP)
      SEN(I)=SC
      SFUEL(I)=FENTROPY+FSH*ALOG(Y(3)/300.)
      VERI(I)=ABS((SEN(I)-SENO-(QHR(I)-QHL(I))/Y(3)/M)*300.)
      ELSE IF (THETA .LE. (THETAS+THETAB)) THEN
      AHRB(I)=QHR(I)*(1.-300./Y(2))
      AHLB(I)=Y(5)*(1.-300./Y(2))
      AHLU(I)=Y(5)*(1.-300./Y(3))
      CALL FARG(Y(1),Y(3),PHI,F,HCOO,UCOO,VCOO,SCOO,Y1,CP,
     +          DLVLT,DLVLP)
      SENN(I)=SCOO
      CALL ECP(Y(1),Y(2),PHI,HCO,UCO,VCO,SCO,Y2,CP,
     +      DLVLT,DLVLP,IER)
      SEN(I)=SCO
      SFUEL(I)=FENTROPY+FSH*ALOG(Y(2)/300.)
      VERI(I)=(X*SEN(I)+(1.-X)*SENN(I)-SENO-(-X*QHL(I))/Y(2)/M-
     +          (-(1.-X)*QHL(I))/Y(3)/M)*300.
      SEN(I)=X*SEN(I)+(1.-X)*SENN(I)
      ELSE
      AHRB(I)=QHR(I)*(1.-300./Y(2))
      AHLB(I)=Y(5)*(1.-300./Y(2))
      AHLU(I)=0.0
```


Reproduced with permission of the copyright owner. Further reproduction prohibited without permission.

```
      CALL ECP(Y(1),Y(2),PHI,HE,UE,VE,SE,Y2,CP,DLVLT,DLVLP,IER)
      SEN(I)=SE
      SFUEL(I)=FENTROPY+FSH*ALOG(Y(2)/300.)
      VERI(I)=(SEN(I)-SENO-(-QHL(I))/Y(2)/M)*300.
      END IF
      AHL(I)=-(X*AHLB(I)+(1.-X)*AHLU(I))/M
      ACHFL(I)=XFUELO*(1.-X)*ACHO
      LF=(FMF-FMS)*ACHO/MNOT
      LFA(I)=LF*XBURN(I)
      AW(I)=-(Y(4)-ENW(I))
      SAW(I)=-AW(I)/M
      ATH(I)= AW(I)+AHRB(I)-(1.-X)*AHLU(I)-X*AHLB(I)
      SATH(I)=-SAW(I)+AHRB(I)/M+AHL(I)-VERI(I)
      AL(I)=SATH(I)+ACHFL(I)

      TERNAL(I)=(1.-X)*UCOMPR(I)+X*UCOMBU(I)

      WRITE(6,20) THETA, V, X,(Y(J),J=1,5),M,Y(6),QHR(I),UCOMPR(I),
     +         UCOMBU(I),TERNAL(I),SEN(I)
      WRITE(20,20) THETA,V,X,(Y(J),J=1,5),M,Y(6),QHR(I),UCOMPR(I),
     +         UCOMBU(I),TERNAL(I),SEN(I)
      WORKOUT=Y(4)
27    FORMAT('THETA',8X,'A-WORK-J',4X,'EN-WORK-J',4X,
     +        'A-HRB-J',6X,'AHLU-J',6X,'AHLB-J',6X,'ENTROPY-J/g*K')

28    FORMAT(8(1PE11.4))
      DO 26 J=1,6
26    YO(J)=Y(J)
30    CONTINUE
      WRITE(6,27)
      WRITE(30,27)
      THETAO=-180.
      WRITE(6,28)THETAO,AWO,ENWO,AHRBO,AHLUO,AHLBO,SENO
31    FORMAT(6(1PE11.4))
      WRITE(30,28)THETAO,AWO,ENWO,AHRBO,AHLUO,AHLBO,SENO
      DO 35 I=1,360
      THETAO=THETAO+1.
      WRITE(6,28)THETAO,AW(I),ENW(I),AHRB(I),AHLU(I),
     +              AHLB(I),SEN(I)
      WRITE(30,28)THETAO,AW(I),ENW(I),AHRB(I),AHLU(I),
     +              AHLB(I),SEN(I)
35    CONTINUE
      WRITE(6,37)
      WRITE(30,37)
37    FORMAT('THETA',6X,'SATH-J/g',2X,'SACH-J/g',2X,
     +        'IVVER-J/g',2X,'A-HL-J/g',2X,'SAW-J/g',2X,
     +        'A-TOL-J/g',4X,'A-WASTE.F-J/g')

      THETAO=-180.
      WRITE(6,28) THETAO,SATHO,SAO,VERIO,AHLO,SAWO,SAO
      WRITE(30,28) THETAO,SATHO,SAO,VERIO,AHLO,SAWO,SAO
      MAXTH=0.
      DO 36 I=1,360
      THETAO=THETAO+1.
      WRITE(6,28) THETAO,SATH(I),ACHFL(I),VERI(I),AHL(I),SAW(I),AL(I)
      WRITE(30,28)THETAO,SATH(I),ACHFL(I),VERI(I),AHL(I),SAW(I),AL(I)
```


Reproduced with permission of the copyright owner. Further reproduction prohibited without permission.

```
      IF (SATH(I) .GT. MAXTH) THEN
      MAXTH=SATH(I)
      MAXTHETA=THETAO
      END IF
36    CONTINUE

      WRITE(40,37)
      THETAO=-180.
      WRITE(40,28)THETAO,SATHO,SAO,VERIO,AHLO,SAWO,SAO,LFAO
      THETAO=-180.
      DO 38 I=1,360
      THETAO=THETAO+1.
      IF (PHI .LE. 1.0) THEN
      ACHF(I)=ACHFL(I)
      ELSE
      ACHF(I)=ACHFL(I)+LFA(I)
      WRITE(60,*)LFA(I)
      EFA(I)=LFA(I)
      END IF
      A(I)=ACHF(I)+SATH(I)

      WRITE(40,28)THETAO,SATH(I),ACHF(I),VERI(I),AHL(I),SAW(I),A(I),
     +              EFA(I)
38    CONTINUE

C
C     COMPUTE AND WRITE THE ETA, IMEP AND ERRORS
C
      CALL ECP(Y(1), Y(2), PHI, HB, U, VB, SB, Y2, CP, DLVLT, DLVLP,
     +         IER)
      UFINAL = U*M
      ERROR1 = 1.0 - VB*M/V
      ERROR2 = 1.0 + Y(4)/(UFINAL - UNOT + Y(5) + Y(6))

      ETA=Y(4)/(FMF*AO*(1.-F))
      ETF=Y(4)/(FMF*CALR*(1.-F))

      CIMEP=Y(4)/CIMEPC*10.
      POWER=8.*Y(4)*RPM/120./1000.
      TORQUE=POWER/(PI*RPM/30.)*1000.
      BSFC=1000.*3600.*FMF/Y(4)
      WRITE(6,40) ETA, CIMEP, ERROR1, ERROR2
      WRITE(20,40) ETA,CIMEP,ERROR1,ERROR2
40    FORMAT('ETA = ',1PE11.4,'IMEP =',1PE11.4,' ERROR1 =',1PE11.4,
     +       ' ERROR2 = ',1PE11.4)
      WRITE(6,50) POWER, TORQUE,BSFC
      WRITE(20,50) POWER,TORQUE,BSFC
50    FORMAT('POWER=',1PE11.4,'[kW]',3X,'TORQUE=',1PE11.4,'[N.m]',
     +         'BSFC=',1PE11.4,'[g/kW.h]')
      WRITE(6,*)'A-HL-J/g',AHL(360),'IRREV-J/g',VERI(360)
      WRITE(6,*)'A-WORK-J/g',SAW(360),'A-TH-J/g',MAXTH,MAXTHETA,'deg'
      WRITE(6,*)'A-EXHAUST',SATH(360)
      WRITE(6,*)'A-Fuel-J/g',ACHF(1), 'A-
                FUEL.WASTE',ACHF(360),ACHFL(360)
      WRITE(6,*)'Fuel-Stoich',FMS
      WRITE(6,*)'Fuel-Actual',FMF,   'TOTAL-MASS',MNOT
      WRITE(6,*)'First.Law.Efficiency',ETF, 'Work',Y(4)
```


Reproduced with permission of the copyright owner. Further reproduction prohibited without permission.

```
      CIMEP1= Y(4)/CIMEPC*10.
      POWER1=8.*Y(4)*RPM/120./1000.
      TORQUE1=POWER/(PI*RPM/30.)*1000.
      WRITE(6,*) CIMEP1,POWER1,TORQUE1
      CLOSE (20)
      CLOSE (30)
      CLOSE (40)
      CLOSE (50)
      CLOSE (60)
      CLOSE (70)
      END


      SUBROUTINE RATES(N, THETA, HTC,Y, YPRIME)

      DIMENSION Y1(6), Y2(10)

      REAL Y(N), YPRIME(N), M, MNOT
      COMMON /ENGINE/ R, BORE, STROKE, EPS, RPM, HEAT, CEE, THETAB,
     +                THETAS, PHI, F, P1, T1, TW, MNOT, OMEGA, UNOT,
     +                UFINAL
      DATA PI/3.141593/, Y2/10*0.0/

      DATA A1/3.653/,A2/-0.001337/,A3/.000003294/,
     +       A4/-.000000001913/,A5/.000/
      CALL AUXLRY(THETA, V, X, EM)
      M = EM*MNOT
      RAD = THETA*PI/180.


      DUMB = SQRT(1. - (EPS*SIN(RAD))**2)
      DV =PI/8.*BORE**2*STROKE*SIN(RAD)*(1.+EPS*COS(RAD)/DUMB)
      A = (DV + V*CEE/OMEGA)/M
C      C1 = HEAT*(PI*BORE**2/2. + 4.*V/BORE)/OMEGA/M/10000.
      C1=HTC*(PI*BORE**2/2.+4.*V/BORE)/OMEGA/M/10000.
      C0 = SQRT(X)
C
C     THREE DIFFERENT COMPUTATIONS ARE REQUIRED DEPENDING
C     UPON THE SIZE OF THE MASS FRACTION BURNED
C
      IF( X .GT. .999 ) GO TO 20
      IF( X .GT. .001 ) GO TO 10
C
C     COMPRESSION
C
      CALL FARG(Y(1), Y(3), PHI, F, HL, U, VU, S, Y1, CP, DLVLT,
     +          DLVLP)


      B = C1*VU/CP*DLVLT*(1.0-TW/Y(3))
      C = 0.
      D = 0.
      E = VU**2/CP/Y(3)*DLVLT**2 + 10.*VU/Y(1)*DLVLP
      YPRIME(1) = (A + B + C)/(D + E)*10.
      YPRIME(2) = 0.
      YPRIME(3) = -C1/CP*(Y(3) - TW) + VU/CP*DLVLT*YPRIME(1)/10.
```


Reproduced with permission of the copyright owner. Further reproduction prohibited without permission.

```
      GO TO 30
C
C     COMBUSTION
C
10    CALL FARG(Y(1), Y(3), PHI, F, HU, U, VU, S, Y1, CPU, DLVLTU,
     +          DLVLPU)
      CALL ECP(Y(1), Y(2), PHI, HB, U, VB, S, Y2, CPB, DLVLTB, DLVLPB,
     +         IER)
      CPB=1.65
C     CPB=1.25

      B = C1*(VB/CPB*DLVLTB*C0*(1. - TW/Y(2)) + VU/CPU*DLVLTU*
     +    (1. - C0)*(1.0-TW/Y(3)))
      DX=0.5*SIN(PI*(THETA-THETAS)/THETAB)*180./THETAB

      C = -(VB - VU)*DX - VB/Y(2)*DLVLTB*(HU - HB)/CPB*(DX - (X -
     +    X**2)*CEE/OMEGA)
      D = X*(VB**2/CPB/Y(2)*DLVLTB**2 + 10.*VB/Y(1)*DLVLPB)
      E = (1. - X)*(VU**2/CPU/Y(3)*DLVLTU**2 + 10.*VU/Y(1)*DLVLPU)
      HL = (1.0 - X**2)*HU + X**2*HB
      YPRIME(1) = (A+ B + C)/(D + E)*10.
      YPRIME(2) = -C1/CPB/C0*(Y(2) - TW) + VB/CPB*DLVLTB*
     +            YPRIME(1)/10. + (HU - HB)/CPB*(DX/X - (1. - X)*
     +            CEE/OMEGA)
      YPRIME(3) = -C1/CPU/(1. + C0)*(Y(3) - TW) + VU/CPU*DLVLTU*
     +            YPRIME(1)/10.
      GO TO 30
C
C     EXPANSION
C
20    CALL ECP(Y(1), Y(2), PHI, HL, U, VB, S, Y2, CP, DLVLT, DLVLP,
     +         IER)
      CP=1.4
C     CP=1.25
      B = C1*VB/CP*DLVLT*(1. - TW/Y(2))
      C = 0.
      D = VB**2/CP/Y(2)*DLVLT**2 + 10.*VB/Y(1)*DLVLP
      E = 0.
      YPRIME(1) = (A + B + C)/(D + E)*10.
      YPRIME(2) = -C1/CP*(Y(2) -TW) + VB/CP*DLVLT*YPRIME(1)/10.
      YPRIME(3) = 0.
C
C     ALL CASES
C
C30   IF (THETA. GE. -180. .AND. THETA .LE. 0.) THEN
C     PRESS1=1.
C     YPRIME(4)=PRESS1*DV/10.
C     ELSE IF (THETA .GT. 0. .AND. THETA .LE. 180.) THEN
C     PRESS2=9.5
C     YPRIME(4)=PRESS2*DV/10.
C     END IF

30    YPRIME(4)=Y(1)*DV/10.
      YPRIME(5) = C1*M*(C0*(Y(2) - TW) + (1. - C0)*(Y(3) - TW))
      YPRIME(6) = CEE*M/OMEGA*HL

      DO 40 I = 1,N
```


Reproduced with permission of the copyright owner. Further reproduction prohibited without permission.

```
40     YPRIME(I) = YPRIME(I)*PI/180.
       RETURN
       END


       SUBROUTINE AUXLRY(THETA, V, X, EM)

       COMMON /ENGINE/ R, B, S, EPS, RPM, H, C, THETAB, THETAS,
      +                PHI, F, P1, T1, TW, EMNOT, OMEGA, UNOT, UFINAL
       DATA PI/3.141593/
       RAD = THETA*PI/180.
C      STROKEE=(155.4+43.25-43.25*COS(RAD)-
C     +    (155.4**2.-43.25**2.*(SIN(RAD))**2.)**0.5)/10.
C      V=PI*B**2.0*STROKEE/4.+64.5
       VTDC=PI/4.*B**2*S/(R-1.)
       V=VTDC*(1.+(R-1.)/2.*(1.-COS(RAD)+1./EPS*(1.-
      +    SQRT(1.-(EPS*SIN(RAD))**2))))
       X  = 0.5*(1. - COS(PI*(THETA - THETAS)/THETAB))
       IF(THETA .LE. THETAS) X = 0.
       IF(THETA .GE. THETAS + THETAB) X =1.
       EM = EXP(-C*(RAD + PI)/OMEGA)
       RETURN
       END



       SUBROUTINE TINITL(P, TU, PHI, F, TB)
       DIMENSION Y1(6), Y2(10)
       DATA MAXITS/50/, TOL/.001/, Y2/10*0.0/
       TB = 300.
       CALL FARG(P, TU, PHI, F, HU, U, V, S, Y1, CP,DLVLT,DLVLP)
       DO 10 I = 1,MAXITS
       CALL ECP(P, TB, PHI, HB, U, V, S, Y2, CP,DLVLT,DLVLP,IER)
       CP=1.7
       DELT = (HU - HB)/CP
       TB = TB + DELT
       IF(ABS(DELT/TB) .LT. TOL) RETURN
10     CONTINUE
       WRITE(6,20)
20     FORMAT('CONVERGENCE FAILURE IN TINITL')
       RETURN
       END



       SUBROUTINE FARG (P, T, PHI, F, H, U, V, S, Y, CP, DLVLT, DLVLP)
C
C      PURPOSE:
C         COMPUTE THE PROPERTIES OF A FUEL, AIR, RESIDUAL
C         GAS MIXTURE
C
C      GIVEN:
C         P        - PRESSURE (BARS)
C         T        - TEMPERATURE (K)
C         PHI      - FUEL AIR EQUIVALENCE RATIO
C         F        - RESIDUAL MASS FRACTION
C
```


Reproduced with permission of the copyright owner. Further reproduction prohibited without permission.

```
C     RETURNS:
C        H        - ENTHALPY (J/G)
C        U        - INTERNAL ENERGY (J/G)
C        V        - SPECIFIC VOLUME (CM**3/G)
C        S        - ENTROPY (J/G/K/)
C        Y        - A SIX DIMENSIONAL COMPOSITION VECTOR OF
C                   MOLE FRACTIONS
C                   1=CO2, 2=H2O, 3=N2, 4=O2, 5=CO, 6=H2
C        CP       - SPECIFIC HEAT AT CONSTANT PRESSURE (J/G/K)
C        DLVLT    - DERIVATIVE OF LOG VOLUME WITH RESPECT TO LOG
C                   TEMPERATURE AT CONSTANT PRESSURE
C        DLVLP    - DERIVATIVE OF LOG VOLUME WITH RESPECT TO LOG
C                   PRESSURE AT CONSTANT TEMPERATURE
C
C     REMARKS:
C        1. VALID FOR 300<T<1000
C        2. ASSUMES THE FUEL IS GASOLINE. TO CHANGE FUELS
C           ONLY THE FUEL DATA STATEMENT NEEDS MODIFICATION.
C        3. ENTHALPIES OF O2, H2, N2 AND C(S) ARE SET TO ZERO
C           AT 298K
C        4. THE FUEL MOLE FRACTION IS UNITY MINUS THE SUM OF Y(I)
C
C********
C
      REAL M, MW, MRES, MFA, MFUEL, K, NU, N2
      LOGICAL RICH,LEAN
      DIMENSION A(7,6), TABLE(6), M(6), NU(6), Y(6), CP0(6), H0(6),
     +          S0(6)
C
C     FUEL DATA
C
      DATA ALPHA/1.0/,BETA/4.0/,GAMMA/0./,DELTA/0./,
     +   A0/1.971324/,B0/7.871586E-03/,C0/-1.048592E-06/,
     +    D0/-9.930422E+03/,E0/8.873728/
C
C     TABLE 3.1, I = 1,6
C
      DATA A/
     1 .24007797E+01, .87350957E-02, -.6607878E-05, .20021861E-08,
     1 .63274039E-15, -.48377527E+05, .96951457E+01,
     2 .40701275E+01, -.11084499E-02, .41521180E-05, -.29637404E-08,
     2 .80702103E-12, -.30279722E+05, -.32270046E+00,
     3 .36748261E+01, -.12081500E-02, .23240102E-05, -.63217559E-09,
     3 -.22577253E-12, -.10611588E+04, .23580424E+01,
     4 .36255985E+01, -.18782184E-02, .70554544E-05, -.67635137E-08,
     4 .21555993E-11, -.10475226E+04, .43052778E+01,
     5 .37100928E+01, -.16190964E-02, .36923594E-05, -.20319674E-08,
     5 .23953344E-12, -.14356310E+05, .2955535E+01,
     6 .30574451E+01, .26765200E-02, -.58099162E-05, .55210391E-08,
     6 -.18122739E-11, -.98890474E+03, -.22997056E+01/
C
C     OTHER DATA
C
      DATA RU/8.315/, TABLE/-1.,1.,0.,0.,1.,-1./, M/44.01, 18.02,
     +        28.008, 32.000, 28.01, 2.018/
C
C     COMPUTE RESIDUAL GAS COMPOSITION ACCORDING TO TABLE 3.3
```


Reproduced with permission of the copyright owner. Further reproduction prohibited without permission.

```
C
      RICH = PHI .GT. 1.0
      LEAN = .NOT. RICH
      DLVLT = 1.0
      DLVLP = -1.0
      EPS = .21/(ALPHA + 0.25*BETA - 0.5*GAMMA)
      IF (RICH) GO TO 10
      NU(1) = ALPHA*PHI*EPS
      NU(2) = BETA*PHI*EPS/2.
      NU(3) = 0.79 + DELTA*PHI*EPS/2.
      NU(4) = 0.21*(1.0 - PHI)
      NU(5) = 0.
      NU(6) = 0.
      DCDT = 0.
      GO TO 20
10    Z = 1000./T
      K = EXP(2.743 + Z*(-1.761 + Z*(-1.611 + Z*.2803)))
      DKDT = -K*(-1.761 + Z*(-3.222 + Z*.8409))/1000.
      A1 = 1.0 - K
      B = .42 - PHI*EPS*(2.*ALPHA - GAMMA) + K*(.42*(PHI - 1.) +
     +    ALPHA*PHI*EPS)
      C = -.42*ALPHA*PHI*EPS*(PHI - 1.0)*K
      NU(5) = (-B + SQRT(B*B -4.*A1*C))/2./A1
      DCDT = DKDT*(NU(5)**2 - NU(5)*(.42*(PHI - 1.) + ALPHA*
     +        PHI*EPS) + .42*ALPHA*PHI*EPS*(PHI - 1.))/
     +        (2.*NU(5)*A1 + B)
      NU(1) = ALPHA*PHI*EPS - NU (5)
      NU(2) = .42 - PHI*EPS*(2.*ALPHA - GAMMA) + NU(5)
      NU(3) = .79 + DELTA*PHI*EPS/2.
      NU(4) = 0.
      NU(6) = .42*(PHI - 1.) - NU(5)
C
C     COMPUT MOLE FRACTIONS AND MOLECULAR WEIGHT OF RESIDUAL
C
20    TMOLES = 0.
      DO 30 I = 1,6
30    TMOLES = TMOLES + NU(I)
      MRES = 0.
      DO 40 I = 1,6
      Y(I) = NU(I)/TMOLES
40    MRES = MRES + Y(I)*M(I)
C
C     COMPUTE MOLE FRACTIONS AND MOLECULAR WEIGHT OF FUEL-AIR
C
      FUEL = EPS*PHI/(1. + EPS*PHI)
      O2 = .21/(1. + EPS*PHI)
      N2 = .79/(1. + EPS*PHI)
      MFA = FUEL*(12.01*ALPHA + 1.008*BETA + 16.*GAMMA + 14.01*
     +      DELTA) + 32.*O2 + 28.02*N2
C
C     COMPUTE MOLE FRACTIONS OF FUEL-AIR-RESIDUAL GAS
C
      YRES = F/(F + MRES/MFA*(1. - F))
      DO 50 I = 1,6
50    Y(I) = Y(I)*YRES

      YFUEL = FUEL*(1. - YRES)
```


Reproduced with permission of the copyright owner. Further reproduction prohibited without permission.

```
      Y(3) = Y(3) + N2*(1. - YRES)
      Y(4) = Y(4) + O2*(1. - YRES)
C
C     COMPUTE COMPONENT PROPERTIES
C
      DO 60 I = 1,6
      CP0(I) = A(1,I) + A(2,I)*T + A(3,I)*T**2 + A(4,I)*T**3 +
     +         A(5,I)*T**4
      H0(I) = A(1,I) + A(2,I)/2.*T + A(3,I)/3.*T**2 + A(4,I)/4.*
     +        T**3 + A(5,I)/5.*T**4 + A(6,I)/T
60    S0(I) = A(1,I)*ALOG(T) + A(2,I)*T + A(3,I)/2.*T**2 +
     +        A(4,I)/3.*T**3 + A(5,I)/4.*T**4 + A(7,I)
C
      MFUEL = 12.01*ALPHA + 1.008*BETA + 16.000*GAMMA + 14.01*DELTA
      CPFUEL = A0 + B0*T + C0*T**2
      HFUEL = A0 + B0/2.*T + C0/3.*T**2 + D0/T
      S0FUEL = A0*ALOG(T) + B0*T + C0/2.*T**2 +E0
C
C     COMPUTE PROPERTIES OF MIXTURE
C
      H = HFUEL*YFUEL
      S = (S0FUEL - ALOG(AMAX1(YFUEL,1.0E-25)))*YFUEL
      CP = CPFUEL*YFUEL
      MW = MFUEL*YFUEL
      DO 70 I = 1,6
      IF(Y(I).LT.1.0E - 25) GO TO 70
      H = H + H0(I)*Y(I)
      S = S + Y(I)*(S0(I) - ALOG(Y(I)))
      CP = CP + CP0(I)*Y(I) + H0(I)*T*TABLE(I)*DCDT*YRES/TMOLES
70    MW = MW + Y(I)*M(I)
C
      R = RU/MW
      H = R*T*H
      U = H - R*T
      V = 10.*R*T/P
      S = R*(-ALOG(.9869*P) + S)
      CP = R*CP
C
      RETURN
      END


      SUBROUTINE ECP (P, T, PHI, H, U, V, S, Y, CP, DLVLT, DLVLP, IER)
C
C     PURPOSE:
C        COMPUTE THE PROPERTIES OF EQUILIBRIUM COMBUSTION
C        PRODUCTS
C
C     GIVEN:
C        P          - PRESSURE (BARS)
C        T          - TEMPERATURE (K)
C        PHI        - FUEL AIR EQUIVALENCE RATIO
C
C     RETURNS:
C        H          - ENTHALPY (J/G)
C        U          - INTERNAL ENERGY (J/G)
```


Reproduced with permission of the copyright owner. Further reproduction prohibited without permission.

```
C         V         - SPECIFIC VOLUME (CM**3/G)
C         S         - ENTHALPY (J/G/K)
C         Y         - A TEN DIMENSIONAL COMPOSITION VECTOR OF
C                     MOLE FRACTIONS
C                     1=CO2, 2=H2O, 3=N2, 4=O2. 5=CO. 6=H2
C                     7=H, 8=O, 9=OH, 10=NO
C         CP        - SPECIFIC HEAT AT CONSTANT PRESSURE (J/G/K)
C         DLVLT     - DERIVATIVE OF LOG VOLUME WITH RESPECT TO LOG
C                     TEMPERATURE AT CONSTANT PRESSURE
C         DLVLP     - DERIVATIVE OF LOG VOLUME WITH REPSECT TO LOG
C                     PRESSURE AT CONSTANT TEMPERATURE
C         IER       - AN ERROR MESSAGE
C                   0 - NORMAL
C                   1 - CONVERGENCE FAILURE: COMPOSITION LOOP
C                   2 - CALLED WITH TOO HIGH AN EQUIVALENCE RATIO; C(S)
C                       AND OTHER SPECIES WOULD FORM
C
C     REMARKS:
C         1. VALID FOR 300 < T < 4000
C         2. ASSUMES THE FUEL IS GASOLINE. TO CHANGE FUELS
C            ONLY THE FUEL DATA STATEMENT NEEDS MODIFICATION.
C         3. THE ENTHALPIES OF H2, O2, N2 AND C(S) ARE SET TO
C            ZERO AT 298K
C         4. SUBROUTINES REQUIRED: FARG, LEQIF (IMSL)
C         5. IF ESTIMATES OF Y(I) I=1,10 ARE AVAILABLE THEY SHOULD
C            BE INPUT THROUGH THE ARGUMENT LIST. OTHERWISE INPUT
C            ZERO'S AND THE ROUTINE WILL MAKE ITS OWN ESTIMATES
C
C*********************
C
      REAL M, MW, K, KP, MT, MP
      LOGICAL CHECK
      DIMENSION M(10), K(6), C(6), Y(10), D(3), B(4), A(4,4), Y0(6),
     +          KP(5,6), DFDT(4), DCDT(6), DKDT(6), DCDP(6),
     +          DYDT(10), DYDP(10), A0(7,10), DFDP(4), CP0(10),H0(10),
     +          S0(10), NPIV(10)
C
C     FUEL DATA
C
      DATA ALPHA/1.0/,BETA/4.0/,GAMMA/0./,DELTA/0./
C
C     SPECIFIC HEAT DATA FROM GORDON AND MCBRIDE (1971)
C
      DATA A0/
     1   .44608041E+01,  .30981719E-02, -.12392571E-05,  .22741325E-09,
     1  -.15525954E-13, -.48961442E+05, -.98635982E+00,
     2   .27167633E+01,  .29451374E-02, -.80224374E-06,  .10226682E-09,
     2  -.48472145E-14, -.29905826E+05,  .66305671E+01,
     3   .28963194E+01,  .15154866E-02, -.57235277E-06,  .99807393E-10,
     3  -.65223555E-14, -.90586184E+03,  .61615148E+01,
     4   .36219535E+01,  .73618264E-03, -.19652228E-06,  .36201558E-10,
     4  -.28945627E-14, -.12019825E+04,  .36150960E+01,
     5   .29840696E+01,  .14891390E-02, -.57899684E-06,  .10364577E-09,
     5  -.69353550E-14, -.14245228E+05,  .63479156E+01,
     6   .31001901E+01,  .51119464E-03,  .52644210E-07, -.34909973E-10,
     6   .36945345E-14, -.87738042E+03, -.19629421E+01,
     7   .25000000E+01, 0., 0., 0., 0.,  .25471627E+05, -.46011763E+00,
```


Reproduced with permission of the copyright owner. Further reproduction prohibited without permission.

```
     8   .55420596E+01, -.27550619E-04, -.31028033E-08,  .45510674E-11,
     8  -.43680515E-15,  .29230803E+05,  .49203080E+01,
     9   .29106427E+01,  .95931650E-03, -.19441702E-06,  .13756646E-10,
     9   .14224542E-15,  .39353815E+04,  .54423445E+01,
     #   .31890000E+01,  .13382281E-02, -.52899318E-06,  .95919332E-10,
     #  -.64847932E-14,  .98283290E+04,  .67458126E+01/
C
C     EQUILIBRIUM CONSTANT DATA FROM OLIKARA AND BORMAN (1975)
C
      DATA KP/
     1  .432168E+00, -.112464E+05,  .267269E+01, -.745744E-04,
     1  .242484E-08,
     2  .310805E+00, -.129540E+05,  .321779E+01, -.738336E-04,
     2  .344645E-08,
     3 -.141784E+00, -.213308E+04,  .853461E+00,  .355015E-04,
     3 -.310227E-08,
     4  .150879E-01, -.470959E+04,  .646096E+00,  .272805E-05,
     4 -.154444E-08,
     5 -.752364E+00,  .124210E+05, -.260286E+01,  .259556E-03,
     5 -.162687E-07,
     6 -.415302E-02,  .148627E+05, -.475746E+01,  .124699E-03,
     6 -.900227E-08/
C
C     MOLECULAR WEIGHTS
C
      DATA M/44.01, 18.02, 28.008, 32., 28.01, 2.018, 1.009, 16.,
     +       17.009, 30.004/
C
C     OTHER DATA
C
      DATA MAXITS/100/, TOL/3.0E-05/, RU/8.31434/
C
C     MAKE SURE SOLID CARBON WILL NOT FORM
C
      IER = 2
      EPS = .210/(ALPHA + 0.25*BETA - 0.5*GAMMA)
      IF( PHI .GT. (.210/EPS/(0.5*ALPHA - 0.5*GAMMA)) ) RETURN
      IER = 0
C
C     DECIDE IF AN INTIAL ESTIMATE TO THE COMPOSITION IS
C     REQUIRED OR IF T < 1000 IN WHICH CASE FARG WILL SUFFICE
C
C



      SUM = 0.
      DO 10 I = 1,10
10    SUM = SUM + Y(I)
      IF ( T .GT. 1000. .AND. SUM .GT. 0.998 ) GO TO 20
      CALL FARG(P,T,PHI,1.,H,U,V,S,Y0,CP,DLVLT,DLVLP)
      DO 30 I = 1,10
30    Y(I) = 0.0
      DO 40 I = 1,6
40    Y(I) = Y0(I)
      IF( T .LE. 1000. ) RETURN
20    CONTINUE
C
```


Reproduced with permission of the copyright owner. Further reproduction prohibited without permission.

```
C     EVALUATE THE REQUISITE CONSTANTS
C
      PATM = .9869233*P
      DO 50 I = 1,6
50    K(I) = 10.**(KP(1,I)*ALOG(T/1000.) + KP(2,I)/T + KP(3,I) +
     +       KP(4,I)*T + KP(5,I)*T*T)
      C(1) = K(1)/SQRT(PATM)
      C(2) = K(2)/SQRT(PATM)
      C(3) = K(3)
      C(4) = K(4)
      C(5) = K(5)*SQRT(PATM)
      C(6) = K(6)*SQRT(PATM)
      D(1) = BETA/ALPHA
      D(2) = (GAMMA + .42/EPS/PHI)/ALPHA
      D(3) = (DELTA + 1.58/EPS/PHI)/ALPHA
C
C     SET UP ITERATION LOOP FOR NEWTON-RAPHSON ITERATION AND
C     INTRODUCE TRICK TO PREVENT INSTABILITIES NEAR PHI = 1.0
C     AT LOW TEMPERATURES ON 24 BIT MACHINES (VAX). SET
C     TRICK = 1.0 ON 48 BIT MACHINES (CDC)
C
      TRICK = 10.
      CHECK = ABS(PHI - 1.0) .LT. TOL
      IF(CHECK)  PHI = PHI*(1.0 + SIGN(TOL,PHI - 1.0))
      ICHECK = 0
      DO 5 J = 1,MAXITS
      DO 4 JJ = 1,10
4     Y(JJ) = AMIN1(1.0, AMAX1(Y(JJ),1.0E-25))
      D76 = 0.5*C(1)/SQRT(Y(6))
      D84 = 0.5*C(2)/SQRT(Y(4))
      D94 = 0.5*C(3)*SQRT(Y(6)/Y(4))
      D96 = 0.5*C(3)*SQRT(Y(4)/Y(6))
      D103 = 0.5*C(4)*SQRT(Y(4)/Y(3))
      D104 = 0.5*C(4)*SQRT(Y(3)/Y(4))
      D24 = 0.5*C(5)*Y(6)/SQRT(Y(4))
      D26 = C(5)*SQRT(Y(4))
      D14 = 0.5*C(6)*Y(5)/SQRT(Y(4))
      D15 = C(6)*SQRT(Y(4))
      A(1,1) = 1. +  D103
      A(1,2) = D14 + D24 + 1. + D84 + D104 + D94
      A(1,3) = D15 + 1.0
      A(1,4) = D26 + 1.0 + D76 + D96
      A(2,1) = 0.0
      A(2,2) = 2.0*D24 + D94 - D(1)*D14
      A(2,3) = -D(1)*D15 - D(1)
      A(2,4) = 2.0*D26 + 2.0 + D76 +D96
      A(3,1) = D103
      A(3,2) = 2.0*D14 + D24 + 2.0 + D84 + D94 + D104 - D(2)*D14
      A(3,3) = 2.0*D15 + 1.0 - D(2)*D15 - D(2)
      A(3,4) = D26 + D96
      A(4,1) = 2.0 +D103
      A(4,2) = D104 - D(3)*D14
      A(4,3) = -D(3)*D15 - D(3)
      A(4,4) = 0.
C
C     SOLVE THE MATRIX EQUATION 3.81 FOR COMPOSITION CORRECTIONS
C
```


Reproduced with permission of the copyright owner. Further reproduction prohibited without permission.

```
      SUM = 0.
      DO 55 I = 1,10
55    SUM = SUM + Y(I)
      B(1) = -(SUM - 1.0)
      B(2) = -(2.0*Y(2) + 2.0*Y(6) + Y(7) + Y(9) - D(1)*Y(1) -
     +         D(1)*Y(5))
      B(3) = -(2.0*Y(1) + Y(2) + 2.0*Y(4) + Y(5) + Y(8) + Y(9)
     +     +  Y(10) - D(2)*Y(1) - D(2)*Y(5))
      B(4) = -(2.0*Y(3) + Y(10) - D(3)*Y(1) - D(3)*Y(5))
      NDIG=1
      CALL SDCOMP (4, 4, A, NPIV, NDIG)
      CALL SOLVE (4, 4, A, NPIV, B)
      ERROR = 0.
      DO 56 L = 3,6
      LL = L - 2
      Y(L) = Y(L) + B(LL)/TRICK
      ERROR = AMAX1(ERROR,ABS(B(LL)))
      Y(L) = AMIN1(1.0,AMAX1(Y(L),1.0E-25))
56    CONTINUE
      Y(7) = C(1)*SQRT(Y(6))
      Y(8) = C(2)*SQRT(Y(4))
      Y(9) = C(3)*SQRT(Y(4)*Y(6))
      Y(10) = C(4)*SQRT(Y(4)*Y(3))
      Y(2) = C(5)*SQRT(Y(4))*Y(6)
      Y(1) = C(6)*SQRT(Y(4))*Y(5)
      IF(ERROR .LT. TOL) ICHECK = ICHECK + 1
      IF(ERROR .LT. TOL .AND. ICHECK .GE. 2) GO TO 57
5     CONTINUE
      IER = 1
C
C     COMPUTE THE REQUSITE CONSTANTS TO FIND PARTIAL DERIVATIVES
C
57    DO 60 I = 1,6
60    DKDT(I) = 2.302585*K(I)*(KP(1,I)/T - KP(2,I)/T/T + KP(4,I)
     +        + 2.0*KP(5,I)*T)
      DCDT(1) = DKDT(1)/SQRT(PATM)
      DCDT(2) = DKDT(2)/SQRT(PATM)
      DCDT(3) = DKDT(3)
      DCDT(4) = DKDT(4)
      DCDT(5) = DKDT(5)*SQRT(PATM)
      DCDT(6) = DKDT(6)*SQRT(PATM)
      DCDP(1) = -0.5*C(1)/P
      DCDP(2) = -0.5*C(2)/P
      DCDP(5) =  0.5*C(5)/P
      DCDP(6) =  0.5*C(6)/P
      X1 = Y(1)/C(6)
      X2 = Y(2)/C(5)
      X7 = Y(7)/C(1)
      X8 = Y(8)/C(2)
      X9 = Y(9)/C(3)
      X10 = Y(10)/C(4)
      DFDT(1) = DCDT(6)*X1 + DCDT(5)*X2 + DCDT(1)*X7 + DCDT(2)*X8
     +        + DCDT(3)*X9 + DCDT(4)*X10
      DFDT(2) = 2.0*DCDT(5)*X2 + DCDT(1)*X7 + DCDT(3)*X9 -
     +        D(1)*DCDT(6)*X1
      DFDT(3) = 2.0*DCDT(6)*X1 + DCDT(5)*X2 + DCDT(2)*X8
     +        + DCDT(3)*X9 + DCDT(4)*X10 - D(2)*DCDT(6)*X1
```


Reproduced with permission of the copyright owner. Further reproduction prohibited without permission.

```
      DFDT(4) = DCDT(4)*X10 - D(3)*DCDT(6)*X1
      DFDP(1) = DCDP(6)*X1 + DCDP(5)*X2 + DCDP(1)*X7 + DCDP(2)*X8
      DFDP(2) = 2.0*DCDP(5)*X2 + DCDP(1)*X7 - D(1)*DCDP(6)*X1
      DFDP(3) = 2.0*DCDP(6)*X1 + DCDP(5)*X2 + DCDP(2)*X8 -
     +          D(2)*DCDP(6)*X1
      DFDP(4) = -D(3)*DCDP(6)*X1
C
C     SOLVE THE MATRIX EQUATIONS 3.91 FOR THE INDEPENDENT DERIVATIVES
C     AND THEN DETERMINE THE DEPENDENT DERIVATIVES
C
      DO 70 I = 1,4
70    B(I) = -DFDT(I)
      CALL SDCOMP (4, 4, A, NPIV, NDIG)
      CALL SOLVE (4, 4, A, NPIV, B)
      DYDT(3) = B(1)
      DYDT(4) = B(2)
      DYDT(5) = B(3)
      DYDT(6) = B(4)
      DYDT(1) = SQRT(Y(4))*Y(5)*DCDT(6) + D14*DYDT(4) + D15*DYDT(5)
      DYDT(2) = SQRT(Y(4))*Y(6)*DCDT(5) + D24*DYDT(4) + D26*DYDT(6)
      DYDT(7) = SQRT(Y(6))*DCDT(1) + D76*DYDT(6)
      DYDT(8) = SQRT(Y(4))*DCDT(2) + D84*DYDT(4)
      DYDT(9) = SQRT(Y(4)*Y(6))*DCDT(3) + D94*DYDT(4) + D96*DYDT(6)
      DYDT(10) = SQRT(Y(4)*Y(3))*DCDT(4) + D104*DYDT(4) + D103*DYDT(3)
C
      DO 80 I = 1,4
80    B(I) = -DFDP(I)
      CALL SDCOMP (4, 4, A, NPIV, NDIG)
      CALL SOLVE (4, 4, A, NPIV, B)
      DYDP(3) = B(1)
      DYDP(4) = B(2)
      DYDP(5) = B(3)
      DYDP(6) = B(4)
      DYDP(1) = SQRT(Y(4))*Y(5)*DCDP(6) + D14*DYDP(4) + D15*DYDP(5)
      DYDP(2) = SQRT(Y(4))*Y(6)*DCDP(5) + D24*DYDP(4) + D26*DYDP(6)
      DYDP(7) = SQRT(Y(6))*DCDP(1) + D76*DYDP(6)
      DYDP(8) = SQRT(Y(4))*DCDP(2) + D84*DYDP(4)
      DYDP(9) = D94*DYDP(4) + D96*DYDP(6)
      DYDP(10) = D104*DYDP(4) + D103*DYDP(3)
C
      DO 90 I = 1,10
      CP0(I)=A0(1,I)+A0(2,I)*T+A0(3,I)*T*T+A0(4,I)*T**3
     +          +A0(5,I)*T**4
C       CP0(I) = A0(1,I) + A0(2,I)*T + A0(3,I)*T*T + A0(4,I)*T**3
     +       + A0(5,I)*T**4
      H0(I) = A0(1,I) + A0(2,I)/2.*T + A0(3,I)/3.*T*T + A0(4,I)/4.*
     +        T**3 + A0(5,I)/5.*T**4 + A0(6,I)/T
90    S0(I) = A0(1,I)*ALOG(T) + A0(2,I)*T + A0(3,I)/2.*T**2
     +      + A0(4,I)/3.*T**3 + A0(5,I)/4.*T**4 + A0(7,I)
C
C     Y(1),Y(2) ARE REEVALUTED TO CLEAN UP ANY ROUND-OFF ERRORS WHICH
C     CAN OCCUR FOR THE LOW TEMPERATURE STOICHIOMETRIC SOLUTIONS
C
      Y(1) = (2.*Y(3) + Y(10))/D(3) - Y(5)
      Y(2) = (D(1)/D(3)*(2.*Y(3) + Y(10)) - 2.*Y(6) - Y(7) - Y(9))/2.
C
      MW = 0.
```


Reproduced with permission of the copyright owner. Further reproduction prohibited without permission.

```
      CP = 0.
      H = 0.
      S = 0.
      MT = 0.
      MP = 0.
      DO 100 I = 1,10
      IF( Y(I) .LE. 1.0E-25 ) GO TO 100
      H = H + H0(I)*Y(I)
      MW = MW + M(I)*Y(I)
      MT = MT + M(I)*DYDT(I)
      MP = MP + M(I)*DYDP(I)
      CP = CP + Y(I)*CP0(I) + H0(I)*T*DYDT(I)
      S = S + Y(I)*(S0(I) - ALOG(Y(I)))
100   CONTINUE
C
      R = RU/MW
      V = 10.*R*T/P
      CP = R*(CP - H*T*MT/MW)
C     CP=(3.653-0.001337*T+0.000003294*T**2-0.000000001913*
C     +       T**3+0.000000000002763*T**4)*0.287
      DLVLT = 1.0 + AMAX1(-T*MT/MW,0.)
      DLVLP = -1.0 - AMAX1( P*MP/MW,0.)
      H = H*R*T
      S = R*(-ALOG(PATM) + S)
      U = H - R*T
      RETURN
      END


      SUBROUTINE ADODE(O,N,RATE,X0,XEND,HTC,Y0,TOL,HTRIAL,YEND)
C
            INTEGER O,N
            REAL X0,XEND,Y0(N),YEND(N),TOL,HTRIAL
            EXTERNAL RATE
C
C     THIS PROGRAM USES ONE OR MORE STEPS OF RKODE TO APPROXIMATE
C     THE SOLUTION OF AN INITIAL VALUE PROBLEM IN ORDINARY
C     DIFFERENTIAL EQUAIONS OVER THE INTERVAL  [X,XEND].
C     THE STEPSIZE IS CHOSEN TO THAT A NORM OF ERREST(N) IS LESS
C     THAN TOL ON EACH STEP.
C     THE APPROXIMATION IS RETURNED IN  YEND(N).
C
C     References: K.E. Atkinson,
C                 An introduction to numerical analysis, p. 378,
C                 J. Wiley, 1978.
C                 G.E. Forsythe, M.A. Malcolm, C.B. Moler,
C                 Computer methods for mathematical computations,
C                 p.129, 1977.
C      Coded: May, 1986; January 20, 1986
            INTEGER I,J,K
            REAL XL,XR,H,ERREST(10),POWER,EE,EE1
            POWER=1./FLOAT(O+1)
            XL=X0
            H=XEND-X0
            IF (ABS(H) .GT. ABS(HTRIAL)) H=HTRIAL
            XR=XL+H
```


Reproduced with permission of the copyright owner. Further reproduction prohibited without permission.

```
C    REPEAT STEPWISE SOLUTION MAINTAINING LARGEST RELATIVE ERROR
C    LESS THAN TOLERANCE.
     5            CALL RKODE(O,N,HTC,RATE,XL,XR,Y0,YEND,ERREST)
                  EE1=0.
                  DO 10 K=1,N
                       EE=ABS(ERREST(K))/(1.+ABS(YEND(K)))
                       IF (EE .GT. TOL) GOTO 30
                       IF (EE .LT. EE1) EE=EE1
                       EE1=EE
    10                 CONTINUE
                  XL=XR
                  DO 20 J=1,N
                       Y0(J)=YEND(J)
    20                 CONTINUE
                  HTRIAL=XEND-XL
    30            IF (EE .NE. 0.)  HTRIAL=.9*H*(ABS(TOL/EE))**POWER
                  IF (XL+HTRIAL .GT. XEND) THEN
                       H=XEND-XL
                    ELSE IF (XL+2.0*HTRIAL .GT. XEND) THEN
                       H=.5*(XEND-XL)
                    ELSE
                       H=HTRIAL
                    END IF
                  XR=XL+H
                  IF (XR .GE. XEND) XR = XEND
                  IF (.5*(XL+XR+.1*H) .LT. XEND) GOTO 5
             RETURN
             END
```

```
      SUBROUTINE RKODE(O,N,HTC,RATE,XOLD,XNEW,YOLD,YNEW,ERREST)
C
           INTEGER O,N
           REAL XOLD,XNEW,YOLD(N),YNEW(N),ERREST(N)
      EXTERNAL RATE
C
C    THIS PROGRAM USES ONE STEP OF AN ORDER O (O=1,2,3) EXPLICIT
C    RUNGE-KUTTA METHOD TO APPROXIMATE THE SOLUTION OF AN INITIAL
C    VALUE PROBLEM IN ORDINARY DIFFERENTIAL EQUATIONS OVER THE
C    INTERVAL  [XOLD,XNEW].
C    THE APPROXIMATION IS RETURNED IN  YNEW(N)  AND ESTIMATES OF
C    THE ERROR IN THESE COMPONENTS ARE RETURNED IN  ERREST(N).
C
C    Reference: J.D. Lambert,
C               Computational methods for ordinary differential
C               equations, p. 133, Wiley, 1973.
C
           INTEGER I,J,IV,JV,PRCOEF,IWA(3)
           REAL H,RRVX,YTEMP(10),FTEMP(10)
           REAL RWA1(10,10),RWA2(44),RWA3(6),RWA4(5,4),RWA5(2,10)
           DATA IWA/2,3,5/
           DATA RWA2/0.,.5,.5,.5,.5,-.5,.5,
     2 0.,.768,.671,.768,.3922213884,.2787786116,
```


Reproduced with permission of the copyright owner. Further reproduction prohibited without permission.

```
     3 .28025,.17575,.544,-.0296109246,-.20483433562,.2344452604,
     4 0.,.507802064,.7988899,.625100049,.3,.507802064,.389021801,
     5 .409868099,.168925953,.181174096,.275,.2856838905,-.03111754601,
     6 -.2110120491,.2564457045,.2306827929,.1618055266,.2191108292,
     7 .3884008512,0.,-.1778455825,-.6229273286,.2095416274,
     8 -.0875001149,.6787313988/
          S=IWA(O)

          IF (O .GT. 3) THEN
             WRITE(6,*) 'High order methods not available - CHOOSE O<4 '
             STOP
             END IF
C    PUT PARAMETERS IN WORK ARRAYS
          J=-15+S*(26-S)/3
          DO 10 IV = 1,S
               RWA3(IV)=RWA2(J)
               J=J+1
   10          CONTINUE
C         RWA3(S+1)=1.
          DO 20 IV = 2,S
               DO 20 JV = 1,IV-1
                    RWA4(IV,JV)=RWA2(J)
                    J=J+1
   20            CONTINUE
          DO 30 IV = 1,2
               DO 30 JV = 1,S
                    RWA5(IV,JV)=RWA2(J)
                    J=J+1
   30            CONTINUE
C    COMPUTE INTERNAL DERIVATIVE APPROXIMATIONS
          H=XNEW-XOLD
          DO 80 I=1,S
               RRVX=XOLD+H*RWA3(I)
               DO 50 K=1,N
                    YTEMP(K)=YOLD(K)
   50               CONTINUE
               DO 60 J=1,I-1
                    DO 60 K=1,N
                         YTEMP(K)=YTEMP(K) + H*RWA4(I,J)*RWA1(K,J)
   60                    CONTINUE
               CALL RATE(N,RRVX,HTC,YTEMP,FTEMP)
               DO 70 K=1,N
                    RWA1(K,I)=FTEMP(K)
   70               CONTINUE
   80          CONTINUE
C    COMPUTE SOLUTION
               DO 85 K=1,N
                    YNEW(K)=YOLD(K)
   85               CONTINUE
               DO 90 J=1,S
                    DO 90 K=1,N
                         YNEW(K)=YNEW(K) + H*RWA5(1,J)*RWA1(K,J)
   90                    CONTINUE
C      COMPUTE ERROR ESTIMATE
            DO 95 K=1,N
               ERREST(K)=0.0
   95          CONTINUE
```


Reproduced with permission of the copyright owner. Further reproduction prohibited without permission.

```
            DO 97 J=1,S
                 DO 97 K=1,N
                      ERREST(K)=ERREST(K) + RWA5(2,J)*RWA1(K,J)
 97                   CONTINUE
            DO 100 K=1,N
                 ERREST(K)=H*ERREST(K)
100              CONTINUE
            RETURN
            END


      SUBROUTINE SDCOMP(NDIM,N,A,NPIV,NDIG)
C
      INTEGER N,NDIM,NPIV(NDIM),NDIG
      REAL A(NDIM,N)
C
C     PERFORMS THE LU-DECOMPOSITION OF A MATRIX WITH MAXIMAL
C     COLUMN PIVOTING.  THE 1-NORM IS USED TO OBTAIN AN
C     ESTIMATE OF THE CONDITION NUMBER.
C     THIS SUBROUTINE DIFFERS FROM DECOMP BECAUSE IT USES AN
C     ALGORITHM FOR SCALING EACH ROW.  THIS MAY CHANGE THE
C     ORDER IN WHICH PIVOT ELEMENTS ARE SELECTED.  IF A
C     CHANGE OCCURS, THE SOLUTION MAY BE DIFFERENT, AND
C     THE LU-DECOMPOSITION WILL BE FOR A MATRIX WHOSE ROWS
C     ARE PERMUTED FROM THOSE OF THE MATRIX INPUT.
C     FOR EFFICIENCY MATRIX OPERATIONS ARE DONE BY COLUMNS.
C     References: G.H. Golub, C.F. Van Loan,
C                 Matrix Computations, p.66, 1983,
C                 Johns Hopkins.
C                 A.K. Cline, C.B. Moler, G.W. Stewart,
C                 J.H. Wilkinson, An Estimate for the
C                 condition number of a matrix,
C                 SIAM Journal NA, Vol. 2, p.368-375, 1979.
C
      INTEGER NM1,I,J,K,IM1,IP1,KP1,NPIVI,PR
      REAL SUM,MAX,T,EPS,DIG,COND
      REAL P(51),Y(51),YM,YP,SP,SM,ROWMX(51)
      SUM=0.0
      DO 10 I=1,N
           SUM=SUM+ABS(A(I,1))
           ROWMX(I)=ABS(A(I,1))
 10        CONTINUE
      COND=SUM
      DO 20 K=2,N
      SUM=0.0
           DO 15 I=1,N
                T=ABS(A(I,K))
                SUM=SUM+T
                IF (T .GT. ROWMX(I)) THEN
                     ROWMX(I)=T
                     END IF
 15             CONTINUE
           IF (COND .LT. SUM) COND = SUM
 20        CONTINUE
      DO 30 I=1,N
           IF (ROWMX(I) .EQ. 0.) THEN
```


Reproduced with permission of the copyright owner. Further reproduction prohibited without permission.

```
                WRITE(6,*) 'MATRIX HAS A ROW OF ZEROS.'
                RETURN
                END IF
30        CONTINUE
      NPIV(N)=1
      DO 60 I=1,N-1
           MAX=ABS(A(I,I)/ROWMX(I))
           NPIVI=I
           IP1=I+1
           DO 35 J=IP1,N
                T=ABS(A(J,I)/ROWMX(J))
                IF (T .GT. MAX) THEN
                     NPIVI=J
                     MAX=T
                     END IF
35              CONTINUE
           IF (I .NE. NPIVI) THEN
                NPIV(N)=-NPIV(N)
                DO 40 K=1,N
                     T=A(I,K)
                     A(I,K)=A(NPIVI,K)
                     A(NPIVI,K)=T
40                   CONTINUE
                END IF
           NPIV(I)=NPIVI
           DO 45 J=IP1,N
                A(J,I)=A(J,I)/A(I,I)
45              CONTINUE
           DO 55 K=IP1,N
                DO 50 J=IP1,N
                     A(J,K)=A(J,K)-A(J,I)*A(I,K)
50                   CONTINUE
55              CONTINUE
60        CONTINUE
      IF (NDIG .EQ. 0) RETURN
C     EVALUATION OF DETERMINANT
      IF (NDIG .NE. 2 .OR. NDIG .NE. 4) GOTO 70
           DET=A(1,1)
           DO 65 I=2,N
                DET=DET*A(I,I)
65              CONTINUE
           WRITE(6,*) 'DETERM IS ',DET*NPIV(N)
70         CONTINUE
C     ESTIMATE OF CONDITION NUMBER BY CLINE ET AL.
      IF (NDIG .EQ. 2) RETURN
      EPS=1.E-5
75    EPS=EPS/2.
      SUM= 1.+EPS
      IF (SUM .GT. 1.) GO TO 75
      DIG=-ALOG10(EPS)
      DO 80 I=1,N
           P(I)=0.
80         CONTINUE
C     FIND VECTOR  E AND SOLUTION OF  U(trans)*P=E
      DO 100 K=1,N
           YP=(1-P(K))/A(K,K)
           YM=(-1-P(K))/A(K,K)
```


Reproduced with permission of the copyright owner. Further reproduction prohibited without permission.

```
            SP=ABS(YP*A(K,K))
            SM=ABS(YM*A(K,K))
            KP1=K+1
            DO 85 I=KP1,N
                  SP=SP+ABS((P(I)+A(K,I)*YP))
                  SM=SM+ABS((P(I)+A(K,I)*YM))
   85             CONTINUE
                  Y(K)=YP
            IF (SP .LT. SM) Y(K) = YM
            YP=Y(K)
            KP1=K+1
            DO 90 I=KP1,N
                  P(I)=P(I)+A(K,I)*YP
   90             CONTINUE
  100       CONTINUE
            DO 110 I=1,N
                  P(I)=Y(I)
  110             CONTINUE
C   SOLVE L(trans)r = y  AND STORE IN P
       DO 120 I=N,1,-1
            IM1=I-1
            DO 115 K=1,IM1
                  P(K)=P(K)-A(I,K)*P(I)
  115             CONTINUE
  120       CONTINUE
C   1-NORM OF  P
       SUM=ABS(P(1))
       DO 141 I=2,N
            SUM=SUM+ABS(P(I))
  141       CONTINUE
       COND=COND/SUM
C   SOLVE Lw = r  AND STORE IN P
       NM1=N-1
       DO 150 I=1,NM1
            IP1=I+1
            DO 145 K=IP1,N
                  P(K)=P(K)-A(K,I)*P(I)
  145             CONTINUE
  150       CONTINUE
C   SOLVE Uz = w  AND STORE IN P
       DO 160 I=N,1,-1
            P(I)=P(I)/A(I,I)
            IM1=I-1
            DO 155 K=1,IM1
                  P(K)=P(K)-A(K,I)*P(I)
  155             CONTINUE
  160       CONTINUE
C   1-NORM OF  z
       SUM=ABS(P(1))
       DO 170 I=2,N
            SUM=SUM+ABS(P(I))
  170       CONTINUE
       COND=COND*SUM
C      IF (NDIG .GT. 2)   WRITE(6,*) 'CONDITION NUMBER IS ABOUT ',COND
       NDIG=DIG+ALOG10(1./COND)
       RETURN
       END
```


Reproduced with permission of the copyright owner. Further reproduction prohibited without permission.

```
      SUBROUTINE SOLVE(NDIM,N,A,NPIV,B)
C
      INTEGER NDIM,N,NPIV(NDIM)
      REAL A(NDIM,N), B(NDIM)
C
C     THIS PROGRAM USES THE DECOMPOSED VERSION OF MATRIX  A
C     OBTAINED BY USING DECOMP TO SOLVE THE PROBLEM  AX = B
C     BY FORWARD AND THEN BACKWARD SUBSTITUTION.  THE VECTOR
C     NPIV CONTAINS THE INFORMATION REQUIRED FOR PIVOTING.
C     FOR EFFICIENCY MATRIX OPERATIONS ARE DONE BY BY COLUMNS
C     References: G.H. Golub, C.F. Van Loan,
C                 Matrix Computations, p.57, 1983,
C                 Johns Hopkins.
C
      INTEGER I,J,K,NM1
      NM1=N-1
      DO 10 I=1,NM1
           IF (I .EQ. NPIV(I)) GO TO 5
                T=B(I)
                B(I)=B(NPIV(I))
                B(NPIV(I))=T
 5              CONTINUE
10         CONTINUE
      DO 20 K=1,NM1
           KP1=K+1
           DO 15 I=KP1,N
                B(I)=B(I)-A(I,K)*B(K)
15              CONTINUE
20         CONTINUE
      DO 30 K=N,2,-1
           B(K)=B(K)/A(K,K)
           KM1=K-1
           DO 25 I=1,KM1
                B(I)=B(I)-A(I,K)*B(K)
25              CONTINUE
30         CONTINUE
      B(1)=B(1)/A(1,1)
      RETURN
      END
```


Reproduced with permission of the copyright owner. Further reproduction prohibited without permission.

Appendix B

Curve Fit Coefficients for Thermodynamic Properties of Various Ideal Gases and Fuels

The tables of coefficients of CO_2, H_2O, CO, H_2, O_2, N_2, OH, NO, O, H in the temperature range from 300K to 4000K and different fuels in the temperature range from 300K to 1000K.

Reproduced with permission of the copyright owner. Further reproduction prohibited without permission.

Reproduced with permission of the copyright owner. Further reproduction prohibited without permission.

Table B-1 Curve Fit Coefficients for Thermodynamic Properties (300<T<1000 K)

Species	a_{i1}	a_{i2}	a_{i3}	a_{i4}	a_{i5}	a_{i6}	a_{i7}
1--CO_2	0.24007797E+01	0.87350957^{I}-02	-0.66070878^{I}-05	0.20021861^{I}-08	0.63274039^{E}-15	-0.48377527^{I}+05	0.96951457^{I}+01
2--H_2O	0.40701275E+01	-0.11084499^{E}-02	0.41521180^{I}-05	-0.29637404^{E}-08	0.80702103^{E}-12	-0.30279722^{E}+05	-0.32270046^{I}+00
3--N_2	0.36748261E+01	-0.12081500^{I}-02	0.23240102^{I}-05	-0.63217559^{E}-09	-0.22577253^{E}-12	-0.10611588^{E}+04	0.23580424^{E}+01
4--O_2	0.36255985E+01	-0.18782184E-02	0.70554544E-05	-0.67635137E-08	0.21555993E-11	-0.10475226E+04	0.43052778E+01
5--CO	0.37100928E+01	-0.16190964E-02	0.36923594E-05	-0.20319674E-08	0.23953344E-12	-0.14356310E+05	0.2955535E+01
6--H_2	0.30574451E+01	0.26765200E-02	-0.58099162E-05	0.55210391E-08	-0.18122739E-11	-0.98890474E+03	-0.22997056E+01
7--H	0.25000000E+01	0	0	0	0	0.25471627E+05	-0.46011762E+00
8--O	0.29464287E+01	-0.16381665E-02	0.24210316E-05	-0.16028432E-08	0.38906964E-12	0.29147644E+05	0.29639949E+01
9--OH	0.38375943E+01	-0.10778858E-02	0.96830378E-06	0.18713972E-09	-0.22571094E-12	0.36412823E+04	0.49370009E+00
10--NO	0.40459521E+01	-0.34181783E-02	0.79819190E-05	-0.61139316E-08	0.15919076E-11	0.97453934E+04	0.29974988E+01

Reproduced with permission of the copyright owner. Further reproduction prohibited without permission.

Table B-2 Curve Fit Coefficients for Thermodynamic Properties (1000<T<4000 K)

Species	a_{i1}	a_{i2}	a_{i3}	a_{i4}	a_{i5}	a_{i6}	a_{i7}
1--CO_2	0.446080E+1	0.309817E-2	-0.123925E-5	0.227413E-9	-0.155259E-13	-0.489614E+5	-0.986359
2--H_2O	0.271676E+1	0.294513E-2	-0.802243E-6	0.102266E-9	-0.484721E-14	-0.299058E+5	0.663056E+1
3--N_2	0.289631E+1	0.151548E-2	-0.572352E-6	0.998073E-10	-0.652235E-14	-0.905861E+3	0.616151E+1
4--O_2	0.362195E+1	0.736182E-3	-0.196522E-6	0.362015E-10	-0.289456E-14	-0.120198E+4	0.361509E+1
5--CO	0.298406E+1	0.148913E-2	-0.578996E-6	0.103645E-9	-0.693535E-14	-0.142452E+5	0.634791E+1
6--H_2	0.310019E+1	0.511194E-3	0.526442E-7	-0.349099E-10	0.369453E-14	-0.877380E+3	-0.196294E+1
7--H	0.25E+1	0	0	0	0	0.254716E+5	-0.460117
8--O	0.554205E+1	-0.275506E-4	-0.310280E-8	0.455106E-11	-0.436805E-15	0.292308E+5	0.492030E+1
9--OH	0.291064E+1	0.959316E-3	-0.194417E-6	0.137566E-10	0.142245E-15	0.393538E+4	0.544234E+1
10--NO	0.3189E+1	0.133822E-2	-0.528993E-6	0.959193E-10	-0.648479E-14	0.982832E+4	0.674581E+1

Reproduced with permission of the copyright owner. Further reproduction prohibited without permission.

Table B-3 Curve Fit Coefficients for Thermodynamic Properties of Selected Fuels (300<T<100K)

Fuel		a_1	a_2	a_3	a_6	a_7
Methane	CH_4	1.971324	7.871586E-03	-1.048592E-06	-9.930422E+03	8.873728
Gasoline	C_7H_{17}	4.0652	6.0977E-02	-1.8801E-05	-3.5880E+04	1.545E+01
Diesel	$C_{14.4}H_{24.9}$	7.9710	1.1954E-01	-3.6858E-05	-1.9385E+04	-1.7879
Methanol	CH_3OH	1.779819	1.262503E-02	-3.624890E-06	-2.525420E+04	1.50884E+01
Nitromethane	CH_3NO_2	1.412633	2.087101E-02	-8.142134E-06	-1.026351E+04	1.917126E+01

VITA AUCTORIS

Shengmei Zhang

Birth January 14th, 1974 Beijing, P.R.China

Education

1999-2000 University of Windsor, Windsor, ON, Canada
Master's of Applied Science, Mechanical Engineering

1993-1997 Jilin University, Chanchung, P.R.China
Bachelor of Engineering, Automotive Engineering

Experience

2000 Ford Motor Company of Canada Ltd., Windsor, ON, Canada
Engineering Intern, Windsor Casting Plant
- Involve lean manufacturing projects and applications
- Report engineering small working group meeting minutes
- Project design for power and free conveyor

1998-1999 Sun Inter-Technology (China) Ltd, Beijing, P.R.China
Project Manager, Auto Industry Division
- Monitor and track existing and potential projects in automotive industry
- Coordinate with other project managers and engineers for proposals and quotations
- Report China's automotive market

1997-1998 China Geo-Engineering Corporation, Beijing, P.R.China
Associate Engineer, Technical Center
- Make technical drawing

Volunteer Activities

Volunteer, Millennium Open House at University of Windsor
- Set exhibition and interact with the general public

Volunteer, Engineering Department Student Union, Jilin University
- Organize and promote events for engineering students

Personal Interests

Paint and sketch
Languages learning
Travel
Art and humanities studies

Reproduced with permission of the copyright owner. Further reproduction prohibited without permission.